Polyolefin Pyrolysis via Liquid Metal Catalysis

by

Christopher Eliot Parker

B.S.E. Chemical Engineering, University of Michigan, 2015

Submitted to the Graduate Faculty of the

Swanson School of Engineering in partial fulfillment

of the requirements for the degree of

Master of Science in Chemical Engineering

University of Pittsburgh

2022

UNIVERSITY OF PITTSBURGH

SWANSON SCHOOL OF ENGINEERING

This thesis was presented

by

Christopher Eliot Parker

It was defended on

November 30, 2021

and approved by

Susan Fullerton
Professor, Department of Chemical and Petroleum Engineering

Mohammad Masnadi Shirazinejad
Assistant Professor, Department of Chemical and Petroleum Engineering

Götz Veser
Professor, Department of Chemical and Petroleum Engineering

Polyolefin Pyrolysis via Liquid Metal Catalysis

Christopher Eliot Parker, MS

University of Pittsburgh, 2022

Plastic production is expected to double in the next thirty years, which is the subject of environmental and health concerns. Improving end-of-life options for plastics can mitigate these concerns, and one solution is for plastic waste to be ‘upcycled’: broken down to its constituent components for re-use in high quality plastic manufacturing. Polyolefins are a particularly concerning type of plastic in this regard, making up about 49% of all plastic in use and to date there are few end-of-life processes that are both sustainable and economically feasible. Pyrolysis, also known as thermal decomposition, is a technically feasible method of upcycling polyolefins; however, without the aid of catalysts the process is energetically expensive and produces a set of low value heterogenous products. An improvement on this process could enable improved rates of recycling, and a catalyst that has a high activity, resistant to coking, and able to handle a diverse set of feeds could provide the needed improvement.

Liquid metals may be such a catalyst. When used a reaction media low-melting metals such as bismuth provide a base for dissolving high-melting catalytically active metals such as nickel, while providing a reaction environment with excellent separation and heat transfer properties. Solutions of liquid metals have shown catalytic activity in similar reactions, and when paired with the thermal and physical properties of liquid metal are promising for use in polyolefin pyrolysis.

This thesis proposes that liquid metals could act as catalysts in pyrolysis of polyolefins, and explores the development of reactors, methods of characterization, and experimental methods required to demonstrate said catalytic activity. It goes on to apply these methods, models, and reactors to proof-of-concept experiments in application to polypropylene and polyethylene pyrolysis, as well as ethane dehydrogenation reactions. The liquid metals tested have yet to demonstrate catalytic activity, and the tools developed can be used to perform further testing on potential liquid metal catalysts for the pyrolysis of polyolefins.

Table of Contents

List of Tables

List of Figures

Preface

Thank you to my wife Emily for your encouragement and tolerance of my early mornings in the lab, and to Dorothy and Piper showing me how promising the future can be.

This work would never have come to be without the support and guidance of my advisors, Professors Goetz Veser, and Eric Beckman. Thank you so much for your encouragement and insight—words cannot express. I am eager to see where your research goes from here.

Thank you to Professor Susan Fullerton for your alacrity in graduate student management, and to Professor Masnadi for your enthusiastic discussions on experimental design and living life.

Thanks to Bob Maniet and Rita Leccia—without you the department would cease to function overnight.

And finally: thank you to Yahui Yang, Aime Laurent, Aaditya Bharanidharan, Yifan Deng, Nasser Al Azri, Sean Graham, and all the other students of the Veser Lab for their countless answers to my countless questions, collaboration, and good times.

1.0 Introduction and Background

The overall motivation of this thesis is to explore whether liquid metals can be used as catalysts to recycle plastics. The attainable objectives are to design a reactor for studying reactions with liquid metals, develop experimental methods for studying such reactions, and explore how liquid metals' catalytic quality can be characterized—these objectives will be discussed in depth in section 2. This investigation involves the intersection of the fields of sustainability, polymer physics, and catalysis. The concepts explored may best be understood individually prior to being brought together in this application, and the objective of this section is to provide sufficient background knowledge to understand the challenges and objectives of this thesis—particularly in answering the high-level objectives: how can plastics be efficiently recycled, and how can liquid metals be put to use in recycling processes.

1.1 Plastic Recycling

Plastics have been in production for about 70 years, and most of these plastics are landfilled or incinerated at the end of their use. The production of plastic is expected to double by 2030, and there is therefore a need for sustainable end-of-life management for plastic in order to reduce the amount of plastic released into the environment (Geyer et al. 2017). This provides an opportunity to make use of this waste and avoid the environmental and health hazards of their accumulation. In the United States ca. 2015, only 9% of plastic waste is recycled (Thiounn et al. 2020)—this is far behind the progress that has been made in Europe which recycled 17% of their plastics in 2003 (Achilias et al. 2006). This demonstrates that even with present technology plastic waste could be better managed in the US that it is now, and improvements in recycling technology could improve the financial feasibility of employing recycling processes.

From a materials cost perspective, it is important to note that only 8% of crude oil is used in plastic production. This is notable because recycling plastics may save oil resources, it will likely not have widespread effects on the global oil demand. Although there are cost savings in recycling plastics to save oil resources and reduce overall production due to the availability of waste, virgin plastics have been historically significantly less expensive than recycled stock, and only in recent years have become cost-competitive due to an increase in consumer demand and improvement of quality (Victory M. and Tudball M. 2021). It is a point of interest whether the reduction of fuel used in transportation will affect the financial feasibility of recycling plastics into, and a thorough investigation by an economist's perspective may shed light on that topic.

From an engineering perspective, industrial waste and consumer plastic waste have different considerations for recycling, including availability, transportation, cleaning, and composition of plastics (Ragaert et al. 2017). PP and PE are found in both post-consumer and post-industrial waste, taking up approximately 49% of plastics used today, and therefore recycling of these polymers is much desired (Ragaert et al. 2017). At the same time, there have been few methods to upcycle these materials—which will be discussed later in this thesis.

Most plastic recycling is considered "Downcycling", as the recyclate is of lower quality and has limited use in products. "Upcycling", in which recycling produces products of equal or great quality and can be used to produce equivalent or even superior products—this typically involves breaking polymers down to their monomeric components for re-polymerization. This creates a circular economy of material management, where the bulk of materials used come from waste.

Circularity is valuable from an economic standpoint and environmental standpoint due to the removal of the need for extensive extraction of raw materials and decrease in hazardous waste generation. Particularly for halogenated plastics, PVC specifically, simply landfilling, or environmental dispersal of materials can release significant greenhouse gases and harmful chemical, for example PVC incorporates chloring into its backbone and will inevitably release hydrogen chloride given sufficient time to degrade. Even using energy recovery mechanisms and controlled degradations can reduce the end-of-life impacts of plastic disposal (Lithner et al 2011). Waste disposal, energy recovery, and recycling are not necessarily mutually exclusive, and can obviously be used in tandem. However, from a global resource perspective, there is a fairly conventional mass balance at play: All polymers produced need to have their materials come from somewhere and go somewhere after use. A useful visualization of those production and end of life mechanisms is reproduced below in Figure 1—ultimately, the use of plastic can be performed as a mass balance between gaseous degradation products and raw materials. There are many methods of disposal, and if more material could be recovered chemically, then less raw material would need to be processed.

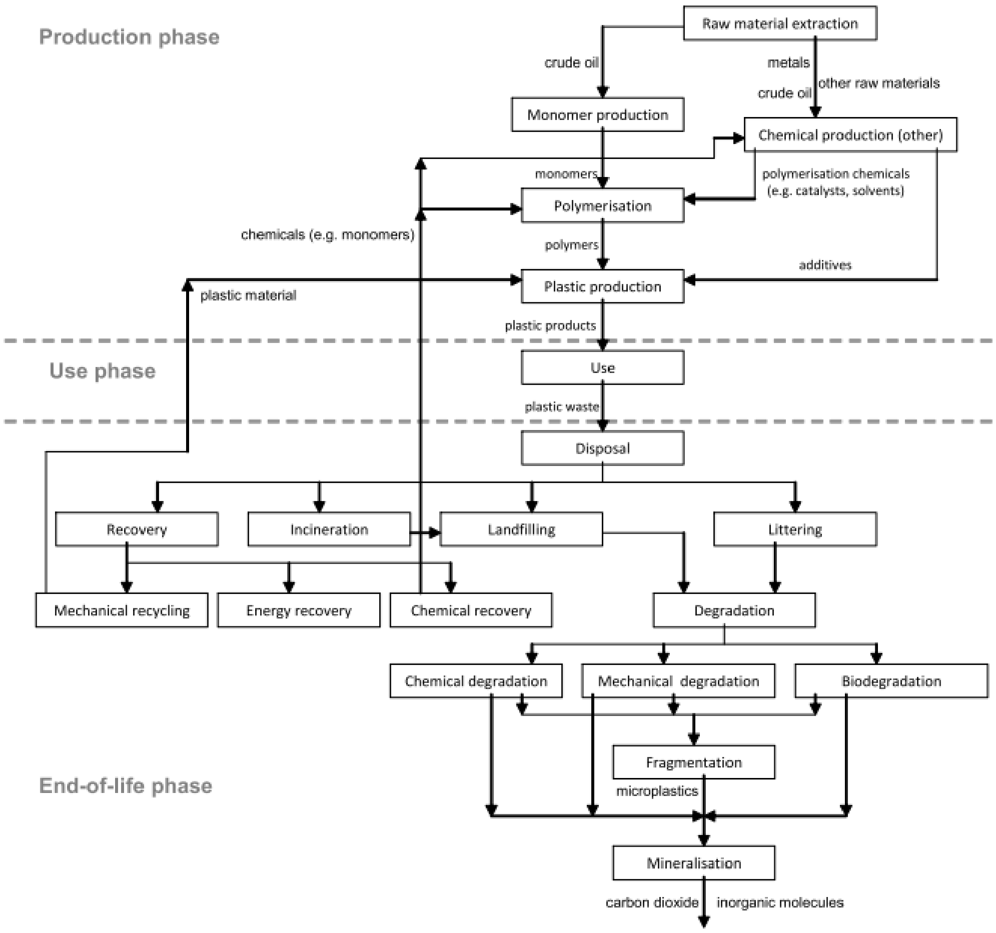

Figure 1 - The Life cycle of plastic products (Lithner et al. 2011)

Some forms of end-of-life management such as incineration are particularly challenging from a health perspective, as many plastics and additives release carcinogenic organic compounds and toxic metal bi-products that have been reported to negatively affect workers in processing plants as well as the infants in the surrounding communities—a topic that has been studied in-depth (Hahladakis et al. 2018). Additionally, post-consumer and post-industrial wastes accumulate chemical contamination during their lifecycle, which contributes to the inherent lower quality of downcycled plastics (Horodytska et al. 2020).

As previously stated, most plastic is not recycled. The end-of-life management of plastics does vary on the type of plastic, as end of life management exists for some plastics such as PLA (Payne et al. 2019), or PET-Contaminated PP streams (Ragaert et al. 2018). It is concerning, and the focus of this research, that the most widely used plastics are polyolefins, particularly polyethylene and polypropylene as seen in Figure 2 below, and these plastics have traditionally had the least sustainable end of life management (Payne et al. 2019). Some experts consider switching away from such plastics with poor options for end-of-life management, however 'alternative' plastics often come with their own environmental and economic concerns, particularly in the high cost of retooling processes and products to use different types of plastics, and the need for collection and end of life management for biodegradable plastics, such as composting of PLA (Prata et al. 2019).

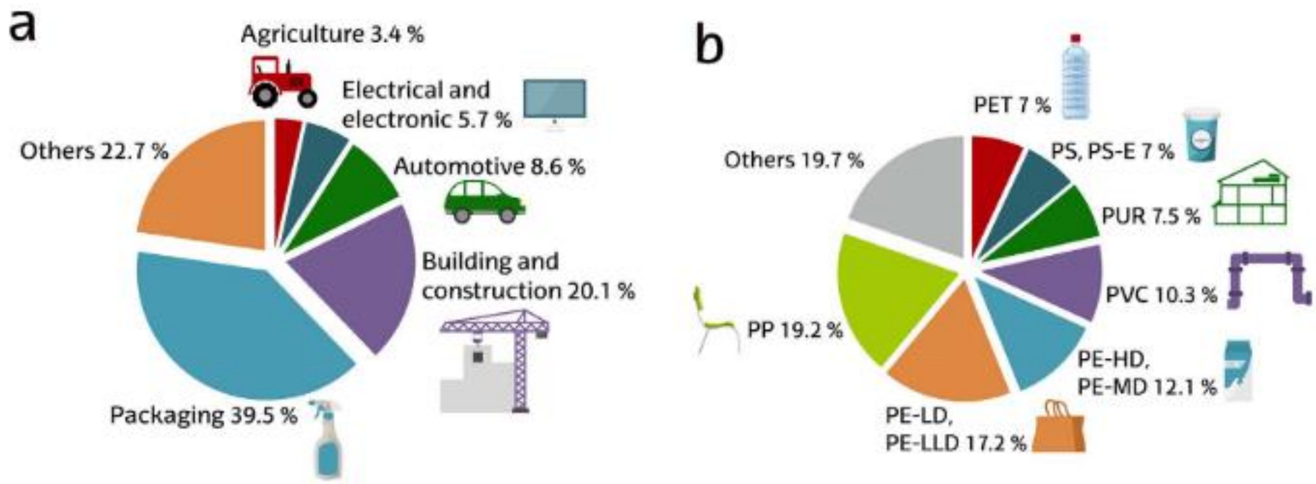

Figure 2 – a: Applications of plastic products. b: types of polymers used. (Lopez 2017).

(PET: Polyethylene terephthalate, PS: Polystyrene, PUR: Polyurethane, PVC: Polyvinyl Chloride, PE-HD: High Density Polyethylene, PE-MD: Medium Density Polyethylene, PE-LD: Low Density Polyethylene, PE-LLD: Linear-Low Density Polyethylene, PP: Polypropylene.)

1.1.1 Chemistry and Recycling of “Plastics”

“Plastic” technically is an adjective meaning ‘easily shaped or molded’. From an engineering perspective, materials that are considered “plastics” are chemical formulations consisting of polymer chains and additives. The physical and chemical properties of plastics depend on their base units, the degree of polymerization, and the stereochemical character of a given polymer, as well as any effects contributed by additives to the material. Despite widely varying the isomerization, stereochemistry, and degree of polymerization, polymers of a particular type typically have similar elemental compositions—this is convenient from an end-of-life management perspective as it means their degradation products will also contain a similar elemental makeup. However, additives to plastics can contain many organic and inorganic compounds that may interrupt any mechanisms of degradation, which may be particularly relevant if there are catalysts involved. This is inconvenient, as varying plastic products of the same polymer type may not break down in identical product spectra.

Plastics have a variety of additives from a variety of sources, as seen in Appendix A. Many polymers are readily oxidized which can cause premature breakdown of material, so antioxidants which are typically phenolic, or phosphates are used to improve stability. Plasticizers or stiffeners can be added to change the mechanical properties, as well as brominated fire retardants to improve thermal resistance, particularly for use with electronics (Hahladakis et al. 2018).

Unintentional additives can be present in plastics, which are compounds not in the plastic formulation by design. These include dirt and organic compounds which may be coating post-consumer waste, as well as degradation products of both the polymers and additives in plastic formulation (Horodytska et al. 2020). There are additionally metals in plastics that enter via additives as well as residual catalysts, which can accumulate particularly in downcycled plastics (Eriksen 2018). Simply put, there is a significant fraction of non-polymer chemicals in post-consumer waste, as outlined in Figure 3 below. At the very least these products will produce non-uniform products during chemical recycling and could potentially interrupt chemical processes which may drastically change reaction efficacy for better or worse.

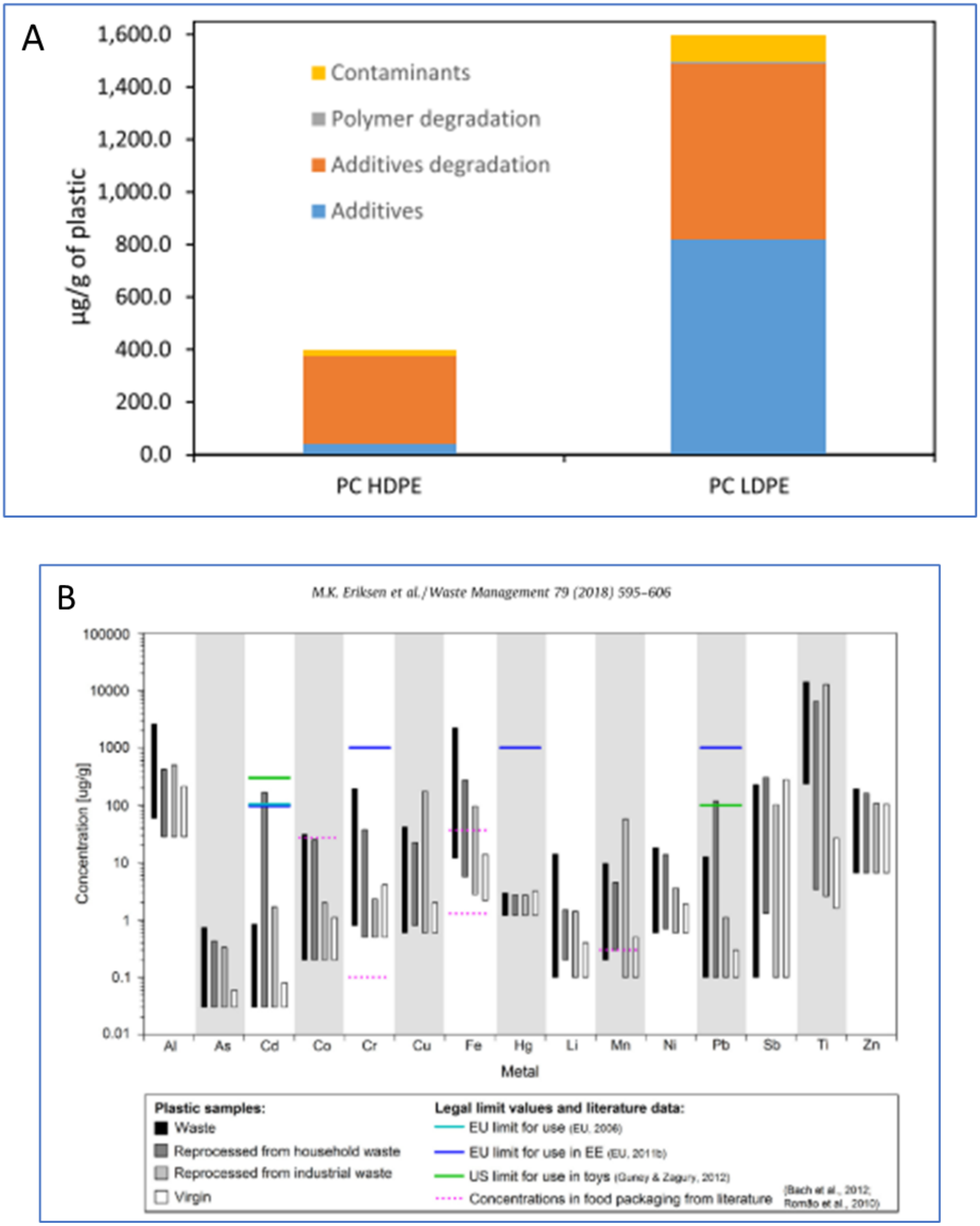

Figure 3 – A: concentration of compounds found in post-consumer plastics according to their nature (Horodytska et al. 2020). B: A summary of weight of metals found in plastics and plastic waste on a per gram of material basis (Eriksen et al. 2018).

1.1.2 Chemistry and Recycling of Polyolefins

“Polyolefin” technically means “Many Olefins”, and when used in this work will follow the industry convention of referring specifically to polyethylenes (PEs) and polypropylenes (PPs), and no other polymerized olefins such as polystyrene. It is important to remember that no two polymer molecules are the same, and vary in terms of size, isomerization, and stereochemistry—which in turn results in different macro material properties. This heterogeneity can make reactions difficult to predict reactivity and kinetics. For a broad description useful for conceptualizing the molecules broadly, consider that Low Density PE (LDPE) has a molecular weight as low as 20,000 g/mol, and High-Density PE (HDPE) may have a molecular weight exceeding 1,500,000 g/mol. These macromolecules form entangled coils that are entangled and typically immobile. The carbon backbone is extremely strong and containing the same electronic character of carbon bonds found in diamonds, and ultra-high molecular weight polyethylene can be found in physically demanding products such as body armor and prosthetic hips. The flexibility of the polymer comes from the ability for the carbon bonds to rotate around stiff bonds of stable length. A representative PE chain is shown below in Figure 4 to help visualize the chemistry of these molecules, and for an excellent review of polymer science consider “Fundamentals of Polymer Science” (Coleman and Painter 1997).

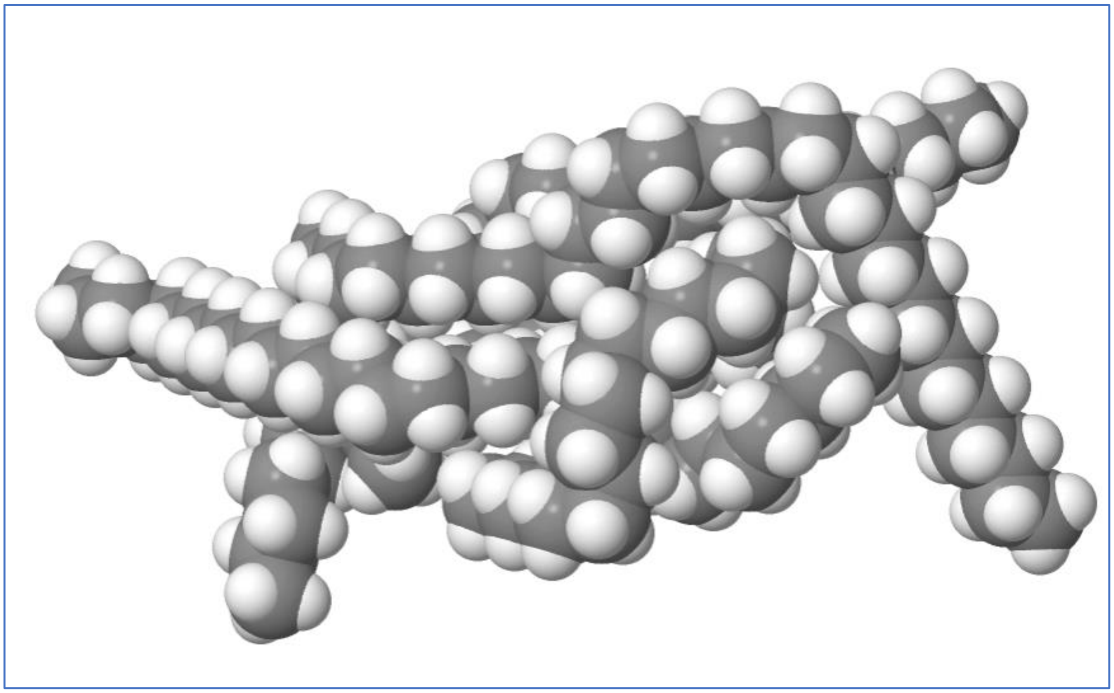

Figure 4 - A schematic of a pair of entangled PE molecules, with a total molecular weight of 2,744 g/mol (Harrison K. 2007).

PEs can be mechanically recycled via purification, melting, and recasting—within this process viscosity is increased and they become more brittle due to a combination of degradation and crosslinking. Blends of polyethylenes can be mechanically recycled through the addition of virgin polymer stocks (Hamad et al. 2013).

PPs have been recycled mechanically as well, and like PEs the melt viscosity of recycled PPs is shown to decrease with increasing processing cycles, presumably due to decreasing PP molecular weight. A variety of polypropylene composites, including talc/PP and EPDM/PP and PP/Organophilics, have been investigated, and it is shown that while the PP thermally degrades through reprocessing, fibrous materials are able to stabilize the product after reprocessing (Hamad et al. 2013).

PEs can be chemically recycled via dissolving PEs in toluene and feeding into fluid catalytic cracking systems, producing mainly naphtha. A similar process has been performed by breaking down PEs thermally, dissolving into naphtha to form a steam cracking feedstock. Additionally, PEs have been thermally cracked in phenol solvents to produce olefins as main products (Hamad et al. 2013). The Dissolution/reprecipitation of polyolefins via dissolving xylene and reprecipitating in n-hexane has been demonstrated at lab scale (Achilias et al. 2007). Catalytic pyrolysis has been investigated using zeolite catalysts, resulting in the production of volatile hydrocarbons (Wei et al. 2010). In recent years, there have been a variety of studies on the thermal and chemical pyrolysis of PEs, and a variety of products can be produced depending on reaction conditions (Lopez et al. 2017).

Thermal degradation of polyolefins promotes random scission of hydrocarbon chains, which results in a distribution of products from longer chain waxes to short alkane gases, as illustrated inf Figure 5 below. Low temperature pyrolysis, i.e.: 500 C, results in waxy products. Pyrolysis at moderate temperatures with longer residence times promotes production of benzene, toluene, xylenes (BTXs). Finally, thermal pyrolysis at high temperatures with a short residence time can result in short alkanes and gaseous products (Lopez et al. 2017).

Figure 5 - Typical Reaction Conditions and Products of Polyolefin Thermal Pyrolysis (Lopez et al. 2017).

A challenge with thermal degradation is that a wide distribution of products is generated. Catalysts can be used to narrow the product distribution from thermal pyrolysis, and as before mentioned zeolites of varying acidity and porosity have been utilized in polyolefin degradation reactions (Lopez et al. 2017). Several reaction systems have been investigated, a couple of notable works involve a two-step reaction system, the first of which breaks polyolefins into smaller waxes and oils, and a second catalytic or higher temperature thermal step to product light olefins (Della Zassa et al. 2010, Artetxe et al. 2012). These reaction systems are very sensitive to pyrolysis conditions of temperature and residence time, and a variety of aluminosilicate catalysts have been used. Although catalysts allow for pyrolysis at lower temperatures and narrow the product spectrum, the porous nature of the catalysts and production of coke in pyrolysis reaction, result in demonstrable deactivation (Marcilla et al. 2004).

1.1.3 Chemistry and Recycling of Mixed Plastics

Theoretically, there are countless ways that plastics can be mixed between polymer species and within a polymer with varying formulations. It is found that there are synergistic effects, and that different plastic blends break down at different temperatures and into different products. This presents a challenge in that most plastic waste will not be entirely pure and it may not be possible to assume the same reactor conditions will produce the same results with different plastics. Conversely, this presents a challenge in that if a plastic mixture that contributes favorably to degradation can be found, then plastics can be intentionally mixed prior to pyrolysis to improve the reaction process.

Such co-pyrolysis processes have been studied in relavent thermal processes; polyolefins have been co-pyrolyzed with other plastics, as well as biomass, with some results showing increasing liquid yields—which indicates that there is a synergetic effect in pyrolyzing mixed systems (Lopez 2017). Notably, the pyrolysis product spectrum is measurably shifted by the addition of polypropylene to polyethylene, predictably in the formation of C3 and C4 gaseous fractions, however also the fraction of C10-C20 hydrocarbons is increased with a corresponding decrease in C24-C40 fraction. Presumably, this shift in distribution is due to the polypropylene’s promotion of radical formation, resulting in increased breakdown of both PP and PE (Palza et al. 2017).

As polyolefin pyrolysis involves complex chemical mechanisms, it is challenging to evaluate via conventional kinetic characterization methodologies. Degradation of solid materials can be analyzed via isoconversional methods.

Isoconversional methods are an evaluation of reaction rate given two assumptions: 1) the rate is a function of temperature and conversion, demonstrated in Equation 1 below, and 2) that the relationship between rate and temperature, and rate and conversion are independent, which allows simplification of Equation 1.1 into Equation 1.2 below (Simon 2004).

$$\frac{d\alpha}{dt} = \Phi(T, \alpha) \qquad \text{Eq. 1.1}$$

$$\frac{d\alpha}{dt} = \mathrm{k(T)f(\alpha)} \qquad \text{Eq. 1.2}$$

α: conversion, t: time, Φ: Rate function, T: Temperature

k: $t$hermal component of rate function, f: convresion component of rate function

Equations 1.1 & 1.2 – Fundamental Assumptions of Isoconversional Methods

k(T) can be assumed to be an Arrhenius relationship, and f(α) contains the contribution of unknown mechanism of degrading solids. Typically, the objective of isoconversional methods is to determine the kinetic model of a system via a kinetic triplet of a system, which is Activation Energy, pre-exponential factor, and conversion function. Linear heating models are particularly useful, as a series of experiments with varying heating rates can be used to parse out the relationship k(T) and allow for analysis of f(α) (Simon 2004).

When applied to polymer degradation, kinetic information for identical systems varies widely (Peterson et al. 2001), which is presumably due to slight changes in reaction design, feedstock, and calculation methods. Therefore, it would be advantageous to establish a method of screening catalysts for activity with a well understood model reaction prior to applying the catalysts for polymer degradation specifically. Short chained alkanes, such as pentadecane, are chemically similar to longer polyolefins, and can be handled in a liquid, and potentially gas, phase much more easily than viscous melts.

The inherently heterogenous recyclate will require a reaction system able to handle varieties of polymers, as well as separate out any non-polymer compounds—all while providing an excellent thermal and catalytic environment. Liquid Metals may be an innovative path to meet these reaction criteria.

1.2 Liquid Metal Catalysts

Liquid metals have long been subject of interest due to their curious physical properties. Perhaps the most apparent liquid metal is mercury, famously toxic and expensive—if an increase in temperature can be managed then there are several more, safe candidates for liquid metals, and their thermal, catalytic, and physical properties can be explored and exploited.

What is particularly remarkable of liquid metals when used in pyrolysis processes is their ability to separate out waste products, namely coke, from the reaction zone which allows for catalysts to maintain their effectiveness overtime. In this scenario, liquid metals can operate within process intensification paradigms, as they act as both catalytic agents and separative agents within a single unit process.

1.2.1 Material Properties of Liquid Metals

Liquid metals have fascinating material properties, most well-known among these are their high density, high surface tension, and unique electromagnetic properties. Post transition metals, and eutectic mixes, have lower melting points and can even be liquid at room temperature (Daeneke et al. 2018). Recently, liquid metals have been employed in soft robotics due their ability to be flexible and perform controlled locomotion and have even been functionalized to tune their electromagnetic and physical properties (Kalantar-Zadeh et al. 2019, Liu et al. 2019). Additionally, there are applications for liquid metals within heat transfer system, particularly in nuclear reactor cooling systems and coupled desalinization operations (IAEA 2007).

Hydrodynamics of liquid metals are of great importance as any reactor involving moving fluid would need to be understood. Bubbles rise in fluids and can have a variety of shapes (Park et al. 2017). However, the dense and opaque nature of liquid metals is challenging to understand, although some experimental (Keplinger et al. 2019) and modelling (Catalan & Rezaei 2020) work has been done in this area and will be discussed later in this paper.

Wettability of metals, particularly with glass as a reactor vessel, is a point of interest. Metals bead upon glass surfaces, and rarely form films along capillaries (Munera Parra et al. 2017). Intuitively, the surface tension of the metals plays a major role in this wettability, and surface character can be tuned by modifying surface composition (Palmer et al. 2019).

Liquid metals have successfully been used in supported heterogenous catalysts with research done on Supported Catalytically Active Liquid Metal Systems, aka SCALMS. These reactive systems tend to be designed and characterized like traditional supported catalysts, which may not take advantage of the bulk material properties of Liquid Metals. Every material property of liquid metal has a potential exploit in unit operation design, as outlined in Table 1 below.

Table 1 - Material Properties and potential exploits of Liquid Metals.

Property	Qualitative Value Bismuth (T = 400 C)	Potential Engineering Exploitations
Surface Tension	High 388 mJ/m^2 (Aqra and Ayyad 2010)	• Surface can be maintained as a boundary in chemical reactors, allowing for variable reactor volume while maintaining containment. • Low wettability allows for the metal to be contained by a porous substrate, such as glass frit, which allows for containment of metal while allowing gas exchange.
Density	High 9224 kg/m^3 (atomistry.com)	• Allows for floating of material on top to form an atomically flat surface, such as glass panes manufactured on molten metal baths. • Allows for organic components to be easily separated from metals via gravimetric force.
Magnetism	Highly Diamagnetic -16.6×10^{-5} (Young & Freedman 2004)	• Hydrodynamic flow is affected by the application of magnetic fields, which can be used to speed or slow bubble speeds. • Magnetic fields may be used for agitation or pumping, particularly if charged with ferrous particles. • May be susceptible to Induction heating, particularly if charged with ferrous particles.
Electrical Resistivity	High ~100 μΩ cm (Ginter et al. 1986)	• High resistivity indicates a susceptibility for efficient joule heating. • Running a current through liquid metal during reaction may result in excitation of electrons and higher activity, particularly for electron donor reactions.
Viscosity	Low 2.4E-03 Pa s (Aqra and Ayyad 2010)	• Low viscosity allows for little friction in pumping of material, and efficient agitation.
Thermal Conductivity	High 14.8 W/m K (atomistry.com)	• High conductivity allows for a more homogeneous reaction temperature, and efficient heat delivery to active sites.
Solubility	Various	• Gases, particularly Hydrogen (Zuraiqi et al. 2020) and Oxygen (Tyrer 1932) may be dissolved in liquid metal, allowing for separation from insoluble materials in-situ. • Solubility will be obfuscated by gas-metal reactions, particularly in the formation and reduction of metal oxides.

Please note that the material properties above are taken from sources studying Bismuth at near ambient pressures and temperature, and that at high temperatures and pressures can result in emergent of a more randomly ordered high temperature liquid, with changes of material properties including observable ferromagnetism (Shu et al. 2017). It is clear that the electronic and physical properties of metals in a liquid state at a high temperature may not be fully understood, and care should be taken in making assumptions about their behavior in catalytic analysis.

1.2.2 Catalytic Behaviors of Liquid Metals

Liquid metals have been explored as catalysts in a variety of reactions, referred to in this work as Liquid Metal Catalysts -- “LMCs”, and in cases where they are used as supported nanoparticles as Supported Catalytic Liquid Metal Systems – “SCALMS”.

The key point of this section is to demonstrate that that a variety of systems have been studied, to gather their key details in once place, and to note a few key observations. The reactions are broken into arbitrary categories where the chemistry and/or applications are similar in order to ease the reader in digesting this system and sorted by date to give a chronology of the depth of history involved in this field. An index of the work done in each area in Tables 2 through 5.

Methane Cracking and Hydrogen Production:

This is the biggest body of work, with a history tracing back to before WWII. Most of this research involves valorizing Methane into Hydrogen in an energy efficient way, and the liquid metal is uniquely able to handle carbon biproducts via carbon solubility and CO2 generation or as purified coke.

Table 2 - Methane Cracking and Hydrogen Production.

Reference	Metals and Catalysts	Reaction	Temperature	Reactor	Notes
Tyrer 1931	Metals: Fe, FeNi, FeMn	Methane -> Hydrogen + Dissolved Carbon Dissolved Carbon + Oxygen -> Carbon Dioxide	1200-1300 C	Conjoined Reaction Tanks	• Explicitly applicable to all Hydrocarbon gases • Mn is included to increase solubility of Carbon • Ni is included to catalyze the reaction
Oblad 1956	Al, Al/Ni	Hydrocarbon Gases ->	1200-2000 F	Bubble Column	• Methane and Propane degradation is experimentally investigated, and a variety of catalysts are described.
Steinberg 1996	Metals: Sn, Fe	Methane -> Carbon + Hydrogen	800-1000 C	Bubble Column	• Methane cracking is the first step in a two step process culminating in Methanol synthesis, the "Carnol Process" • Carbon Deposition on the molten metal is expected to act as an auto-catalyst.
Serban 2003	Metals: Pb, Sn Suspended Catalysts: Al2O3, NiMo, SiC	Methane or Natural Gas -> Hydrogen + Carbon	600-900 C	Bubble Column	• Uses heat from a nuclear reactor • Carbon analyzed with EDS and XRD
Gulevich 2008	Metals: Pb, Pb-Bi	Pb + H2O -> H2 + [O] + Pb CH4 + PbO -> CO + 2H2 + Pb CH4 + 2H2O -> CO2 + 4H2 CH4 -> C + 2H2	400-1000 C	Bubble Columns Discusses ancillary unit operations	• Focus on utilizing Heavy Liquid Metal Coolants from nuclear power plants. • Presents nice diagrams, calculations for feasibility, and thermodynamic data.

Table 2 – Continued

Plevan 2015	Sn	CH4 -> C + 2H2	750-900 C	Bubble Column	• Comparison of Methane cracking with molten metals with a non-catalytic PFR. • Computational and Experimental work is presented, and the experimental conversions do not match computational predictions.
Schultz 2015	Sn	CH4 -> C + 2H2	1100 C	Slug Flow Capillary Reactor	• Residence times above 10 seconds are required for high conversion.
Munera Parra 2017	Sn, GaInSn	CH4 -> C + 2H2	1300 C	Slug Flow Capillary Reactor	• Discussion of wettability of metal alloys and materials, and characterization of reactor system.
Upham 2017	Ni/Bi, Ni/Au, Ni/Pb, Ni/Ga, Ni/In, Ni/Sn, Cu/Sn, Ag, Pb, Ga, Sn, Bi, In	CH4 -> C + 2H2	950-1065 C	Bubble Column Reactor Stagnation Point Screening Reactor	• Ni/Bi at its solubility limit is shown to have their higher rate of hydrogen production. • DFT Discussion shows Pt atoms form dimer clusters.
Palmer 2019	Ni/Bi, Cu/Bi, Bi, Cu	CH4 -> C + 2H2	1000 – 1100 C	Stagnation point reactor.	• Copper and Bismuth shown to be non-catalytic, though mixtures of the metals are catalytic. • Analyzed surface concentrations via surface tension measurements.
Palmer 2020	Ni/In	CH4 + CO2 -> CO + H2	1000 C	Bubble Column Reactor Stagnation Point Reactor	• Stagnation point reactor is used for kinetic analysis. • Cycling of CO2 and CH4 is performed to make a redox catalytic cycle. • SEM and Raman Spectroscopy are used to evaluate the carbon formed in the reaction.

Degradation and Pyrolysis Reactions:

There are only a couple of reactions utilizing LMCs for pyrolysis in recent years, work notable works in plastic and Biomass Pyrolysis. Further back in history there have been a few applications, particularly in coal liquefaction.

Table 3 - Degradation and Pyrolysis Reactions

Reference	**Metals and Catalysts**	**Reaction**	**Temperature**	**Reactor**	**Notes**
Matsuura 1981	Zn, Cd, Ga, In, Tl, Bi, Sn, Bi	Coal -> Gas + Oil + Saturates	400 – 420 C	Batch Reactor	• A clear volcano shaped relation between activity and heat of metal oxidation is demonstrated. • Degradation never reaches 100% conversion of coal.
Komiyama 1982	Bi, Cd, Ga, In, Pb, Sn	Asphalt -> Gas + Saturates + Aromatics + Resins + Asphaltenes	250 – 366 C	Semi Batch Reactor	• Builds from work in coal liquification from the same research group. • Notably produces sulfurous gases including H_2S.
Matsuura 1983	Sn	H_2 + Coal -> Liquids + Gases	360 – 440 C	Batch Reactor	• Effects of agitation are investigated, as well as temperature and catalyst loading.
Nagel 1996	Sn, Sn/Zn, Sn/Cu/Zn	Organic Liquids -> Liquids + Gases Hexanes -> Ethylene	700-900 C	Vapor inlet swept over metal Vapor inlet bubbled through metal	• Molten Metal Technologies also included a variety of other patents for inletting organic compounds into molten metal baths. • Molten Metal Technologies is literally a textbook example of the rise and scandalous fall of a mismanaged technology scale-up [Hoffman et al. 1999].
Stelmachowski 2010	Sn/Pb	PP -> Oils + Gases PE -> Oils + Gases	360-430 C	Tube in a Tube	• Piston Driven Plastic into a reactor, with the assumption that the Tin and Lead are not catalyzing the reaction and are enhancing heat transfer. • It is not clear whether degradation occurs within contact of the molten metal, or in the headspace of the reactor.

Table 3 – Continued

Desai 2019	Ni/Ga, Sn	Hydrocarbon decomposition	600-900 C	Bubble Column with Regeneration	• Broad patent covering feeding organic liquids and gases into a liquid metal bath containing a catalyst and allows for separation of spent metal catalyst and regeneration in a continuous project.
Arenova 2019	Sn/Bi, Sn/Bi/Ni	Cellulose -> Organic Volatiles + Hydrocarbon Gases + Char + Tar Aspen Wood -> Organic Volatiles + Hydrocarbon Gases + Char + Tar	500-800 C	Semi-Batch Reactors	• Eutectic tin and bismuth are used to pyrolyze biomass. • Higher temperature reaction allows for more gaseous products.

Dehydrogenations

Many of these reactions are to dehydrogenate amines and alcohols, however, recent work with alkanes has been taken on using SCALMS.

Table 4 – Dehydrogenations

Reference	**Metals and Catalysts**	**Reaction**	**Temperature**	**Reactor**	**Notes**
Schwab 1961	Hg, Sn, Tl With Pt, Au, Ag, Cd, In, Sn, Pb, Sb, Bi	Formic Acid -> H2 + CO2	311 – 501 C	Flow over the Metal	• “Heterogeneous catalysis on liquid metal surfaces is not yet of any technical relevance, but is hoped to give some basic information…”
Kashiwadate 1971	Zn, Ga, In	Butanol -> Butyraldehyde	450 – 520 C	Bubble Column Reactor	• Butanol is fed at a very slow rate of ~0.09 mol/hr, vaporized in a preheater.
Miyamoto 1972	In	Butanol -> Butyraldehyde	450-550 C	Flow over Reactor	• Kinetic analysis shows decomposition at surface of In is the rate limiting step.
Takahashi 1978	Te, Te/Se	Cyclic Aromatic Hydrocarbons -> Dehydrogenated Cyclic Aromatic Hydrocarbons	500 - 580 C	Unknown	• It is assumed that toxic H2Se is formed in reaction, and Benzene is used a solvent for reactants. • This work is progress towards coal liquefication.
Honda 1980	K/In, K/Pb, Na/Pb	Butenes -> Butadienes	568 – 618 C	Bubble Column Reactor	• Butanes are mixed with helium prior to reaction, and products are analyzed via GC.
Ogino 1987	In, Tl, Ga, Zn	Alcohol Dehydrogenation	550-700 C	Unknown	• Incorporated into a larger study on alcohol dehydrogenation—see Fig. 2 in chapter 3 of Catalysis and Surface Properties of Liquid Metals and Alloys (Ogino 1987).
Okano 1971	Zn, In, Tl, Ga, Pb, Cd, Bi	n-Butylamine -> n-butyronitrile + H2	440 – 500 C	Bubble Column Reactor	• Liquid product analysis is performed via IR.
Taccardi 2017	PdGa/AlO$_x$	Butane -> Butene	445 C	Supported Liquid Metals	• Nice results in coking of catalyst compared to conventional catalysts.

Table 4 – Continued

Kettner 2019	PdGa/AlO_x	CO Adsorption onto catalyst	310-446 K	Supported Liquid Metals	• Model system with CO adsorptions onto GaPd SCALMS. • Synthesis procedure, characterization of catalysts, and DFT Analysis of Adsorption is investigated
Raman 2019	Ga_nRh/AlO_x	Propane -> Propene	100 – 650 C	Supported Liquid Metals	• In Situ exploration of Ga/Rh nanoparticles with TEM. • DFT exploration of Rh atoms in a gallium surface.
Bauer 2019	$Ga_{37}Pt/Al_2O_3$	Propane -> Propene	200-450 C	Supported Liquid Metal catalysts	• In situ Operando DRIFT analysis of reaction. • AIMD simulations of Pt atoms in Ga nanoparticles.

Other Reactions

This is an catchall category covering the remaining studies on LMCs. Several of these studies are focused on developing a fundamental understanding of Liquid Metal's participation in reactions and characterization of the surfaces of LMCs

Table 5 - Other Reactions

Reference	**Metals and Catalysts**	**Reaction**	**Temperature**	**Reactor**	**Notes**
Bergstrom and Carson 1941	Na, Li	H2 + Alkenes -> Alkanes	137 – 280 C	Batch Reactor	• A variety of unsaturated compounds are investigated with a variety of metals. Calcium investigated is not in liquid form.
Friedman 1971	Li, Na, Na/K, Na/Rb, Na/Cs	H2 + Alkenes -> Alkanes	200-350 C	Rocking Autoclave Reactor	• A variety of polycyclic aromatic and polyaryl hydrocarbons are investigated.
Miyamoto 1976	In	Ethanol + 2-Butanone -> Acetaldehyde + Butanol Ethanol + cyclopentanone -> Cyclopentanol + Acetaldehyde	405 – 460 C	Microreactor	• A variety of hydrogen transfer, including isotope effects, are investigated.
Balooch 1984	In, Pb	Cl_2 + Pb -> $PbCl_2$	300-900 K	Molecular Beam-Mass Spec	• Kinetic investigation of adsorption of Cl onto the surface of Pb and In
Sun 2018	Rh/GaInSn (supported)	Olefin + CO/H2 -> Aldehydes	100 C	SLMCs	• Focusing on low temperature reactions with a variety of Olefin reactants.

It is notable that the research on LMCs spans nearly a century, and there is not a single reference to a successful scaled up operation of a reaction involving LMCs. This indicates that there have been shortcoming of the technology, or lack of appropriate use-case, that made them insolvent for industrial use. Several notable challenges for working with LMCs are noted in the conclusion section of this work.

Additionally, the breadth of metals used is quite large, and certain metals act as catalysts for some reactions and not others. This indicates that an application-first approach to studying LMCs (such as looking for a method of upcycling plastic waste) would benefit from a wide screening of potential LMCs to evaluate whether or not the efficacy of LMCs in that application.

1.2.3 Characterization of LMCs

Characterizing liquid metals is extremely difficult, as the liquid nature of the catalyst is sensitive and volatile. Few methods of in-situ characterization have been developed to characterize bulk liquid metals, except for thermogravimetry, diffuse reflectance infrared Fourier transform spectroscopy (DRIFTS) (Bauer et al. 2019), and high-resolution thermogravimetric analysis coupled with mass spectrometry (HRTGA-MS) (Wolf et al. 2020). Surface analysis has been performed via Molecular Beam analysis (Balooch et al. 1984) and analysis of surface tension (Palmer et al. 2019). It appears to be a broad assumption that liquid metal alloys are well dispersed.

Due to the phase change upon quenching of liquid metal, any characterization of catalyst ex situ is of questionable value for dispersion analysis and activity measurements, though could be of value in closing mass balances and establishing bulk concentrations.

1.2.4 Reactors using LMCs

There are a variety of reactors that have been developed, with in-line references in Tables 2 through 5 above, and an index of images is reproduced below. Most of the reactors utilize gas-phase reactants, and the only that handle solid or liquid reactants are non-continuous, with the most recent being a pre-heated reactor for biomass pyrolysis (Arenova et al. 2017). Another simple way to perform solid phase reactions is to use TGA and Pyrolizers in a semi-batch fashion, however preparation of catalysts in these instruments is unlikely to be possible.

For gas-phase, heterogenous reactions the use of reactors that flow gas over a metal surface allows for good control of surface contact geometry, as well as a providing a consistent surface to observe. The downside of that reactor configuration is a small reaction interface, particularly as the surface of liquid metals is considered atomically smooth. To achieve a larger surface area over which to react then bubble columns can be used. Conceptually, this allows for continuous re-formation of a liquid metal surface on the walls of the bubbles—however it may be difficult to control, or even measure, the hydrodynamics of reactant flow. A couple groups have tried to overcome these challenges by using capillary reactors, which ended up not being successful due to the low wettability of metal on glass (Munerra Parra et al. 2017), and by designing a reverse bubble column where liquid metal is sprayed through a chamber filled with reaction gas (Gullevich et al. 2008).

Bubble Column Reactors

Tyrer 1931 – Patent 1803221

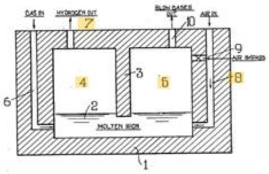

Ogino 1987

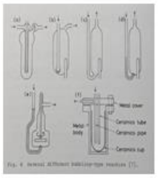

Kashiwadate 1971

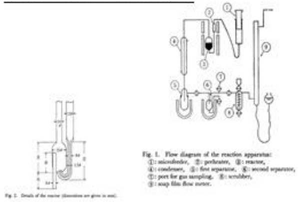

Fig. 1. Flow diagram of the reaction apparatus:
①: microfeeder, ②: preheater, ③: reactor,
④: condenser, ⑤: first separator, ⑥: second separator,
⑦: port for gas sampling, ⑧: scrubber,
⑨: soap film flow meter.

MMT Patent 5543558

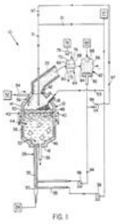

Servan 2003

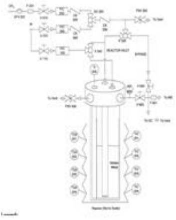

Gulevich 2008

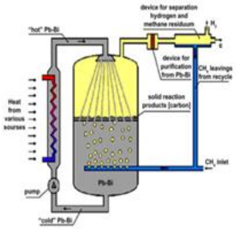

Upham 2017 & Palmer 2020

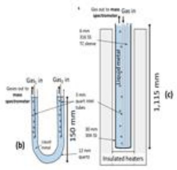

Palo Alto – Patent 019/0055173 A1

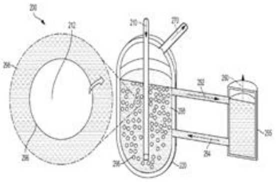

Gas Flown over Pool of Metal

Miyamoto 1972

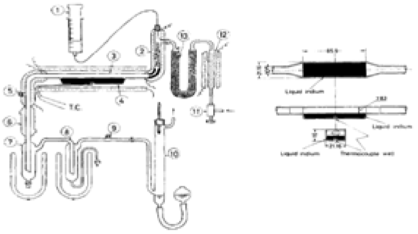

Schwab 1976

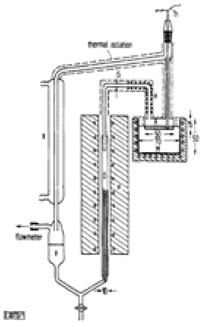

Upham 2017 & Palmer 2019 & Palmer 2020

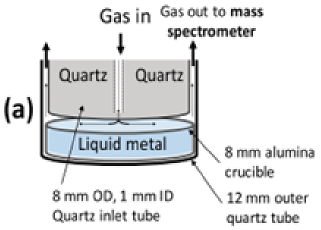

Batch Reactors

Matsuura 1982

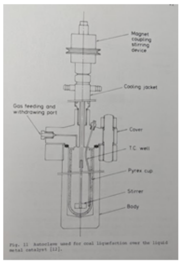

Friedman 1971

[Rocking Autoclave]

Capillary Reactors

Schultz 2015

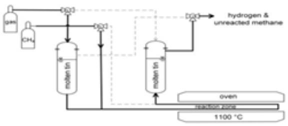

Munera Parra 2017

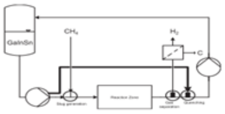

Fig. 3 – New experimental set-up.

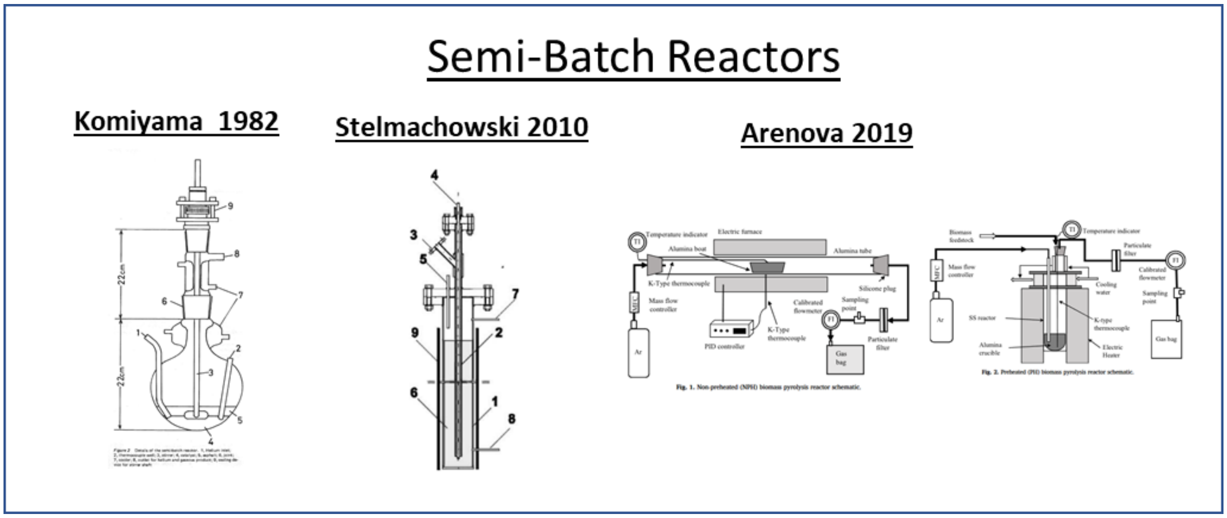

Figure 6 – Index of Reactors using LMCs, by functional category. Please see references for detailed information.

2.0 Research Objectives, Results, Discussion

The ultimate research objective of this project is to evaluate the efficacy of liquid metal catalysts in polyolefin waste upcycling. As discussed in the introductory sections, our understanding of liquid metal catalysts is incomplete, and the mechanisms of polyolefin pyrolysis are complicated. In order to produce meaningful and reproducible results, the objectives of this thesis is to make incremental progress in studying polymer pyrolysis, and perform foundational research on liquid metals as catalysts. Specifically, there are three objectives that will be discussed in detail:

1. Design and construct a reactor for screening liquid metal catalysts
2. Develop a method of experimentation to screen the catalysts
3. Investigate a methods of characterizing the catalysts

These objectives are inherently codependent. An experimental method cannot be developed without a reactor for performing experiments, and inherently requires characterization methods to verify the composition of the catalyst. Likewise, the characterization of a catalyst will require an experimental method that identifies key characteristics of the catalyst, and a reactor that permits catalyst recovery. While these objectives will be discussed in series, please note that they were developed in parallel.

2.1 Develop a reactor for screening Liquid Metal Catalysts

2.1.1 Design Methodology

The screening reactions consist of pyrolysis of off-the-shelf polyolefins, and ethane dehydrogenation. The same reactor does not necessarily need to be used for both of these reactions, though it would be useful to use reactors with as many interchangeable parts as possible. Therefore, the reactors were designed to be useful in a reactions involving liquid metal catalysts generally, not just ethane dehydrogenation and plastic pyrolysis.

Another point of consideration in reactor design is the unknown nature of what will be important variables in liquid metal catalysis. Precise control of reaction temperature, pressure, catalyst composition, and reactant flow rates are known variables, though there may be other factors that are important to the reaction system that are as of now unknown. Therefore, the reactors are designed to be modular in nature to allow for adjustments to be made as the reaction system becomes further understood.

With these concepts in mind, a summary of the key design parameters are outlined below:

Table 6 – LMC Reactor Design Criteria.

Must have safety procedures for reactor failure and loss of containment.	**LMC reactors are hazardous even in the absence of reactive materials. All experiments involving LMC must be conducted within a fume hood and have a catch-basin for broken glass and hot metal.** In two years of reactor development and experiments with LMCs, there were a series of critical failures: • Reactors shatter mid-reaction due to thermal expansion. • Unintended combustion occurs due to oxygen penetration into the system. • Reactors and/or piping fail rubber seals due to clogging with quenched metal exiting the heated zone.
Must minimize use of metals in reaction zone.	• Metal expands while being heated in the solid phase, and tends to contract upon melting, and the metal may expand or contract while heated in the liquid phase. All of this is to say that catalyst geometry, and therefore contact area, may change at different temperatures, and has repeatedly shatter glass reactors if heated or cooled too quickly. • If less LMC is used, it can be easier to recover from the reactor—large pieces are hard to extract and tend to appear physically heterogenous. • If less LMC is used, then preparing the catalyst can occur more quickly—for example, if reducing gas is used to remove surface oxides, that can be done much more quickly if there is less metal to reduce.
Must be cheap enough to dispose of after each use, or otherwise be cleanable.	• Glass reactors often break due to aforementioned thermal expansion challenges. • Plastic pyrolysis can leave seemingly uncleanable organic residues, and metal can leave metallic deposits that are likewise difficult to clean. • Upon cooling, LMC can be welded to the reactor, which often requires shattering the reactor to recover.
Must allow for excellent sealing from the room atmosphere.	• LMCs are particularly sensitive to oxidation at high temperature, and even a trace amount of oxidizing agent can allow for metal oxide contamination.

2.1.2 Reactor Configurations

There were several reactors utilized for screening reactions, some of which were entirely unsuccessful though nevertheless provided experience that contributed to future reactor and experimental design. This section outlines the design and key takeaways from notable reactor configurations, and pictures to give a suggestion of the physical design of the reactors; in literature pyrolysis results vary wildly and a contributing factor to that is differences in reactor design—the impetus for this section is to be as clear as possible about how these reactors are designed and operated.

TGA

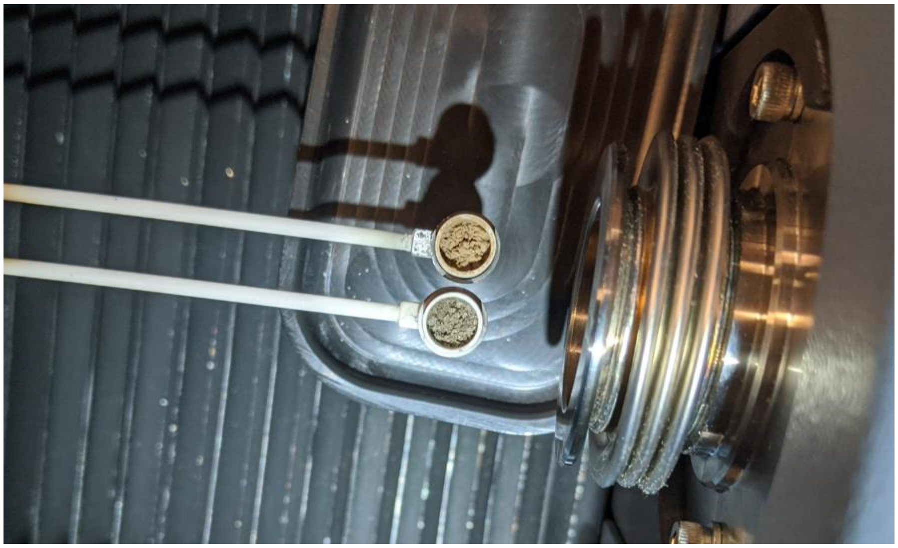

Figure 7 – TGA Cups loaded with PE mixed with Bismuth and ZSM5 (bottom), and PE mixed with ZSM5 (top)

Initial tests on LMCs with PO pyrolysis involved the use of a Thermal instruments SDT Q600 to evaluate the degradation of plastics, where the weight loss of plastics indicates conversion. This is a method used in solid state pyrolysis, typically used in conjunction with an isoconversional method where the kinetic triplet is unknown (Peterson et al. 2001). The objective of these experiments, which will be discussed later in this thesis, is to determine whether or not liquid metals demonstrate a catalytic effect.

The plastic and catalyst are loaded into an alumina cup and stirred with a pair of tweezers until visually mixed. Some powdered metals were used, however, sometimes it appeared that the metals were oxidized or otherwise contaminated with a dull surface and did not appear to bead in the pan upon the completion of the reaction.

Ultimately, the TGA was useful in replicating studies in literature regarding plastic degradation (Peterson et al. 2001, Das et al. 2017, Marcilla et al. 2004), however, the contacting between the LMC and plastic may not be consistent, particularly due to visual inspections showing noticeably different residue after each experiment. Additionally, collection of products is proved infeasable in this reaction system due to the high flow of inert gas, small amount of plastic pyrolyzed, and non-hermetically sealed DSC outlet.

One major source of concern is that the mass of metal in the system at higher temperatures, which indicates vaporization of the catalyst. This is concerning due to loss of control of the catalyst composition and loading, as well as risk of damage to the machine.

The DSC function of the SDT is useful in determining the homogeneity of the metal, as well as contaminations of oxides. It may also be used to evaluate coking on the metal via TPO samples, as well as metal composition via specific heat measurements.

Pipe Reactor

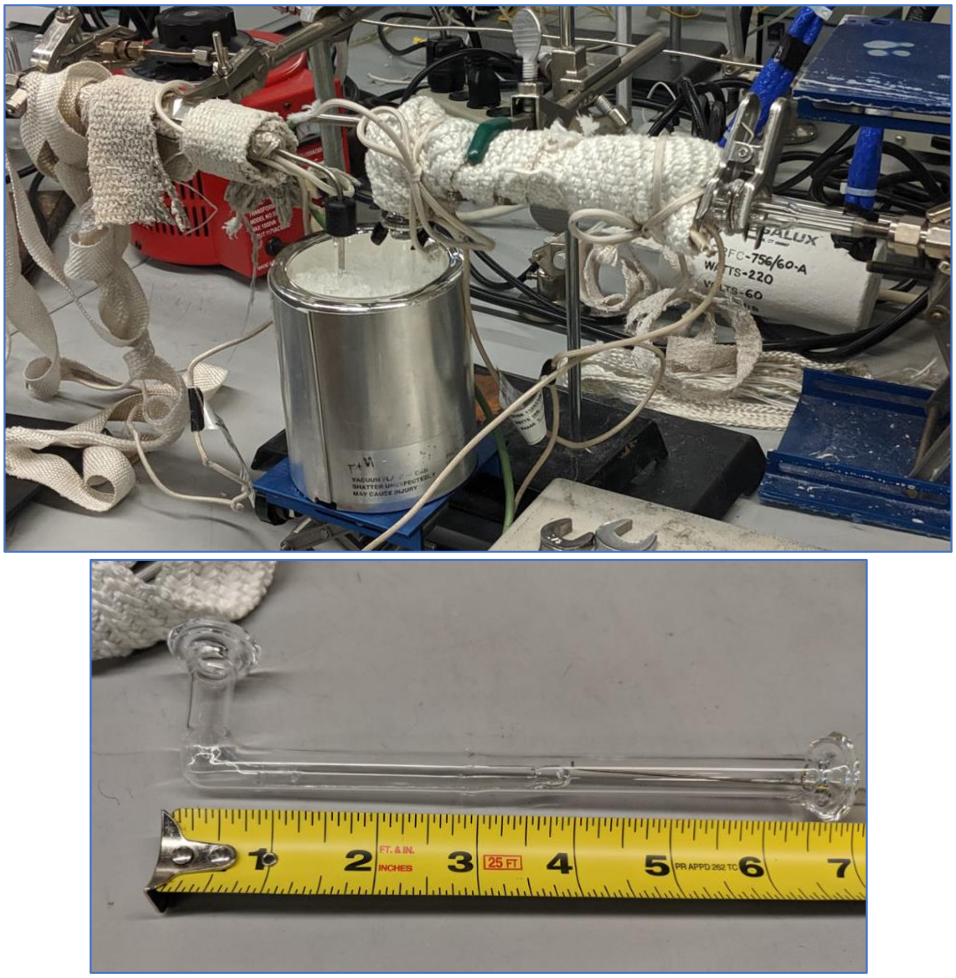

Figure 8 – Experimental setup of Pipe Reactor (top), and pipe reactor (bottom).

A reactor was created with an alumina TGA pan placed in a quartz glass tube via a quartz sled, which is like literature examples of LMC Biomass Pyrolysis (Arranova 2019). The quartz tube is then wrapped with heating tape and insulation, and then a purge gas is flown through the reactor, and over the metal.

By design, the reactor will operate in a semi-batch fashion, where it is heated to a set point of 420 C, and the PE and PP will be pyrolyzed, and exit the tube as gas. The gas will enter a cold trap with ice water, which would condense any condensable species, and the remainder of the gas would flow through to a Mass Spec and exhaust.

The reactor failed to produce more than trace amounts of gases, and almost no condensation products were found in the cold trap—those that were found were extremely waxy, and clung to the outlet of the reactor itself, indicating that they condensed above room temperature. Upon visual inspection it appeared that the plastic bubbled during reaction, and that caused it to exit the section of the reactor that was up to temperature, so it was never fully pyrolyzed. This phenomenon of plastic overflowing via bubbling or expansion during pyrolysis has been noticed in other plastic pyrolysis systems, and during reactions plastic should verified to stay in the reaction zone (Luff et al. 1968). Caps can be used to help contain bubbling and having a slow temperature ramp can help minimize any bubbling. Subsequent reactor designs will either incorporate bubbling into the design itself, or to create the reaction zone in such a way that bubbling doesn't allow for the plastic to leave the reaction zone.

The chief challenges with this reactor are twofold. First: there is a small amount of plastic, as only so much as can fit in a TGA pan. This causes some of the same problems seen within the TGA itself, specifically: even in perfect reaction conditions so little pyrolysis products are produced that is difficult to detect them. Secondly: the temperature profile along the reactor is not perfectly consistent. A slight misplacement of the alumina pan, or a slightly different heating tape wrapping, or the escape of the plastic out of the pan itself, could result in significantly different reaction temperature.

On a safety note, O-rings were used to seal the glass pieces together, and once the seal was imperfect allowing oxygen to enter the reactor. This caused combustion of the plastics, which is a safety hazard and caused damage to the reactor. It is critical to ensure that all seals are very strong in these reaction systems due to the sensitivity of pyrolysis reactions to oxygen, as well as the LMC's themselves.

Vial Reactor

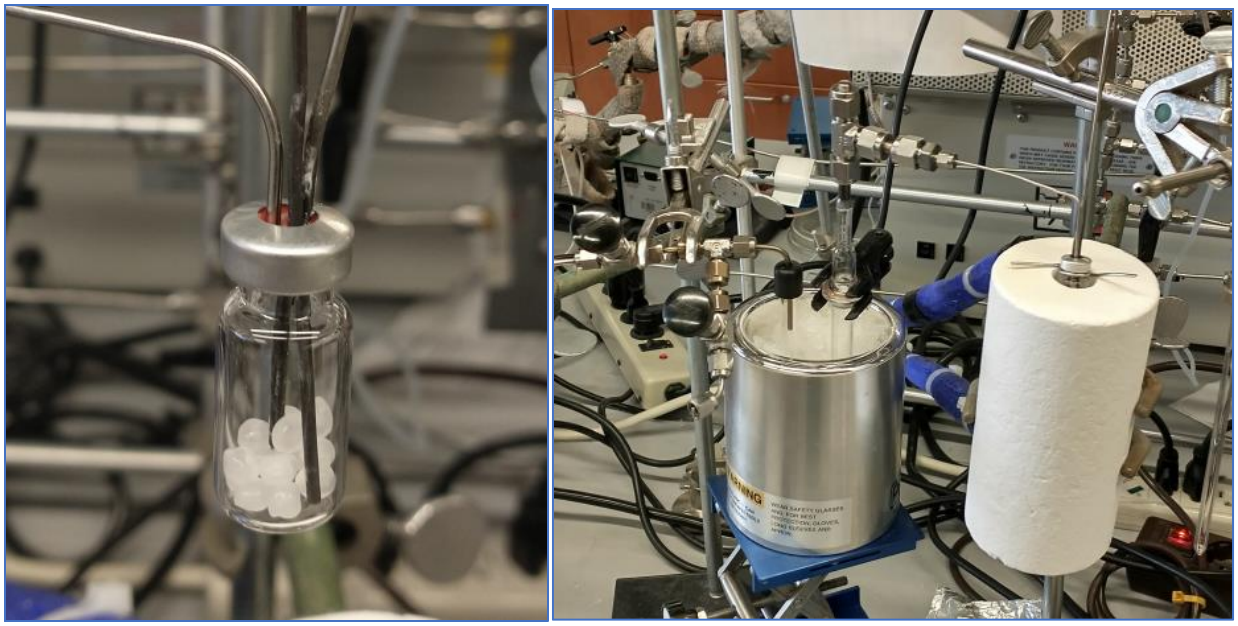

Figure 9 – Vial Reactor with gas inlet, gas outlet, and thermocouple (left), Vial Reactor configuration (right). Thermostating heat tape for gas outlet is not shown in these pictures, which was used to prevent condensation prior to cold trap.

The next generation of reactor is a Vial reactor, i.e.: a simple borosilicate vial with a PTFE septum, that consists of cheap materials so it can be discarded after each use. It can hold over 10x the amount of plastic as the alumina cup in previous reactors, and any challenges with reactor contamination are a non-concern as it does not need to be cleaned. The reactor can be operated in a semi-batch mode, where plastic and catalysts are mixed into the reactor and heated up to temperature, and the product gas is purged from the system, sent through a cold trap, and then through a Mass Spec. Conceptually, it could also be operated in a continuously, via pumping molten plastic into the vial through a 1/16” pipe with a sharpened point.

The heat for this reactor is provided by a ceramic furnace, which provides more control over temperature and less opportunity for user-error than previous heating-tape solutions, as the reactor can simply be slotted into the furnace directly.

This reactor worked well when there were no leaks, however, it was found that most all experimental runs produced leaks, due to the fragility of the PTFE lid. Specifically, the PTFE is rated to go up to about 380 C, and the pyrolysis reaction is occurring at about 420 C. Although the lid is far away from the reaction zone, the prolonged exposure to high temperature, with three pipes running through the septa, appears to allow for much air to enter the system. Some combustion was witnessed, and the mass spec signals measured were not at all consistent.

From a safety perspective, one time there was a leak, and a floral smell was noticed around the reactor, and it became clear that this reaction system should operate within a fume hood to ensure that any known or unknown toxic systems are handled appropriately. Because of the concerns with containment of the system, all future work with LMC is done in a fume hood from this point on with few exceptions.

Ultimately, this reactor was abandoned because most runs were not replicable, but much of the design pieces of this reactor were incorporated into the Quartz test tube.

Quartz Test Tube

Figure 10 – Top Left: ½” Diameter Test Tube Reactor, filled with metal ingots that will melt into a 1” column. Top Right: Test Tube Reactor configuration, for EDH. Bottom Left: 1” of LMC in a bubble-through configuration, and sputtered metal above reaction zone. Bottom right: ¼” of LMC used for melting plastic pellets dropped onto LMC, with a quartz sheath on the thermocouple, and a gas inlet to purge the system.

The quartz test tube reactor is the logical next step from the vial reactor, it operates in precisely the same way, but is made of more resilient materials of quartz and steel, with the only polymer component being an O-Ring around a vacuum junction to keep the quartz-steel seal hermetic, which is well away from the reaction zone and has never deteriorated. The heating for this tube is provided by a stand. The product outflow could line be achieved via an inserted 1/16" tube or using a Swagelok junction with a T-Joint.

This reactor was first used to characterize EDH reactions, which were critical in testing and refining this reactor concept and paving the way for polymer systems in the future. The EDH reactions occur above 700 C, so the entire reactor system had to be made of materials stable above 800 C, specifically quartz and steel.

The same furnace is used for this reactor as with the vial reactor, however the depth that the reactor is inserted could be varied, depending on the desired conditions of the experiment. A thermocouple inside the reactor is often included, which is sealed to the Swagelok via a Supeltex ferrule. 1/16" holes were drilled to allow for multiple lines into the reactor for gas inflow, reactant inflow, gas outflows, and thermocouples. In a couple of occasions, the thermocouple inserted appeared to melt into the metal bath (although upon later inspection the temperature of the reactor may have been incidentally above 1000 C). To protect the thermocouple from corrosion, and to remove any catalytic activity on the surface of the TC, a quartz sheath was developed. This quartz sheath will decrease the sensitivity of the thermocouple to temperature changes in the reaction zone, and temperature verification experiments were be performed to verify that the steady state temperature is reported by both the quartz sheathed and non-quartz sheathed thermocouple.

There were three configurations used with a quartz tube

1. A ¼" test tube, sealed it to a vacuum Swagelok fitting, and inserted with a 1/16" steel pipe, which was used to bubble purge and/or reaction gas through the reactor loaded with about 1" of LMC.

No bubbling is seen, however, a channel of gas appeared along the side of the reactor, and there was no observed pressure buildup.

2. A ½” test tube, sealed it to a vacuum Swagelok fitting, and inserted a thermocouple and a 1/16” gas inlet line through which was used to bubble purge and reaction gas through about 1” of LMC, as shown in Figure 11 on the Bottom Left. This worked well, and bubbling was seen with no channeling through the metal, and at flow rates above 60 SCCM which resulted in sputtering of metal out of the reaction zone. Notably, the inner 1/16” gas inlet was often clogged with metal upon re-use, or the entire bulk of metal welded the bottom of the reactor together. This challenge was overcome via taking off the reactor using temperature resistant gloves, so that the metal was always liquid while it was in contact with the gas inlet.
3. A 1/2” test tube to test plastic degradation by loading it with ¼” of LMC, and then dropping pellets down on the metal, as shown in Figure 11 on the Bottom Right. The product gases were flowed out of the reactor and into a cold trap, precisely as was done with the vial reactor. The dropping of pellets was fairly successful and will be talked about in more detail in the solids feeding section of this thesis. Notably, sometimes the pellets would melt slightly en-route to the reaction zone, and cling to the much cooler upper-reactor, thermocouple, or purge line and never pyrolyze.

From a safety perspective there were a couple instances where the cooling or heating metal shattered the reactor and loss of containment. The cause is somewhat unclear, and likely has to do with thermal expansion and/or phase change behavior building up pressure—it could also be thermal stress on the quartz upon cooling. This hazard was mitigated by placing a sand trap beneath the reactor and furnace to catch any falling metal.

These reactors have been useful in a variety of experiments, and their production is cheap enough to continue. A change was made to reduce the length of the tube from 6” to 4” to reduce the amount of headspace and more quickly cool the product to prevent post-reaction degradation. One of the benefits of this tube reactor is that it much easier to see what is going on inside of the reactor at any given point than previous reactor concepts.

Quartz Stagnation Point

Figure 11 – Stagnation point reactor. Left: Prior to reaction the metal is unmelted, and the insert is raised. Center: During reaction, the metal forms a beading pool of liquid, and the insert is lowered to create a 1/16” inch gap. The thermocouple undergoes thermal expansion, and at point of insert should be halfway through the gap, not touching the metal. Right: Schematic of the cross section of the reactor at its CenterPoint, with glass in blue, LMC in grey, and arrows indicating the gas flow direction.

Most literature on LMC use setups where reaction gas is able to flow over the LMC, which has the benefit of having an observable and well-defined catalytic surface (vs. a bubble-column reactor where hydrodynamic effects come into play). In a similar setup to that used by UCSB (Upham 2017), this reactor includes a design an insert that fits within the existing glass tubes and would deliver gas into the center of the catalyst so that it would flow out along the gas and exit via the annulus between the test tube reactor and insert. The inner tube was roughly 1/12” in inner diameter near the base and can fit a fine thermocouple that would allow for gas to be directed to the center of the LMC while monitoring the temperature at or near the surface of the LMC. To fit the insert into the hermetically sealed Swagelok insert, the piece was sized to be ¼” in OD so it would be sealed by conventional Swagelok vacuum fittings, and then worked with the machine shop to bore the center of the fittings to be ¼” so the insert could fit all the way through.

The insert is big enough to fit a 1/16” feed tube, so independently of the gas flow, another hydrocarbon feed could be inserted, so that reactions other than EDH could be monitored (i.e.: Pentadecane degradation). In theory, the purge gas would keep the feed tube cooled so that any volatile feeds do not evaporate before they reach the reaction zone.

Due to the fine inner diameter of the insert, a solid feed was unable to be dropped into the reactor in this situation, however, the quartz tube with purge gas and dropping of a pellet is designed to give a similar contact of reactant to LMC and gas flow path.

Fixed Frit Reactor

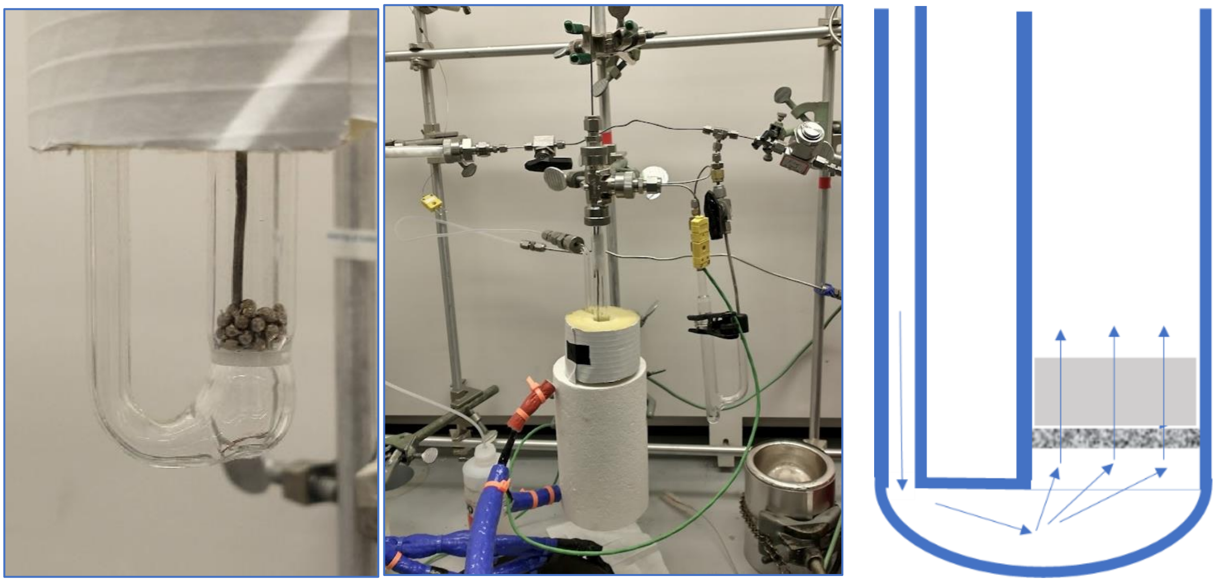

Figure 12 - Fixed Frit Quartz U-Tube. Left: the metal pellets sit upon a quartz glass frit. Center: Configuration of Fritted U-Tube Reactor. Right: Schematic of the reactor, with glass in blue, frit in textured grey, LMC in grey, and arrows indicating gas flow direction.

The latest design of reactor is unlike any seen in literature, and involves placing the LMC is suspended within a quartz U-Tube via a quartz glass frit. This allows for gas to bubble through the metal, and the quartz frit acts as a sparger to disperse the reaction gas or purge gas. This configuration is made possible because the LMC cannot penetrate the glass frit’s pores due to its poor wettability and capillary pressure (Schultz 2015). The penetration of the LMC does not appear to be sensitive to the coarseness of the frit—even the most course frit does not allow the LMC to penetrate within it.

Suspending the LMC within the U-Tube allows for purge and reaction gases to pass through the fit and through the LMC—which allows for good control over the bubbling through the LMC, and—due to the removal of feed tubes above the LMC—allows for a much easier drop of solid reactants into the LMC. It is assumed that the gas is well dispersed as it passes through the frit, and if this assumption is not correct then the hydrodynamics of the system may operate differently than designed—for instance, in an extreme case gas could channel through the metal instead of bubbling. Care should be taken in observing how the gas passes through the frit.

Upon the initial tests it appears that the frit can be contaminated by coke and metal after even a couple hours of use, and cleaning of the reactor (or replacement of the reactor) is required. Cleaning with 5 M nitric acid removes most discoloration, however hydrodynamic behavior of the gas passing through the metal does not match what was seen at initial use; namely, the gas doesn’t bubble through the metal but flows around it, suggesting that the center most pores are clogged.

This reactor could be optimized by using a thin and course of a frit, and to place the temperature probe for the controller below the LMC. If a sufficiently clean metal were achieved, then it might be cost effective to transition to a straight tube reactor with a frit and use a U-Tube bend in steel below the glass in order to catch any metal or coke that penetrates the frit.

This reactor may be able to be used to perform polyolefin cracking reactions with small alkane chains, such as pentadecane. A method of vaporizing the alkanes and controlling their introduction will be required to ensure they can pass through the frit.

2.1.3 Reactant Feeding

A challenge in this experimental work has been the handling of plastic as reactants. Obviously, one of the benefits of characterizing the LMC systems with gaseous reactions is that handling gas reactants sidesteps many of these challenges and can be contacted with metal via flowing over a surface or bubbling through with relative ease.

These are the reactant handling methods pursued in this work:

Solution

Perhaps the simplest way to transport the plastic is to dissolve it in a solvent so it can be pumped as an inviscid liquid. Unfortunately, polyolefins are only soluble at high temperatures in xylenes, and these solvents will likely affect the reaction conditions, product spectrum, and would not scale well. This was ruled out, however, other research specifically looks at dissolution-reprecipitation method for upcycling plastics, and that is sufficient to produce polymers similar to virgin stock (Achillias 2007, Achillias 2009). Dissolving plastics into petrochemical stocks like Naphtha and feeding into FCC systems in extant petrochemical plants is another way that dissolving plastics can be leveraged, however, the fraction of plastics is low compared to the fraction of conventional FCC feeds (Lopez 2017).

Melt: Syringe Pump

Melting the plastic would be ideal as if they could be pumped as a liquid into a reaction system continuously. This was attempted in the lab using a steel syringe and a positive displacement syringe pump, the same pump shown in Figure 13 below. Unfortunately, even pumping through a 6” long ¼” OD pipe was not able to be achieved—the temperature control of the system was unable to be maintained, and either nothing was pumped out, or a smoking waxy black sludge was ejected. Perhaps solid-blocks were formed in the pipe and syringe at cold points, and when the temperature was increased past 200 C the plastic began to combust within the pipe and syringe.

Melt: Screw Feeder/Rotary Kiln

It is expected that a twin-screw feeder could take in a solid pellet feed, which would melt along a screw feeder as has been demonstrated in extant literature (Sasse and Emig 1998). The operation of such a twin screw feeder would involve a two screws feeding plastic pellets along a channel, which would then drop the pellets into the reaction zone. It would likely need to be jacketed with cold water to prevent plastic from sticking to the channel wall. Such screw feeders have a minimum size that might make them acceptable for pilot plant use, but not acceptable for quick lab screening reactions. Also, per discussions with Orbetron technical services, such screw feeders can handle no back-pressure, and may be difficult to hermetically seal.

A screw fed system has not yet been constructed due to its implacability at a small scale, and such feeding systems are expected to be more feasible at a pilot scale.

Melt: Injection Molder

In discussion with Braskem about this project it sounded like the simplest thing to do would be to melt the plastic waste, and load it into an injection molder, which could inject it into the liquid metal bath at a high pressure. This seems like an excellent way forward, however, there will likely be some reactant degradation and crosslinking during the melt and injection process which might skew kinetic analysis.

Liquid Substitutes

To avoid the challenges with pumping viscous melts, one could use a liquid substitute like pentadecane or polyisobutylene which are easier to maintain in their liquid states. This can simplify the reaction setup which would be advantageous for some screening reactions. Pumping pentadecane was achieved without challenges using a plastic syringe and a positive displacement syringe pump, which worked well with the existing test tube setup, as the liquid could be injected or dripped into the system via a 1/16” pipe. One concern with this is that the pentadecane was vaporizing prior to leaving the reactor, which would mean the system is operating with a gas-injection inlet. Polyisobutylene is unlikely to vaporize without pyrolyzing and may be the best liquid substitute for PE or PP pyrolysis.

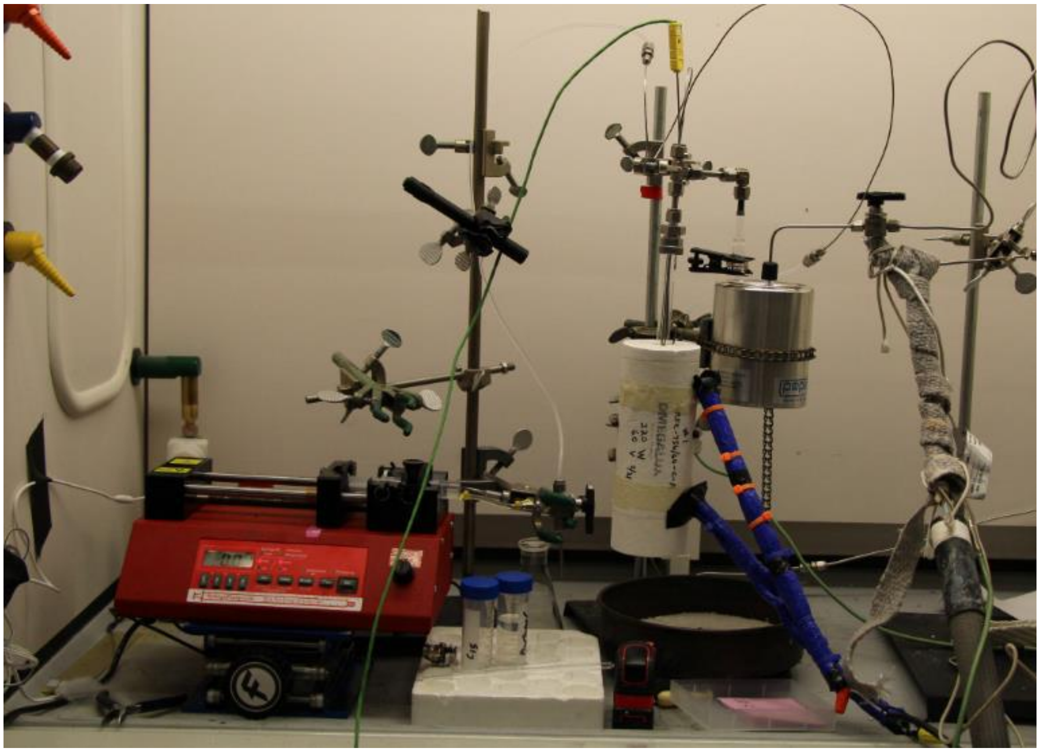

Figure 13 – Syringe pump fed Pentadecane into Test-tube reactor.

Solids

The plastics could be handled directly as solids if they can be controllable as they are fed into the reactor. This has the benefit of not allowing for the plastic to be degraded or crosslinked during a melting process and may scale well as it eliminates the need for melting operations. The plastic could be shredded or pelletized and fed into a reactor by dropping it into the top, and perhaps the LMC could be agitated to improve the contact, so the plastic doesn't merely float on top of the LMC. Additionally, it could be fed as a powder and blown into the reactor. It should be noted that plastic powders (and to a lesser extent pellet) will readily stick to any surfaces that are near their melting point, which can present challenges for handling solid plastic materials. Manual feeding of solid plastics can be achieved via a piston or dropping of plastic directly and metering out of solid feeds can be automated via use of a screw feeder, twin screw feeder, or disc feeder.

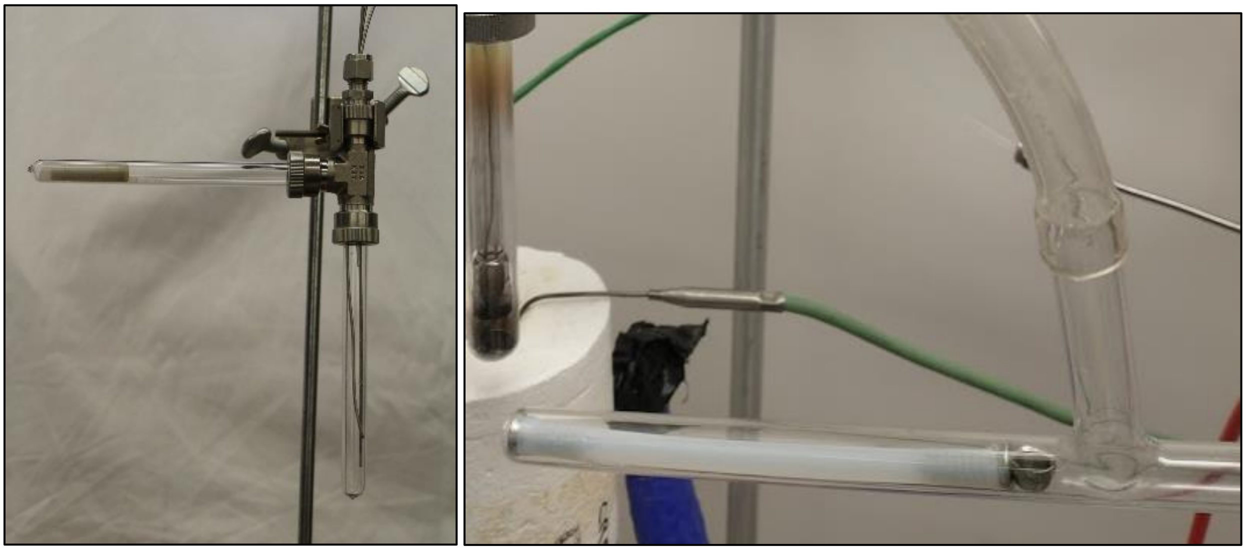

Figure 14 – Magnetically actuated piston for dropping plastic pellets. Left: Single Drop. Right: Reloadable piston.

2.1.4 Reactor Hydrodynamics

When reaction gas is bubbled through a LMC column it behaves as a bubble column with unique properties. A key characteristic of the reactor is the residence time, which is dictated by how quickly bubbles rise through the metal—and being able to measure the residence time is a required if any kinetic analysis is to be made. The opacity of LMC makes it impossible to see at-a-glance how gas bubbles or channels through such a reactor, and whether any hydrodynamic behavior is coming into play such.

Therefore, a CFD model would be useful to help understand the behavior of a LMC bubble column. The hydrodynamics of this system is particularly interested as the velocity of the rising bubble, and bubble geometry will dictate contact area between the reactant and catalyst, as well as the residence time. Two preliminary models are created and discussed, the first being performed of a single bubble rising via COMSOL simulation, and a second model of continuous flow is modeled in ANSYS Fluent.

COMSOL Methods and Results

A preliminary model in COMSOL was used to evaluate the rise time a single sphere of ethylene with a radius of 2 cm, in in a column of liquid bismuth 2 meters high in three dimensions. This model assumes incompressible fluids, laminar flow throughout, constant viscosities, uniform and constant surface tension, isothermicity, radial symmetry and no reaction. The governing equations are continuity, Navier stokes Equation, and a level-set mechanism for separating the gas and liquid phases, with an assumption that the phases are immiscible. These are outlined in Equations 1.3 through 1.8 below, and a snapshot of the model is shown in Figure 15:

Continuity:

$$\rho\nabla * \boldsymbol{u} = \boldsymbol{0} \qquad \text{Eq. 1. 3}$$

Momentum Equation:

$$\left(\frac{\partial \boldsymbol{u}}{\partial \mathrm{t}} + \boldsymbol{u} * \nabla \boldsymbol{u}\right) = -\nabla \mathrm{p} + \tilde{\mathrm{N}} * \left(\nabla \boldsymbol{u} + \boldsymbol{u}^{\mathrm{T}}\right) + \rho \boldsymbol{g} + F_{\mathrm{st}} \qquad \text{Eq. 1. 4}$$

$$F_{st} = \ \nabla * [\sigma\{\mathrm{I} + (-\boldsymbol{n}\boldsymbol{n}^{T})\}\delta] \qquad \text{Eq. 1.5}$$

Level Set Equations:

$$\delta = 6|\nabla\Phi(1-\Phi)||\nabla\Phi| \qquad \text{(At the interface)} \qquad \text{Eq. 1.6}$$

$$\delta\ = 0 \qquad \text{(Not at the interface)} \qquad \text{Eq. 1.7}$$

$$\Phi(\mathrm{r}, \mathrm{z}) = \mathrm{C} \qquad \text{(Level Set Field)} \qquad \text{Eq. 1.8}$$

ρ: **Density**, $\boldsymbol{u}$: ***velocity vector***, t: time, g: acceleration due to gravity, $\boldsymbol{F_{st}}$: **Surface Tension Force**, $\boldsymbol{\sigma}$: **Surface Tension Coefficient**, $\boldsymbol{n}$: ***Interface Normal,*** δ: **Dirac Delta Function**

Equations 1.3 - 1.8 – Governing Equations of the COMOSOL Model

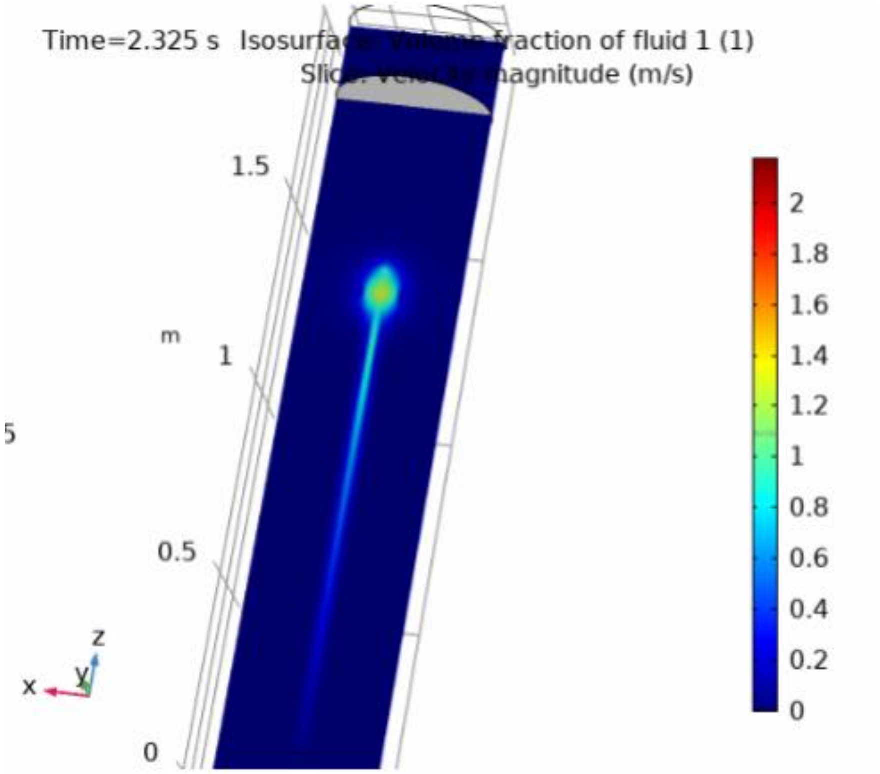

Figure 15 – Velocity contour of a rising bubble of Ethylene, as generated by the COMSOL model.

This model shows that the ethylene bubble will rise with a velocity of approximately 0.4 m/s. This is slightly lower than what would be expected for unhindered rising as estimated by the Mendelson Equation, reproduced below in Equation 1.9, which assumes that sufficiently small bubbles can be generated and no forces other than surface tension and gravity are present (Strumpf 2017). Applying material properties for liquid bismuth, the Mendelson equation suggests the rise velocity of the system likely will reach a minimum around 0.2 m/s, as shown in Figure 16 below.

$$u_{Mendelson} = \sqrt{\frac{2\sigma}{\rho d_{eq}} + \frac{g d_{eq}}{2}} \qquad \text{Eq. 1.9}$$

ρ: Density, $u_{Mendeslon}$: $Mendelson\ Rise\ Velosity$, t: time, d_{eq}: equivalent diameter,

g: $accelleration\ due\ to\ gravity$

Equation 1.9 – Mendelson Equation

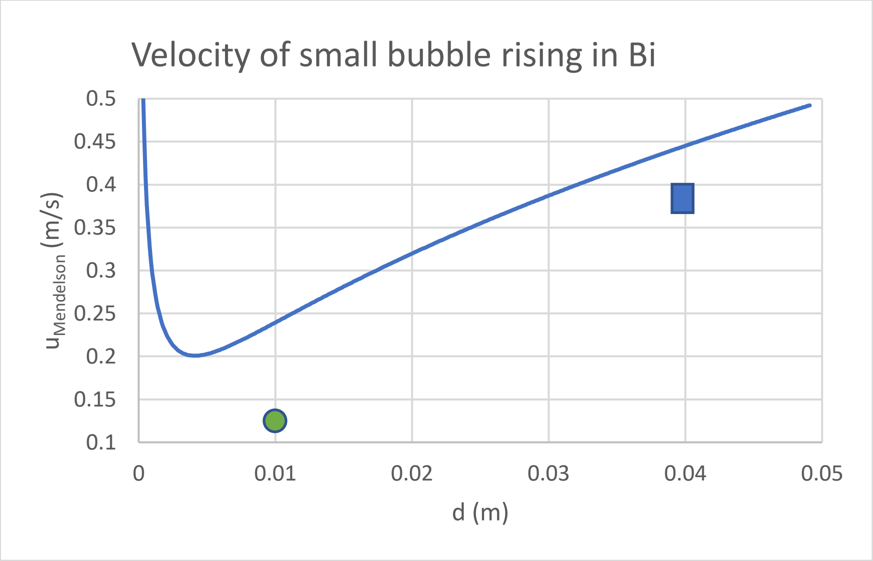

Figure 16 – The Mendelson equation for liquid bismuth. The indicated blue square is the velocity achieved in the COMSOL model, and the indicated green dot is the velocity from the ANSYS FLUENT model discussed in the next section.

It can be noticed that when the diameter is sufficiently small, the first term in equation 9 dominates, and the model is no longer physically relavent. As is, these results are comparable to literature analysis, as seen with other bubbling-liquid metal systems; experimental validation of the Mendelson equation has been performed with inert gases rising in liquid metals via several studies on liquid mercury and Galinstan (Strumpf 2017). Although the model predicted a slower velocity than predicted by the

Mendelsohn equation, the bubble likely deformed to become smaller in effective diameter, which would shift the velocity predicted by the Mendelsohn equation closer to the modeled value.

This model is useful as a baseline for understanding this system conceptually, however it falls short due to a myriad of assumptions it makes, particularly in incompressibility. Additionally, there is little experimental validation to verify that the model is working appropriately.

One of the key uses for this model is to estimate residence time of our bubble column reactors, and although rough estimate of rising velocity can be determined, understanding the flow of a bubble column requires understanding of continuous flow, compressible fluids, and reaction kinetics. This model is an incremental step towards creating a robust model capable of making predictions, and more incremental steps were made with the subsequent model in ANSYS FLUENT.

ANSYS FLUENT Method and Results

A second CFD model was created using the Ansys modeling stem. The object of this study is similarly to extend the hydrodynamic model and include reaction mechanisms. The first step was to create an Ansys Fluid model to corroborate the results in COMSOL and evaluate rising velocity of bubbles and bubble breakup-coalescing behavior given a continuous stream of gas that would mimic the reactive process.

This model operates in a 2D geometry, with a constant flow of Ethane at a superficial velocity of 0.1 m/s into a column of liquid metal 0.09 m high 0.02 m wide, through a 1/16” orifice. It assumes compressible ideal gas and incompressible liquid metal, laminar flow throughout, constant viscosities, constant surface tension, isothermicity, and no reaction. The governing equations are the Navier stokes equation for momentum, continuity of mass, continuity of energy, and a volume-of-fluid (VOF) mechanism for separating the gas and liquid phases with an assumption that the phases are immiscible. The VOF method equations are shown below in equations 1.10 through 1.13. The boundary conditions include no-slip walls, constant pressure outflow at the top of the reactor, and a constant velocity inflow at the bottom. This model is intentionally made similar to study evaluating the breakup of bubbles in water via the VOF method (Zahedi et al. 2014), and snapshots of the bubble rising behavior given by this model is shown in Figure 17 below. Additional data and figures can be found in Appendix B.

Continuity, each phase:

$$\frac{1}{\rho_q}\left[\frac{\partial}{\partial t}\left(\alpha_q\rho_q\right)+\nabla\cdot\left(\alpha_q\rho_q\overrightarrow{v_q}\right)=S_{\alpha_q}+\sum_{p=1}^{n}\left(\dot{m}_{pq}-\dot{m}_{qp}\right)\right] \qquad \text{Eq. 1.10}$$

Momentum Equation:

$$\frac{\partial}{\partial t}(\rho\vec{v})+\nabla\cdot(\rho\vec{v}\vec{v})=-\nabla p+\nabla\cdot\left[\mu\left(\nabla\vec{v}+\nabla\vec{v}^{T}\right)\right]+\rho\vec{g}+\vec{F} \qquad \text{Eq. 1.11}$$

Surface Tension:

$$F_{vol}=\sigma_{ij}\frac{\rho\kappa_i\nabla\alpha_i}{\frac{1}{2}(\rho_i+\rho_j)} \qquad \text{Eq. 1.12}$$

Energy Equation:

$$\frac{\partial}{\partial t}(\rho E)+\nabla\cdot(\vec{v}(\rho E+p))=\nabla\cdot(k_{eff}\nabla T)+S_h) \qquad \text{Eq. 1.13}$$

ρ_q: **Density of Phase q**, α_q: ***Volume Fraction of Phase q*** , $\overrightarrow{v_q}$: ***Velocity of Phase q***, $S_{\alpha q}$: ***Mass Source of Phase q***,

$\dot{m}_{qp}$: ***mass transfer from phase q to p***, p: ***Pressure***, μ: ***Viscosity***, g: ***acceleration due to gravity***,

$\overline{F}$: ***External Force Field***), σ_{ij}: ***Surface Tension Coefficient at interface of i and j***, κ_i: ***Curvature of phase i***

E: ***Energy***, k_{eff}: ***effective thermal conductivity***, T: ***Temperature*** S_h: ***Energy Source***

Equations 1.10 – 1.13 – VOF Method Equations (ANSYS FLUENT Theory Guide, 2009)

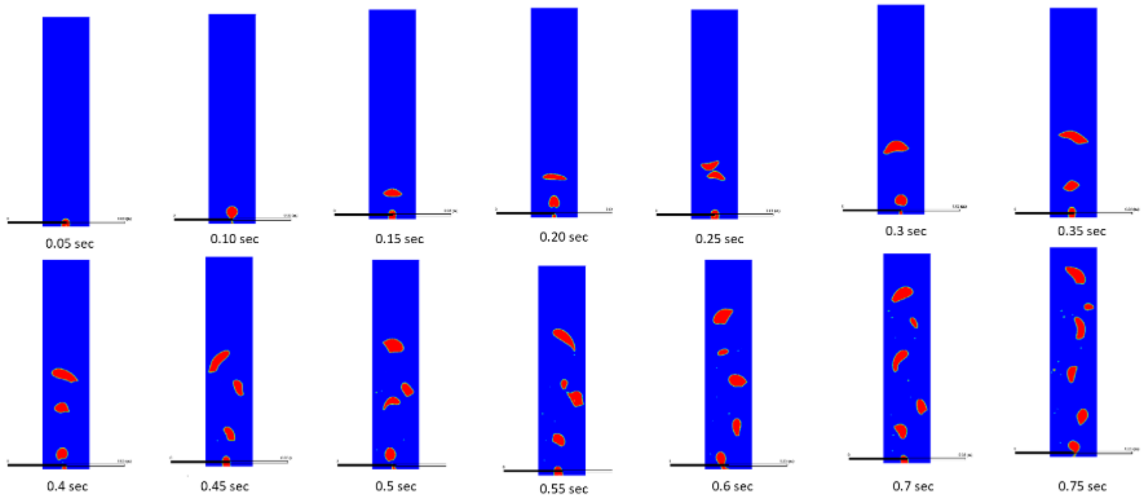

0.05 sec 0.10 sec 0.15 sec 0.20 sec 0.25 sec 0.3 sec 0.35 sec

0.4 sec 0.45 sec 0.5 sec 0.55 sec 0.6 sec 0.7 sec 0.75 sec

Figure 17 - VOF contours from 0.05 seconds to 0.75 seconds. The Red is Ethane, and the Blue is liquid Bismuth.

The bubble diameter varies between these timesteps; however, the velocity appears to somewhat level off around 0.12 m/sec, and the bubble diameter varies widely on the order of magnitude of 0.01 m. Additional data on these metrics can be found in Appendix B This bubbling flow clearly shows bubble deformation, and wake effects, which were expected to be present in a similar, physical, reactor system.

This model shows a slower rising velocity than the COMSOL model, which is at least partially due to the smaller bubble size, and it also a slower rising velocity than predicted by the Mendelson Equation, which indicates that we may have hindered flow from wake effects and wall interference. This hindered flow may conceptually result in turbulent flow regimes, which the physics of this model fail to capture.

This model is useful in showing an order-of-magnitude estimate of bubble rising velocity through LMC, as the model agrees comparably to experimental data with similar metals (Strumpf 2017), and could allow for residence time predictions using a lab-scale bubble column. It also shows the sensitivity of bubble rise velocity with bubble size and could be used in to perform what-if scenarios to understand the sensitivity of bubble size to inlet velocity and geometry.

After the hydrodynamic behavior is understood, then adding in reaction kinetics would be the logical next step. As both EDH and pyrolysis generate product gases, it will be particularly meaningful to understand how the resulting gas expansion will affect bubble geometry and residence time.

A decimeter tall column of liquid metal is a useful representation of the lab scale reactors present in the Veser lab, however, scaling of this technology may result in different hydrodynamic behavior. If this CFD model can be improved to make predictions at lab scale, then it may be useful to perform what-if scenarios for varying reactor geometries for scale-up.

This model could be improved by incorporating turbulent physics, which in a hindered flow scenario are likely to come into play, particularly around bubble coalescence and breakup (Besagni et al. 2018). Additionally, physical considerations such as wall effects and gas introduction geometry could have an effect on rising velocity and bubble size, and thus should be evaluated in future work.Confidence in this model could be raised by validating it against experimental data. This experimental validation could be done by matching the model geometry to extant studies of bubble rising behavior (Keplinger et al. 2019).

2.2 Investigate methods of characterizing liquid metal catalysts

Characterizing liquid metals using conventional catalytic methodology may not feasible due to the high temperatures and non-oxidative requirements required for the catalysts to be in a liquid form. That being said, there are a few things that have been investigated to characterize liquid metals.

2.2.1 Kinetic characterization

Product Recovery and Characterization

Some of the most important data collected from EDH and pyrolysis experiments is the conversion and product spectrum. This can be achieved by identifying and quantifying the reactants and products, which begs the question: what products do are expected to be seen, and how could they be collected and quantified? This is an inherently challenging question as pyrolysis tends to produce a variety of similar compounds that may be difficult to codify and separate.

Other pyrolysis studies have handled this in a few different ways, including measuring the phase of the products between liquids, solids, and gases (Lopez 2019); by separating by chemistry of products i.e.: Paraffins, olefins, BTX, and Coke (Wei et al. 2010); the solubility of the products i.e.: hexane soluble, toluene soluble (Matsuura et al. 1982); carbon number of products (Stlemachowski 2010); and specific products, which can reach more than dozens of species (Onwudili et al. 2009).

Ultimately, the question to be answered is “how effectively can LMCs upcycle polyolefins?”, which lends a particular interest to product fractions that can be fed into polymer synthesis processes. Could pyrolysis produce monomers such as Ethylene and Propylene? Can pyrolysis produce hydrocarbon gases that could be dehydrogenated such as Ethane and Propane, can pyrolysis produce liquid naphtha that can be fed into petrochemical processes such as C4-C12s, can pyrolysis produce longer oils and waxes that may not be liquid and would require solution to feed into petrochemical processes, or is the reactive system hardly breaking down the polymers at all, and in that case, chemically, what is the difference in the reactant plastics and product plastics?

Recovery and Character of Pyrolysis Products

A heterogenous solid material will degrade into a heterogeneous set of products, and polyolefins will be expected to degrade until mostly organic fragments in the gaseous, liquid, or solid form. A challenge in this work is to recover, stabalize, and characterize the reaction products in order to understand the mechanism and kinetics of the reaction. A summary of the expected reaction products and how the can be characterized follows.

Characterization of Volatile and Semi-Volatile Products

Sufficiently small products are consistently gaseous at atmospheric pressure and ambient temperature, such as ethane, ethene, and methane. These products can be easily transported to inline characterization devices or transported to independent characterization devices via gas sampling bags. Semi-Volatile products, such as butane and benzene, have a high vapor pressure but are liquid at ambient conditions. This causes some challenges with transportation to in-line characterization due to risk of condensation, or evaporation from a liquid state. Semi-volatiles have can be recovered by thermostating the product line to avoid condensation, and the forcing through a cold trap or filter that is sufficiently cold to force them into liquid or solid states until they can be recovered (Artetxe et al. 2012, Das and Tiwari 2018).

Both volatile and semi-volatile products are conventionally characterized by mass spectroscopy and gas chromatography—although for heaver semi-volatiles the inlet chambers and columns used may need to be heated to prevent condensation.

Mass Spectroscopy (MS): The gaseous volatile products are most easily detected by MS, which can be gathered in-line with the reactor and acquire excellent overtime data. Due to the nature of hydrocarbons, the MS fragments from the products are quite similar, and a deconvolution mechanism was developed to separate EDH products and calculate conversion and selectivity. A similar deconvolution method could be developed to distinguish between light pyrolysis products, the method for which can be found in Appendix C.

Gas Chromatography (GC), and GC/MS: The bulk of pyrolysis studies use GC to separate pyrolysis products to get around the challenges and uncertainty with determining which MS signals correspond to which compounds. The products can then be detected by a variety of detectors, most commonly MS in a GC/MS format.

Characterization of Non-Volatile Products

Sufficiently large products, such as waxes, residue, and heavy oils, tend to be non-volatile and cannot be flown through a GC or Mass Spec (with the possible exception of using MALDI MS characterization). A couple of methods are available to characterize these products.

Pyrolytic GC/MS (py-GC/MS): this is similar to conventional GC/MS, with the alteration that the analytes are quickly pyrolyzed and the pyrolysis products are flown through the GC/MS. This can allow for characterization of the analytes via analysis of the products themselves, however due to the similarity between pyrolysis products, it is likely that they will produce similar py-GC/MS signals and thus is unlikely to give excellent data.

Differential Scanning Calorimetry (DSC): DSC can be used to analyze when solid waxy components in a mixture melt (Arabiourrutia 2012). It may also be paired with TGA to evaluate the degradation and pyrolysis of the waxes and heavier polymer components to characterize the material (Aguado 2007).

High Performance Liquid Chromatography (HPLC): HPLC may be used to identify non-hydrocarbon components of materials, particularly useful for identifying what additives and additive degradation products are present in pyrolysis products (Ragaert et al. 2017).

Gel Permeation Chromatography (GPC): GPC is synonymous with size exclusion chromatography and can be used to evaluate the length of waxes and smaller polymers. It should be noted that if the polymer fractions are sufficiently large as to not be soluble in THF or Chloroform, then high-temperature GPC is required to fully characterize a MWD (Hillman 1971, Arabiourrutia 2012).

2.2.2 Direct Catalyst Characterization

Direct observation of LMCs is desirable to verify the character of LMCs. Such characterization, either in a liquid or solid phase, may be useful to answer research questions about the composition of the catalyst, how a LMC active site behaves, and the molecular character of the liquid surface. Few LMC systems involve direct investigation of the catalyst itself, and so it may be helpful to perform an overview and set of results that could be used to for LMC characterization.

Liquid Phase Catalyst Characterization

Surface Tension can be determined via the bubble pressure method, where a bubble pressure is processed via the Young-Laplace equation to determine surface tension and density (Palmer et al. 2019).

This measured surface tension can be used to determine the fraction of different components, given that the set of species that can be present is known. This requires excellent removal of surface oxides from metal surfaces which can be achieved via treatment with Hydrochloric Acid (Munera Parra et al. 2017). Whether or not this method of surface character can be used at elevated temperatures needs to be investigated, and if it could be achieved then one would be able to determine the chemical composition of the surface of an LMC.

Supported liquid metal catalysts have been studied in situ via IR spectroscopy. This is especially convenient for monitoring the catalyst before and after reactions (Kettner et al. 2019). Diffuse reflectance infrared Fourier transform spectroscopy (DRIFTS) can be used to evaluate the extent of CO adsorption onto active sites for SCALMS and compare them to conventional solid catalysts (Bauer et al. 2019). These characterization methods can be used to determine if LMCs are being activated, or deactivated, by the binding of oxides, and may demonstrate generally whether or not the character of an LMC changes during the course of a reaction.

Theoretically, SEM can be used to characterize liquids through the use of high temperature chambers and variable pressure systems which would allow for atomic analysis of liquid surfaces. However, this cause concerns due to the vaporization of metal which could collect in the vacuum chamber. This may be circumventable through the use of microfluidic devices, if perhaps only for room temperature liquid metals (Yang 2011).

Secondary ion mass spectrometry can be used on liquid metals, however it has much of the same challenges as SEM. Again, there are possible techniques to proceed, such as a method that has been developed to cover a liquid with a small layer of degradable substance (such as SiN) so that it can be ablated via molecular beam to reveal the liquid beneath for analysis to a sufficiently small extent SIMS Liquid (Zhou 2016).

Measuring the reflectance of liquid metal surfaces may also be useful in determining surface composition, particularly as low melting metals' reflectance is particularly sensitive to presence of surface oxides (Nakakubo et al. 2021), however liquid metal reflectance and other optical properties are temperature dependent and so caution should be taken in this characterization method, or perhaps a novel temperature sensor may be developed (Regan 1997).

Similarly, the resistivity of the liquid metal is intuitively dependent on the metal composition, and this phenomenon could be used to evaluate composition—although conductivity of high temperature liquid metals is likely not well characterized at this point, and a variety of impedance studies could be undertaken to lay the groundwork for this analysis. There is some groundwork in this area for some liquid metals, and models may be useful in extrapolating the electrical properties of LMC systems, though again, conductivity is temperature dependent and so this may require a robust understanding of the LMC system (Assael et al. 2018).

Solid Phase Catalyst Characterization

TGA can be used to evaluate the phases of liquid metal alloys in a couple of fashions. Specifically, DSC can be used to look for the melting endotherm of different alloys, for example validate the phases present in a Bismuth Nickel sample to determine the fractions of BiNi and Bi3Ni, or pure bismuth, as demonstrate in Figure 18.

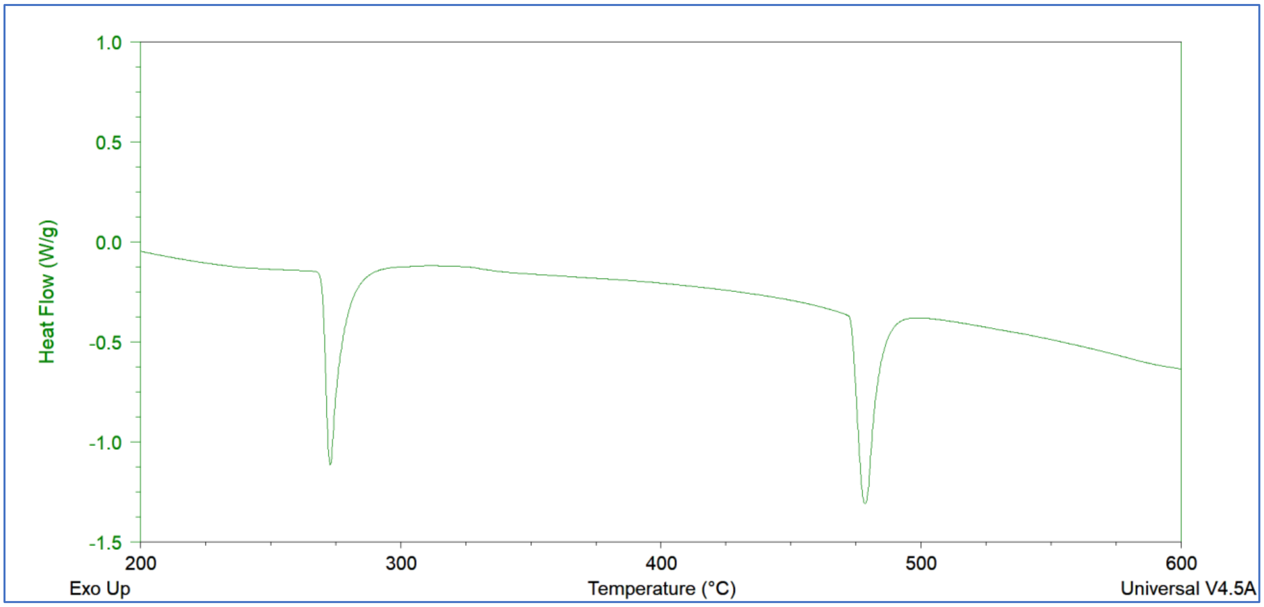

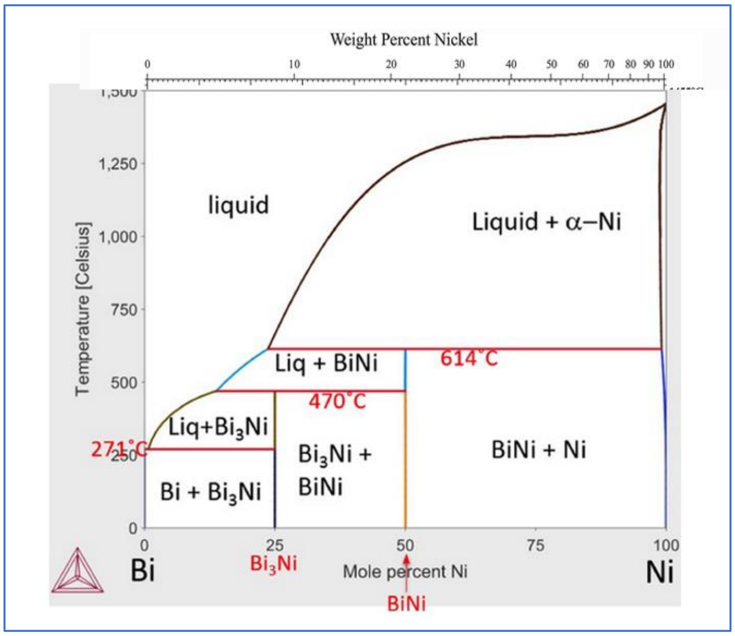

Figure 18 – Top: Heat flow out of a spent Bismuth Nickel catalyst. Bottom: A phase diagram of Bismuth Nickel System, for reference.

This isn’t a direct evaluation of the catalyst, as phase separation would presumably occur upon cooling and cause different solid phases to form depending on quenching conditions. However, it can be used as a sanity check for evaluating the composition of material. After 600 C, the heat flow increases drastically as the bismuth begins to evaporate, and so a potential third peak of BiNi at 614 has not yet been identified.

Scanning Electron Microscopy, Electron Dispersion Spectroscopy, and Electron probe-micro analysis can be used to evaluate the surface composition of the metals. It should be noted that the penetration of electrons into post transition metals is typically only a few hundred nanometers, as can be estimated from CASINO simulation. A proof-of-concept analysis via SEM and EDS on spent 5% weight Nickel and Bismuth is included below in Figure 19, with additional elemental analyses in Appendix D. The graphs below indicate the high-level topology and chemical composition of the catalyst after it is removed from an EDH experiment.

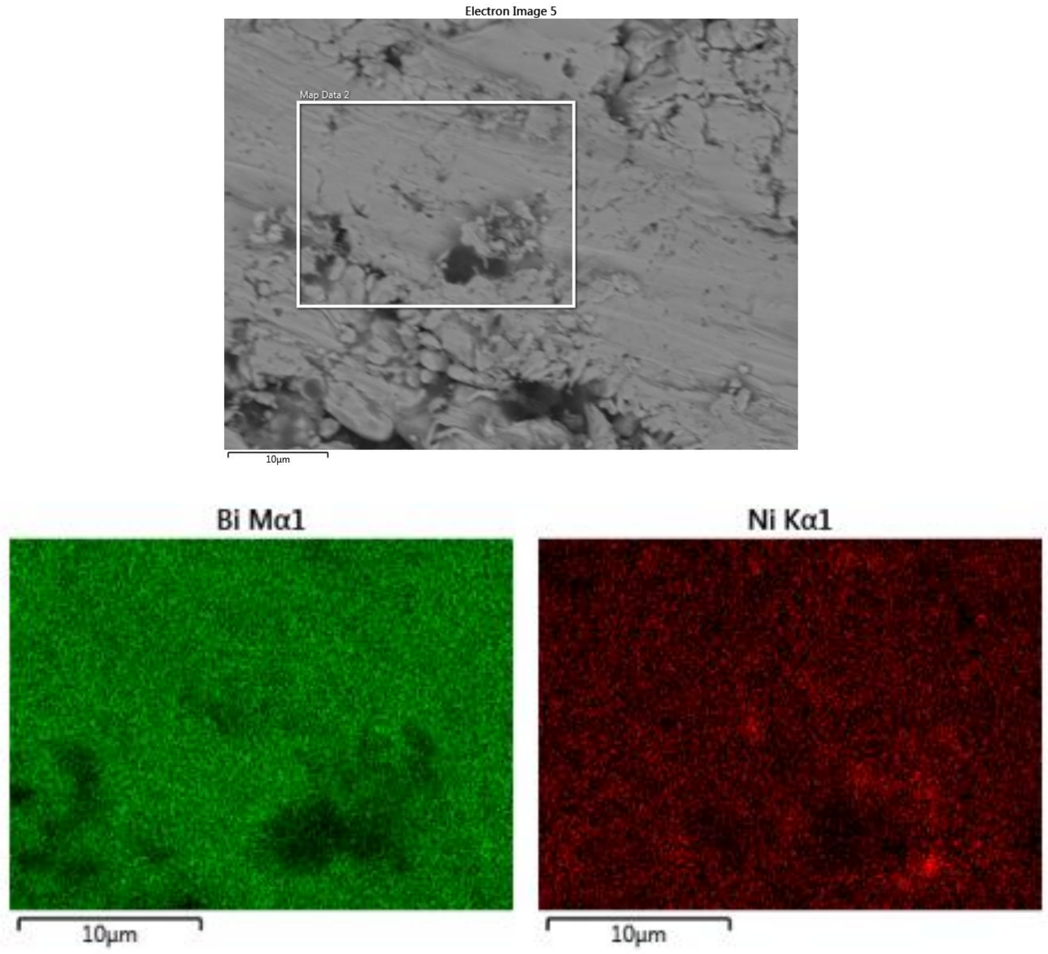

Figure 19 - Top: SEM Image of 5% Bismuth Nickel Catalyst. Bottom: Bitmap of Bismuth and Nickel frequencies within indicated area.

The SEM image shows some topography on the catalyst—this demonstrates a stark contrast with the character of a liquid surface, which is perfectly smooth. The EDS bitmaps reflect some of this topography, and overall, there appears to be little phase separation, with perhaps a couple of spots where the Nickel appears to be accumulating. From these data it is hard to tell if that clumping is the result of surface topography and repeating this analysis on a polished sample of catalyst would give insight into whether or not the LMC phase separated upon quenching.

EDS and/or EPMI may also be able to detect trace elements of expected contaminants. EDS can typically detect impurities at 0.1% n/n and EPMI can be used to go down all the way to 0.01% n/n. This may be particularly relevant in determining whether liquid metal catalysts in pyrolyzing plastics absorb contaminant metals, as tend to accumulate in recycled plastics and is shown in Appendix A (Eriksen 2018).

To evaluate bulk composition with EDS and EPMI, it would be required to cut the catalyst samples and polish the sample in cross section for analysis. The surfaces can be better preserved from oxidation and other contamination by covering the samples with epoxy and grinding it away to expose the surface selectively.

2.3 Develop a method of experimentation to screen liquid metal catalysts

2.3.1 Evaluate efficacy of LM Catalysts in EDH

Confirm operation in thermodynamic range

To evaluate the kinetics of ethane dehydrogenation, one must first confirm that they are operating in the kinetic regime and not quickly reaching equilibrium. This can be done by sweeping ethane through the reactor without a catalyst and evaluating the conversion achieved. One would want to see appreciable conversion at as low of a temperature as possible, as a lowering of activation energy, and thus higher conversion at lower temperature, would be an indication of catalytic potential. Another consideration is the limitation of the reactor materials—the furnace can operate up to 900 C, however at that temperature the interior of the reactor reaches a steady temperature of about 800 C. With that in mind, an operating condition of 750 C at ambient pressure was chosen—when using the stagnation point reactor, or the test tube reactor that the system is observed to pressures by up to 5 psi, this effect is neglected throughout this work, and it assumed that at the reaction zone the reactants and catalysts are under atmospheric pressure. Given Figure 20, at 800 C the equilibrium conversion about 55%.

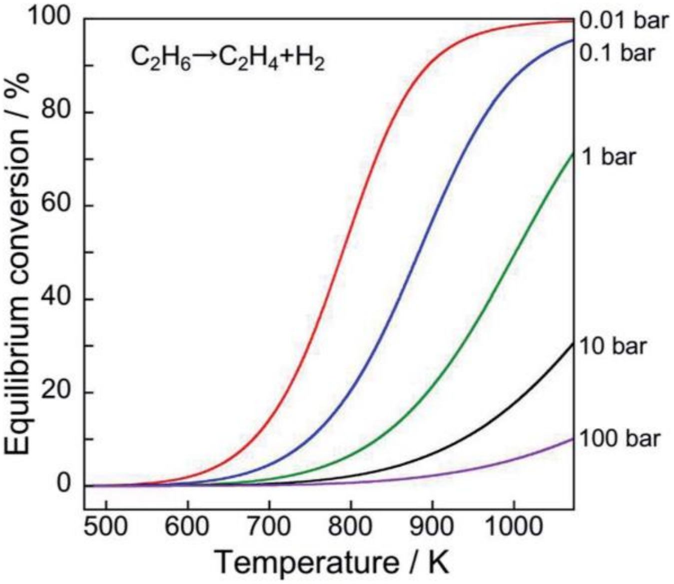

Figure 20 - Equilibrium reaction for EDH reaction at various conditions (Saito et al. 2020).

Ethane is flown through the stagnation point charged with ¼” of LMC, at a temperature of 800 C, at ambient pressure, and flow rates varying between 30 and 150 SCCM. The products were analyzed via MS with a 10% Argon used as an internal standard to evaluate the conversion. Pure Bismuth was analyzed in this fashion, as well as 10% weight Nickel in Bismuth, and an empty reactor as a baseline. The results are summarized in Figure 21 below.

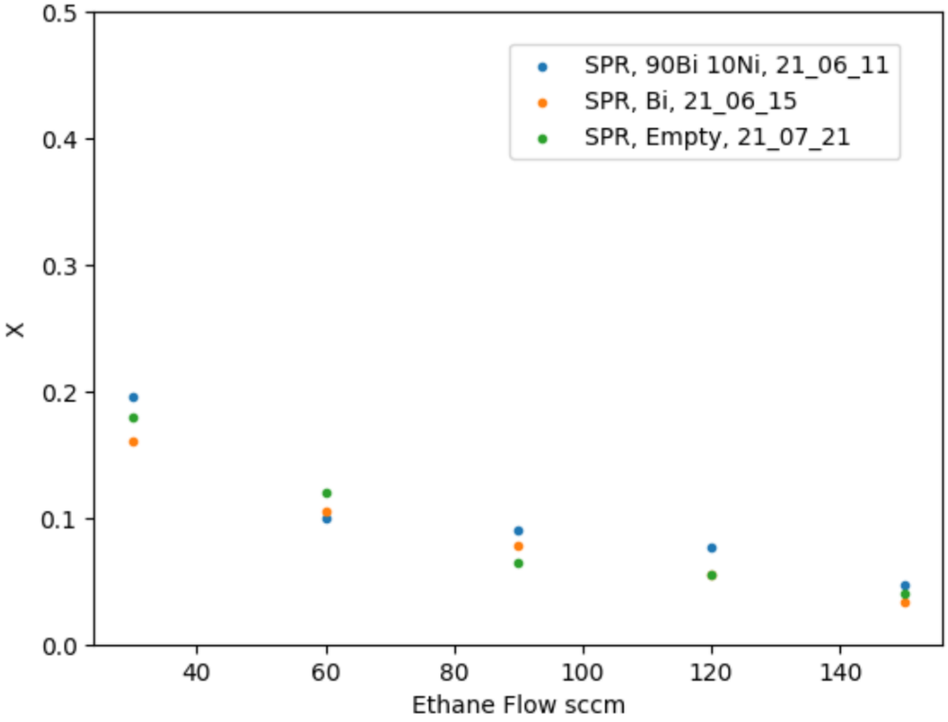

Figure 21 - Conversion of EDH in the stagnation point reactor at 750 C

It is seen that the conversion without a catalyst is well below equilibrium at all flow rates. It is apparent that as the flow rate increases the conversion decreases, which is intuitive as the residence time would be decreasing. Counterintuitively, little difference between any of the experimental conditions is seen.

There are a couple sources of experimental error, namely a difference in temperature and pressure during the reaction, as well as the volume of the reactor due to the spacing of the insert. Nonetheless, one can see that without a catalyst the system is operating well below equilibrium and should be able to proceed with catalyst screening—particularly as this configuration has been used repeatedly in characterization of LMCs with use in Methane Cracking (McFarland et al. 2017).

Perform Proof of Concept EDH Screening

This experiment was repeated with the fixed-frit reactor with identical experimental methods. Ethane was intended to be run in the exact same flowrates as the previous reaction, however the metal began to sputter at a flowrate above 90 SCCM and the experiment was aborted to limit damage to the catalyst and reactor.

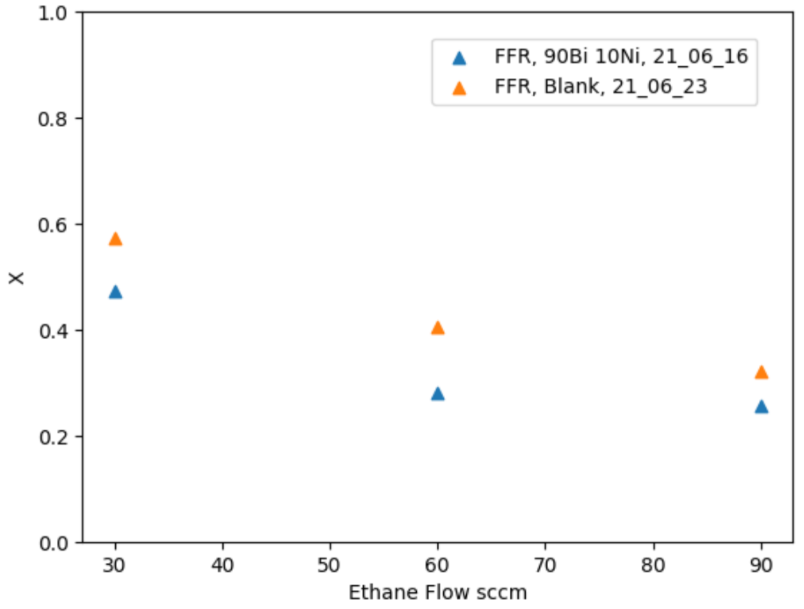

Figure 22 - Conversion of EDH in the Fixed Frit reactor at 750 C

In this analysis it is seen that the homogeneous EDH reaction is dominating as the liquid metal runs have a lower conversion distinctively, which indicates that Nickel/Bismuth Alloy is not catalytic in EDH; though it is possible there is a slight catalytic activity that is obfuscated by a decrease in homogeneous reaction due to the decreased volume in the reaction zone due to the space occupied by the LMC. It is clear from Figure 24 that at 30 SCCM the conversion exceeds the expected equilibrium. This may be the result of hot spots in the reactor, and could also be the result of competing reactions—further investigation may shed some light on this observation. The temperature probe is just above the metal, and thus it may be possible that the metal itself is hotter than 750 C. A temperature profile analysis may be performed of this reactor to clarify the reaction conditions and ensure that the inlet and outlet are not so hot as to promote homogeneous reactions outside of the reaction zone.

The FFR reactor is expected to induce a higher contact area than the stagnation point reactor due to ethane flowing around and bubbling through the metal, and thus would be more sensitive to catalytic dehydrogenation in relation to homogeneous and spontaneous dehydrogenation.

Key Takeaways and Future Work in EDH

The key takeaway from these results is that there has been no evidence of catalytic activity of Bismuth/Nickel LMCs with respect to EDH. The resilience of LMCs to coking is another point of interest, and that study will need to be performed after a catalytically active system can be operated with confidence.

There are many more metal systems to test beyond the bismuth/nickel system, and a thorough analysis of the possibilities may prove fruitful—particularly in reference to recent demonstrations propane dehydrogenation via gallium/platinum SCALMS (Bauer et al. 2019), butane dehydrogenation via gallium/palladium SCALMS (Taccardi et al. 2017), propane dehydrogenation via gallium/rhodium SCALMS (Raman et al. 2019), and methane cracking with bismuth/copper LMCs (Palmer et al. 2019).

2.3.2 Evaluate efficacy of LM Catalysts in polyolefin upcycling

TGA Experiments

Experiments of Polyolefin Pyrolysis in the TGA tested a variety of liquid metals in a TGA and evaluated whether or not the rate of degradation was faster with LMC than pure thermal pyrolysis, and if the pyrolysis onset occurred at a lower temperature.

DSC and TGA data were collected from a Q600 SDT from TA Instruments. Alumina TGA pans were used, loaded with about 0.1 g of LMC, and 0.05 g of polymer. The temperature program employed a ramping rate of 10 K/minute until no change in mass was noticed. Some catalysts were tested at an isothermal program, where the temperature was held constant at 420 C. The catalysts tested included Tin, Bismuth, Bismuth Nickel Alloys, Bismuth Zinc Alloys, and Bismuth Palladium Alloys. Of these experiments only Bismuth and Bismuth / 10% Palladium Alloy were shown to make any noticeable difference on rate of pyrolysis, as shown below in Figure 23.

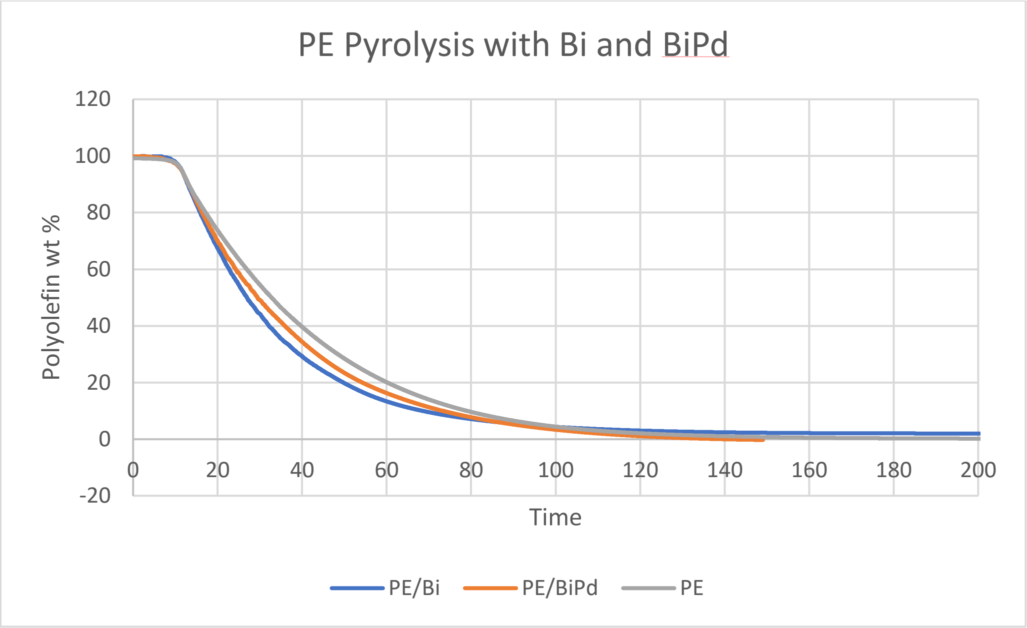

Figure 23 - Isothermal TGA Data for polyethylene degradation in the presence of Bismuth and 10% Pd in Bismuth

These results suggest that Bismuth and Bismuth Palladium alloy accelerate the degradation of PE, however, the onset temperature of pyrolysis remains unchanged—which we would expect to change if the activation energy were reduced. Further analysis is required to confirm that this truly catalysis, which can be done by comparison to a known catalyst, in order to validate that this experimental method is providing reliable results.

ZSM5 has been shown in literature to catalyze PE pyrolysis (Lopez et al. 2017), and a TGA analysis was performed of non-doped H-ZSM5 created and supplied by Yifan Deng of the Veser Lab. In the same method as employed for LMC, ZSM5 was tested for catalytic activity, the results of which are shown below in Figure 24.

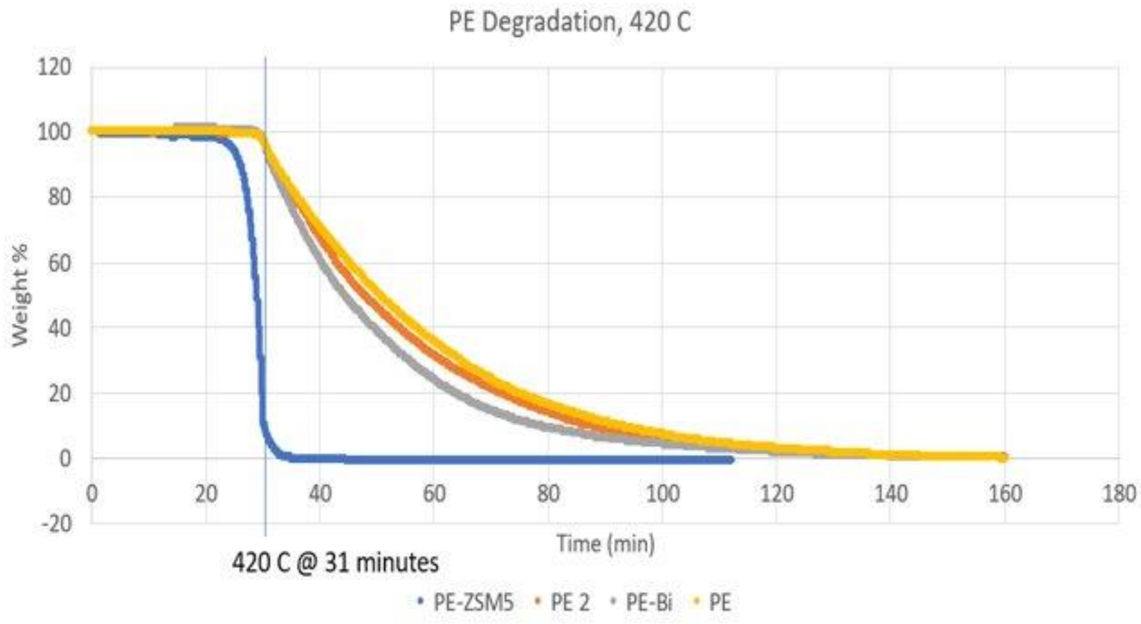

Figure 24 - Degradation of polyethylene in the presence of Bismuth and ZSM5

ZSM5 is clearly having a catalytic effect in decreasing pyrolysis onset temperature, and increasing the rate of degradation. Compared to this effect the Bismuth and 10% weight Palladium in Bismuth is having a much slighter effect. These results show that the LMCs tested are not catalytically active with respect to polyolefin pyrolysis.

Resilience to coking

Although the LMC is not shown to be catalytic, is it preventing catalyst coking? This was investigated via a series of analysis with a ramping temperature in the SDT. One alumina cup contained 0.05 g polyethylene with 0.01 g ZSM5, and another cup prepared with 0.05 polyethylene, 0.01 g ZSM5, and 0.09 g bismuth. The cups are reloaded with polymer after each run, and the results are shown in Figure 25 below, with non-catalytic runs shown for reference. The objective of this experiment is to establish the presence or lack of presence of liquid metals' ability to prevent coking in suspended catalytic systems.

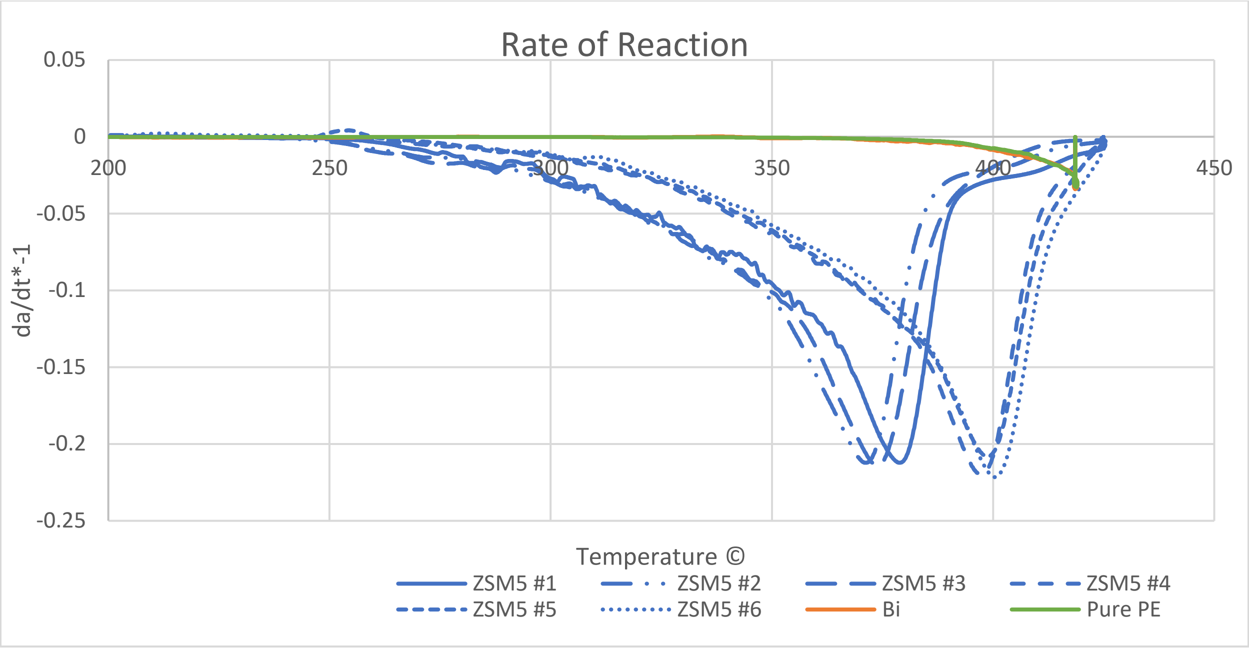

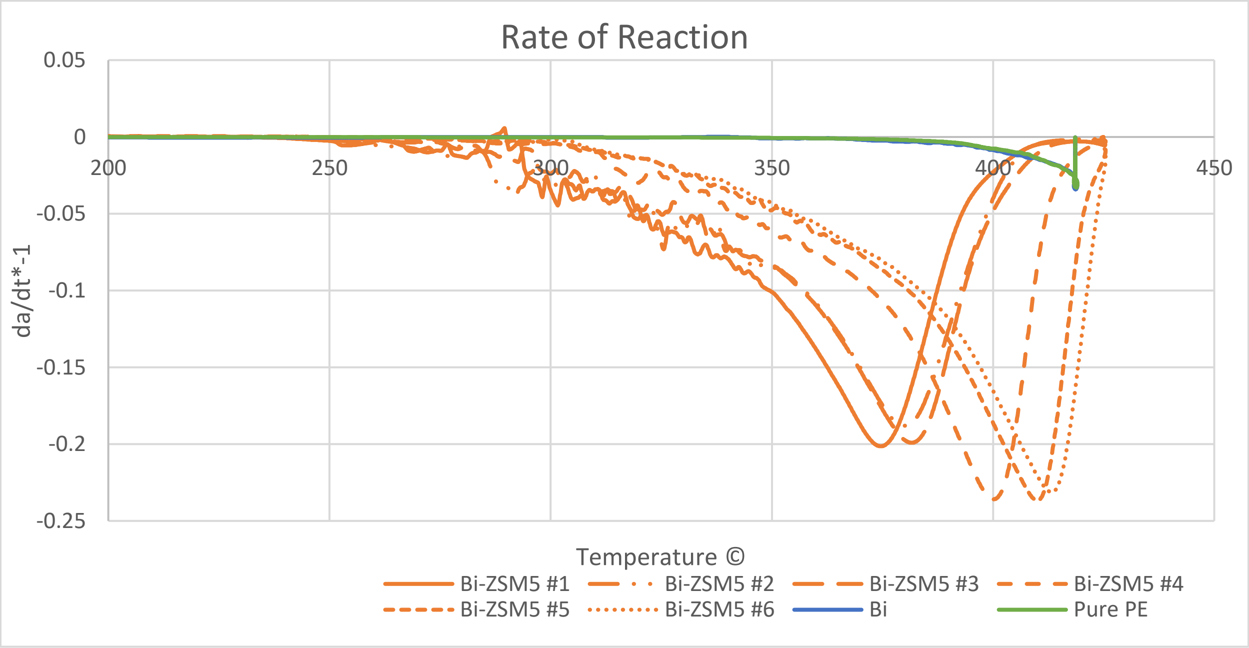

Figure 25– ZSM5 deactivation in PE Pyrolysis over 6 pyrolysis runs. Top: ZSM5. Bottom: ZSM5 and Bismuth.

These results again show a drastic decrease in pyrolysis onset temperature for both systems, and the ZSM5 is seen to partially deactivate after just one pyrolysis run, which matches similar studies in literature (Marcilla et al. 2004). The introduction of bismuth into the system does not appear to inhibit the activity of the ZSM5. These results indicate that LMCs could be used to suspend catalyst particles without inhibiting access to them, which would be useful in reaction design as the LMC would allow for excellent heat transfer to the active sites and other properties of the LMC may be utilized in reaction design.

It is possible that this method is effectively evaluating the activity of LMC. The LMC is unable to be reduced in the TGA prior to pyrolysis, which allows for surface oxides to separate the LMC from the polymer—cutting off any access to active sites on the LMC. The LMC could also be changing the product spectrum, and the product gases would need to be collected and characterized to determine if LMC is participating in the reaction.

The physical limitations of the TGA do not allow for product collection or catalyst preparation, and so additional reactors were employed that allow for these procedures.

Proof of concept experiments in quartz tube

A piston driven feeding system was used to drop plastic pellets into a quartz tube reactor. Each pellet was approximately 0.5 grams, and the reactor was heated to 420 C and a purge gas of 10 SCCM Argon was used to flush out the reactor without ceasing. Product gases were monitored by in-line MS, and a cold trap was used to collect liquid products for analysis with GC/MS.

The results of these experiments were successful pyrolysis, as demonstrated by visual degradation in the reactor, and corresponding product gases causing peaks in the MS reading was seen that matches with expected products including Propene, Ethane & Ethene, and Methane. Additionally, liquid product was recovered in the cold trap which consisted of a variety of carbon chain products per GC/MS analysis and flushed the reactor with solvent and recovered longer carbon chains that appear to be plastic fragments.

No basis for comparison was able to be made between catalyst pyrolysis rates or products, as the experiments did not have similar reaction conditions in practice. A common reason for inconsistency is that the plastic pellets often would get stuck to the sides of the reactor, or on the thermocouple and either never enter the reaction zone or slowly dripped into the reaction zone

The MS signals recovered indicate that when the pellet enters the reactor successfully then pyrolysis proceeds, and if inconsistency can be removed from the feeding process, then pyrolysis products can be quantified, and the reaction rate evaluated. The feeding process can be improved with a transition to the fixed frit reactor fed from a vertical tube. The pellet is less impeded due the absence of an inlet line, and the tall, straight drop allows the pellet to build momentum before it comes into contact with any hot reactor pieces. In proof-of-concept experiments, such a feeding system allows for perfect consistency in delivering a plastic pellet to the reaction zone.

Key takeaways and future work in Polyolefin pyrolysis

The experiments have not given conclusive evidence that LMCs are catalytic in polyolefin degradation. That being said, this has only begun to evaluate the efficacy of LMCs in plastic degradation.

There are a couple of key takeaways from these experiments. Firstly, decoupling thermal degradation from catalytic degradation is necessary. This can be done by operating below 400 C, utilizing isoconversional methods to evaluate reaction mechanisms, using a small amount of plastic to maximize surface-to-volume ratio, or correcting catalytic pyrolysis against a non-catalytic baseline. Secondly, similar reactants and reaction conditions should be used to screen LMCs, and once an experimental system can provide repeatable results, then a rapidly screening many LMC combinations would help understand what LMC systems would be useful. Finally, using a low molecular weight linear polymer will allow for the easiest operation of the system, as viscous effects will be minimized.

3.0 Conclusions

No evidence of catalytic activity of Bismuth-Nickel LMC has been demonstrated thus far, with respect to polyolefin pyrolysis or the dehydrogenation of ethane. There LMCs studies has been limited almost exclusively to Bismuth-Nickel, and there are a variety of successful LMCs that have been used in literature that might be evaluated. Beyond simple solutions of liquid metals, liquid metals may suspend known catalysts such as ZSM5 to improve their reactivity while making use of the unique material and electromagnetic properties of liquid metals. LMCs resilience to coking has not been conclusively confirmed or disproven, and once a LMC is seen to be catalytically active it will be particularly interesting to evaluate it for resistance to coking.

Reactors have been successfully designed and prototyped to handle LMCs. The stagnation point reactor is ideal for studying gas phase reactions, as it performs with few moving parts, and has a well-defined catalyst contact area, and is widely used in recent studies on LMC (Palmer et al. 2019). This reactor could be improved by reducing the variance in reaction zone above the catalyst and quenching the product gases more efficiently via a reduction of headspace volume. The fixed-frit reactor has shown promising proof of concept results in solid-phase reaction as it allows for consistent delivery of polymer to the reaction zone and allows for in-situ catalyst preparation. This reactor could be improved via additional validation for repeatable results and improving temperature control of the reaction zone—which may be possible via changing the reactor geometry to allow for only the reaction zone to be placed in the furnace. The fixed frit reactor is novel in that it contains LMC with porous glass, which is a particularly useful phenomenon that may warrant further study.

Characterization techniques for analyzing quenched LMC have begun to be established, while in-situ exploration of liquid LMC has not yet been achieved. In particular, validation of chemical composition of LMC can be done via EDS, while studies of homogeneity and phase separation may be performed via both EDS and DSC analysis. Understanding the character of liquid LMC remains a priority, and progress might be made via surface tension analysis, such has been performed in methane cracking studies (). Industry-standard catalyst characterization, such as EDS, are not available for use at the high temperatures LMC operate at. Electromagnetic characterization may be fruitful if relationship between resistivity and magnetic susceptibility can be established with LMC composition.

A hydrodynamic model has been developed for bubbling ethane through liquid metal, and the model requires validation against experimental results prior to use as a predictive instrument. Once validated, the model will be useful in understanding the residence time and interfaces in a column of LMC, and may be useful in exploring unique reactor geometries to optimize reaction conditions. Expansion of this model to include reactivity would be useful as well, particularly in understanding how the gas expansion of pyrolysis reactions could be used in reactor design to optimize residence time and reaction conditions.

3.1 Key Takeaways on the Catalytic Effects of Liquid Metal Catalysts

3.1.1 Challenges with Liquid Metal Reactors

There are several conceptual challenges with utilizing liquid metal as catalyst and/or reaction media, this section outlines the salient examples that should be considered when conceptualizing reactor scale-up.

Surface Area

As the participation of LMCs is considered to be heterogenous, with a possible exception for small gas molecules, it is concerning that the surfaces of liquids are extremely smooth. For example, the surface area of ZSM5 may exceed 400 m^2/g. Liquid metal has high surface tension and high density and will seek to minimize its surface area and take on a spherical form. A 1-gram spherical drop of Bismuth will have a volume of 0.1 cm^3, and surface area density of 0.0001 m^2/g. Even if fine bubbles or sprays of LM are produced, they are unlikely to ever approach the surface area achieved by conventional, porous, heterogenous catalysts.

Metal contamination

Oxygen – oxygen will readily react with metals to form metal oxides, and these oxides may accumulate on the surface of LMCs which will reduce the quantity of LMC and possibly obstruct active sites. This is particularly concerning as many plastics and additives contain oxygen, and loading solid feed into a reactor without introducing atmosphere may be challenging. In hydrogen producing reactions, perhaps these oxides can be reduced in situ, or with the addition of a stream of hydrogen feed or syn-gas.

Metals– plastics contain trace metal, waste streams can be contaminated with, laminates contain bulk metal, and reactor housings contain metal. These sources of metal will likely change the composition of the LMC, due to the solubility of metal in the system.

Ceramics – waste streams will likely be contaminated with trace glass, and stable metal carbonates may be formed via interaction with organics and LMC. These ceramics are likely to be less dense than metals and will likely float to the top of any metal surface. On one hand this is a benefit, as the contaminants can be scraped off or otherwise removed from the organic products, however it is unlikely that this removal process will be without challenges, particularly as ceramics floating on the surfaces will reduce the exposed catalytic surface of the LMC.

Metal Loss

Many low-melting metals, particularly zinc and aluminum, have relevantly high vapor pressures. This causes noticeable mass loss in TGA experiments and is likely to be a source of material cost, and damage to downstream equipment due to metal contamination. Other low-melting metals have orders of magnitude lower vapor pressure, so perhaps this challenge can be circumvented.

Hydrodynamic Pressure

Metals are extremely dense and will likely exert an enormous hydrodynamic pressure in columns, particularly as there is little to no void space as there is with conventional column packing. For example, the density of liquid Bismuth is about 10 g/cm^3, therefore, a mere 1-meter column of Bismuth would exert a hydrodynamic pressure of 98 kPa. This may or may not impact material constraints and will likely have an effect on reaction conditions within any bubble-column reactor due to the pressure gradient along the height of the column.

Corrosion

Steel is often used as reactor housings, and unfortunately it is known that liquid metals, including bismuth--corrode such housings. It is likely that housings will need to be specially designed, manufactured, and frequently inspected and/or replaced. There has been visible deterioration of gas inlets and thermocouples in the reactors, which is expected to be due to corrosion, and could also be the result of metal deposition onto the steel to form solid metal alloys. This hazard and cost could be mitigated through the use of low-temperature reactions, and additives that prevent corrosion such as Zr or Ti (Zhang et al. 2009).

3.1.2 Opportunities of Liquid Metal Reactors

There are promising features of liquid metals which may allow for exploitation in catalysis, and chemical engineering at large. A summary of these features is included below.

Catalysis and Unique Active Sites

There are many examples of liquid metals exhibiting catalytic activity, and one of the most notable findings in the field is that single-atom active sites can be achieved, specifically with supported Gallium-Platinum particles (Bauer et al. 2019). These sites are unique in that the platinum sites are separated by swaths of gallium, which prevents for adsorption of species next to each other, which prevents extension of carbon chains to form coke.

As previously mentioned in this thesis, the number of LMCs evaluated barely scratches the surface of the permutations of candidate metals and suspended catalysts, and catalytic activity is sensitive to even slight changes in LMC composition. Until a robust study of the potential catalyst candidates is made, and criteria for what makes a LM an LMC is determined, then this topic will remain filled with potential in the field of catalysis.

Physical Properties

As mentioned previously, liquid metals are unique in their extremely high surface tension, and that property has been successfully exploited to develop the fixed frit reactor. The surface tension and density jointly play a large role in the hydrodynamics of LMC bubble columns, as evidenced by the CFD models described in this work. If those properties can be utilized to control the rise velocity and geometry of bubbles within LMC then potentially self-regulating residence times may be achieved.

Electromagnetic Properties

LMCs are virtually untested in terms of electromagnetic properties. The high resistivity of post-transition metals and metalloids imply that joule heating of reaction media is feasible, and perhaps induction heating could be applied. Studies on magnetohydrodynamics have been made to evaluate the effects of applying magnetic fields to flows of liquid metals (Strumpf 2017), and magnetohydrodynamic applications in reaction engineering could be a standalone subject of study.

If the LMCs are not sufficiently susceptible to magnetic fields to achieve a desired magnetohydrodynamic behavior, then they could be charged with ferrous particles to create functionalized liquid metals with drastically changed electromagnetic properties (Liu et al. 2019). These materials are already being used to make novel electronic devices including liquid-metal driven pumps, and their application in chemical engineering operations appears to be entirely unexplored.

Electrochemical Properties

As LMCs are inherently conductive, and contain direct contact to active sites, then they theoretically have applications in electrochemical reactions—which would be particularly interesting as the active sites themselves would act as anodes or cathodes. No studies on this topic have been located, and this area poses a tentative area for possible future work. Room temperature liquid metal alloys including Galinstan and EGaIn may be ideal candidates for preliminary studies.

3.2 Future Work

3.2.1 High Throughput Screening

As there are many possible combinations of liquid metals that have the potential to be catalytically active, a high-throughput screening regimine may be useful to rule out liquid metals that are not catalytic, and those that may be useful in more detailed studies.

A liquid metal catalyst may consist of a active catalyst suspended or dissolved within an inactive base metal. With that in mind, it may be useful to establish a working set of solvent metals with which to test catalytic metals for efficacy with LMC. A list of potential solvent metals and metal alloys are listed below, and potential suspended or dissolved catalysts are too numerous to meaningfully discuss at this level of specificity.

For reference, while no exposure to metal fumes is considered without risk, particularly over long periods of time. Recall from Figure 1, waste polymers contain heavy metals including toxic Cd and Pb (Horodytska et al. 2020), and therefore any pyroylsis sysetm will produce toxic fumes and biproducts. This is a known challenge with polymer recycling, and when these toxins are not handled appropriately they cause demonstrable concerns to public health for the communities recycling plants are located in (Lopez et al. 2017).

Table 7 – List of Potential Solvent Metals.

Metal	Melting Point	Known Application or Source
E. GaInSn (Aka: Galinstan) -	-19 C	
E. GaIn	14 C	
Ga	30 C	Studied in Methane Cracking (Upham et al. 2017)
E. BiCdPbInSn*	47 C	Produced by Belmont Metals
E. BiPbInSn*	58 C	Produced by Belmont Metals
E. BiCdPbSn* (BEND Metal)	70 C	Produced by Belmont Metals
E. InSn	120 C	
E. BiPb* (Aka: LBE)	124 C	Used as a coolant in lead-cooled fast nuclear reactors
E. BiSn	139 C	Studied in Biomass Pyrolysis (Arenova et al. 2019)
In	157 C	Studied in Methane Cracking (Upham et al. 2017)
E SnPb*	183 C	Studied in Polyolefin Pyrolysis (Stelmachowski 2010)
E. ZnSn*	199 C	
Sn	232 C	Studied in Methane Cracking (Upham et al. 2017)
E. BiTe (Bi Rich)	266 C	
Bi	271 C	Studied in Methane Cracking (Upham et al. 2017)
Cd*	321 C	
Pb*	328 C	Studied in Methane Cracking (Upham et al. 2017)
E. ZnAl*	382 C	
E. BiTe (Te rich)	413 C	
Zn*	420 C	High vapor pressures
Te*	450 C	
E. AlCu*	559 C	
E. CuTe*	617 K	
Al*	660 C	

*** - indicates the metal contains a toxic element, or an element with a known toxic oxide.**

Selection of a active catalyst to dissolve in the base will require understanding of the reaction mechanism. Platinum, Palladium, and Rhodium have been used in SCLAMS to catalyse alkane dehydrogenation, while Nickel and Gold have been used to crack methane. Those metals may be an appropriate starting point for catalyst selection in EDH reactions.

Catalytic pyrolysis of polyolefins benefits from acidic active sites (Lopez et al. 2017). It is an unresolved question how to incorporate acidic sites into a LMC, and may require functionalization of the surface of the liquid metal to include hydrocarbons, or the suspension of acidic zeolites. Operating a metal with a positive oxidation state may allow it to act as a lewis acid, however, study on how to force a LMC to maintain a particular oxidation state would be required.

The list of catalytically active metals could be narrowed down via thermodynamic analysis of carbon adsorption, similar screening done in the analysis below for dry reforming of methane reproduced in Figure 26 below (Palmer et al. 2020).

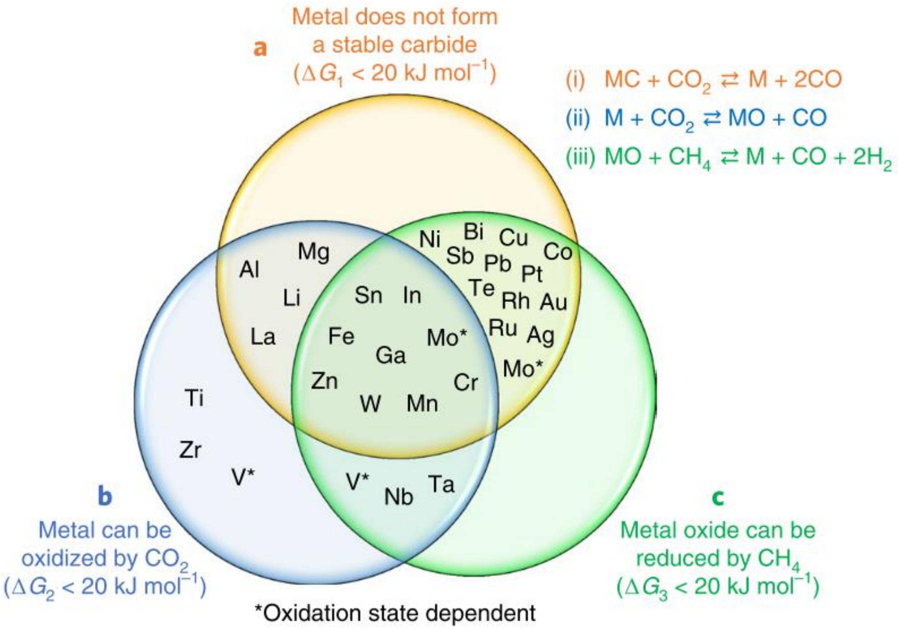

Figure 26– Thermodynamic analysis of candidates metals for the dry reforming of methane (Palmer et al. 2020).

3.2.2 Evaluate Efficacy of LM Catalysts in Plastic Waste Upcycling

Once the methods for performing pyrolysis experiments with LMC are established—and catalysts that effectively catalyze pure-polymer pyrolysis are identified—then there are several incremental steps that can be taken to explore LMCs effectiveness in pyrolyzing real-world plastic waste.

Co-Pyrolysis

Literature shows that there is a demonstrated difference in pyrolysis activity by plastic mixes—specifically that the pyrolysis mechanism is different when a mixture is pyrolyzed (Achilias et al. 2012). It would be useful to confirm that the LMC pyrolysis mechanisms are still valid with co-pyrolysis, particularly with mixtures of HDPE, LDPE, and PP.

It may also be useful to study the co-pyrolysis of Polyolefins with macroscopic contaminants, such as damp and dry paper, glass, and aluminum. These contaminants are concerning to me due to their likelihood of existing in sizable fractions in real plastic waste, and a controlled study of how these contaminants interact with LMC will help us to foresee challenges with actual plastic wastes. Aluminum is included due to the possible application of LMC in pyrolyzing laminated wastes that include aluminum, such as potato chip bags.

Targeting Waste Streams

In discussion with industry partners, the overall efficacy of a recycling system will depend on the plastic waste available to be recycled. These plastic groups are referred to as bales, and will likely need to be acquired at bulk on the scale of a 1-ton pallet of plastic waste, and will need to be systematically and randomly pared down to workable amount at lab scale—similar processes have been studied in literature, and an overview of how this can be systematically achieved can be found in Appendix E. Beyond this, the gaps in what materials can and cannot be recycled vary regionally, and locally there are a variety of bales that could be acquired for analysis test with the LMC pyrolysis system. In order of increasing complexity:

1. Haybale: post use PP, in the form of haybale-twine
2. 1 Bale: post-consumer PE, not washed
3. Lids and tubs bale: PE PP, not washed
4. Multi-layer: Laminates of PP, EDOH, nylon, aluminum, and many additives. These are trimmings from bag manufacturing, post industrial waste.
5. 3,6,7 bale: most complex mix. Residual landfill bale.

Modifications to the reactor are likely required to handle this real plastic waste, as they do not exist in pellet form like the model polyolefin systems. A washing processes can be employed to remove debris, then shred and pelletized as needed to reliably feed the waste into the reactor. Manual steps on how to do this can be found in Appendix E, as illustrated in similar studies (Erikson et al. 2018).

Data collection

The data to be collected for plastic waste experiments is similar to the data already collected for single-polymer pyrolysis; what products are produced, and at what temperature does pyrolysis occur. Beyond that, special attention should be paid to how the product spectrum changes overtime. Specifically: is the LMC resilient to coking and contaminant accumulation of ceramics, organics, trace metals, halogens, and organic compounds.

The groundwork is just laid for studying liquid metals as catalysts, and with additional research an evaluation of how effective they will be in polyolefin pyrolysis can be made, and our understanding of these materials can be enhanced.

Appendices

Appendix A: Plastics Additives

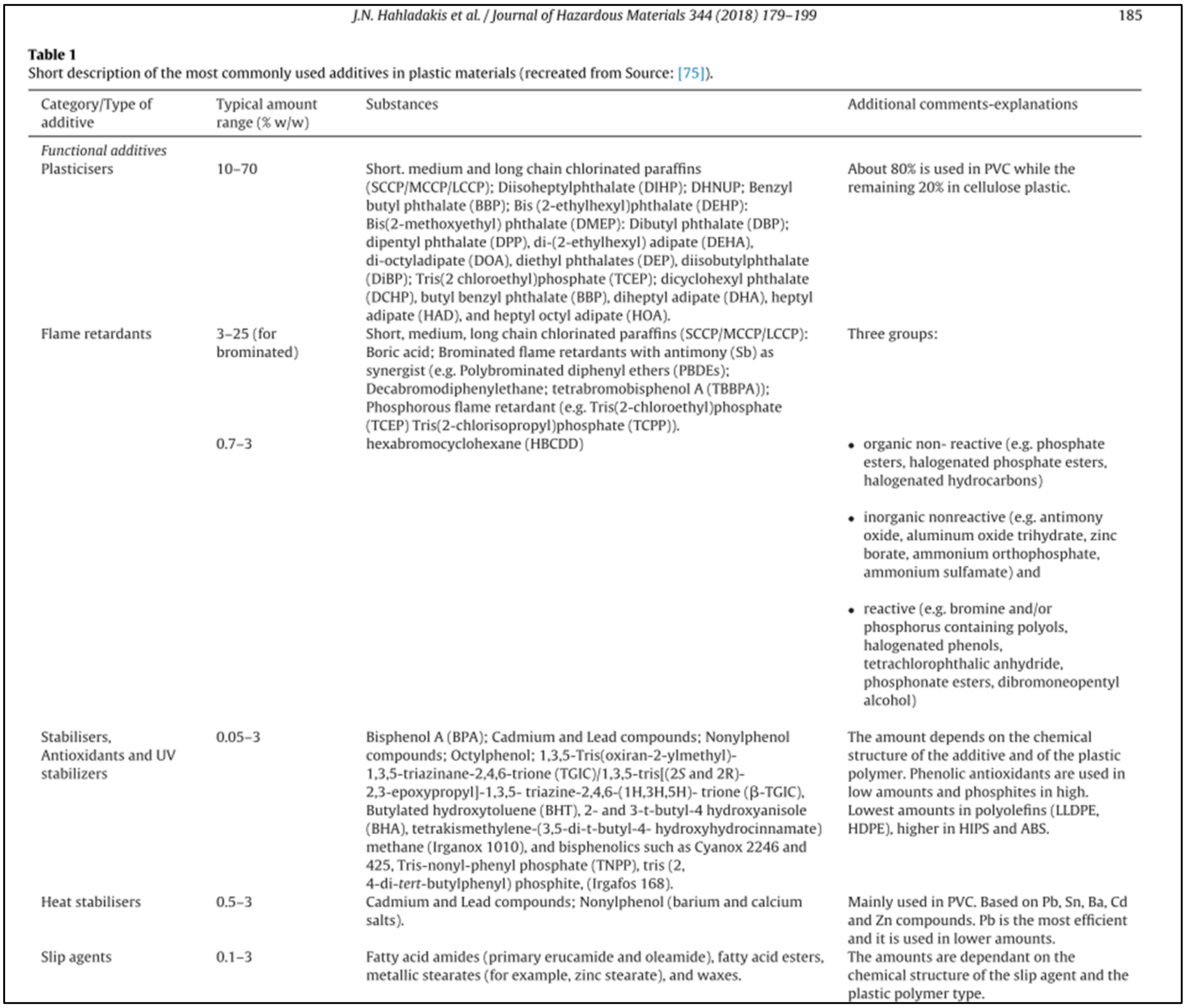

J.N. Hahladakis et al. / Journal of Hazardous Materials 344 (2018) 179–199 185

Table 1
Short description of the most commonly used additives in plastic materials (recreated from Source: [75]).

Category/Type of additive	Typical amount range (% w/w)	Substances	Additional comments-explanations
Functional additives			
Plasticisers	10–70	Short. medium and long chain chlorinated paraffins (SCCP/MCCP/LCCP); Diisoheptylphthalate (DIHP); DHNUP; Benzyl butyl phthalate (BBP); Bis (2-ethylhexyl)phthalate (DEHP): Bis(2-methoxyethyl) phthalate (DMEP): Dibutyl phthalate (DBP); dipentyl phthalate (DPP), di-(2-ethylhexyl) adipate (DEHA), di-octyladipate (DOA), diethyl phthalates (DEP), diisobutylphthalate (DiBP); Tris(2 chloroethyl)phosphate (TCEP); dicyclohexyl phthalate (DCHP), butyl benzyl phthalate (BBP), diheptyl adipate (DHA), heptyl adipate (HAD), and heptyl octyl adipate (HOA).	About 80% is used in PVC while the remaining 20% in cellulose plastic.
Flame retardants	3–25 (for brominated)	Short, medium, long chain chlorinated paraffins (SCCP/MCCP/LCCP): Boric acid; Brominated flame retardants with antimony (Sb) as synergist (e.g. Polybrominated diphenyl ethers (PBDEs); Decabromodiphenylethane; tetrabromobisphenol A (TBBPA)); Phosphorous flame retardant (e.g. Tris(2-chloroethyl)phosphate (TCEP) Tris(2-chlorisopropyl)phosphate (TCPP)).	Three groups:
	0.7–3	hexabromocyclohexane (HBCDD)	• organic non- reactive (e.g. phosphate esters, halogenated phosphate esters, halogenated hydrocarbons) • inorganic nonreactive (e.g. antimony oxide, aluminum oxide trihydrate, zinc borate, ammonium orthophosphate, ammonium sulfamate) and • reactive (e.g. bromine and/or phosphorus containing polyols, halogenated phenols, tetrachlorophthalic anhydride, phosphonate esters, dibromoneopentyl alcohol)
Stabilisers, Antioxidants and UV stabilizers	0.05–3	Bisphenol A (BPA); Cadmium and Lead compounds; Nonylphenol compounds; Octylphenol; 1,3,5-Tris(oxiran-2-ylmethyl)-1,3,5-triazinane-2,4,6-trione (TGIC)/1,3,5-tris[(2*S* and 2*R*)-2,3-epoxypropyl]-1,3,5- triazine-2,4,6-(1H,3H,5H)- trione (β-TGIC), Butylated hydroxytoluene (BHT), 2- and 3-t-butyl-4 hydroxyanisole (BHA), tetrakismethylene-(3,5-di-t-butyl-4- hydroxyhydrocinnamate) methane (Irganox 1010), and bisphenolics such as Cyanox 2246 and 425, Tris-nonyl-phenyl phosphate (TNPP), tris (2, 4-di-*tert*-butylphenyl) phosphite, (Irgafos 168).	The amount depends on the chemical structure of the additive and of the plastic polymer. Phenolic antioxidants are used in low amounts and phosphites in high. Lowest amounts in polyolefins (LLDPE, HDPE), higher in HIPS and ABS.
Heat stabilisers	0.5–3	Cadmium and Lead compounds; Nonylphenol (barium and calcium salts).	Mainly used in PVC. Based on Pb, Sn, Ba, Cd and Zn compounds. Pb is the most efficient and it is used in lower amounts.
Slip agents	0.1–3	Fatty acid amides (primary erucamide and oleamide), fatty acid esters, metallic stearates (for example, zinc stearate), and waxes.	The amounts are dependant on the chemical structure of the slip agent and the plastic polymer type.

Figure 27– Typical plastic additives, and their uses (Hahladakis et al. 2018).

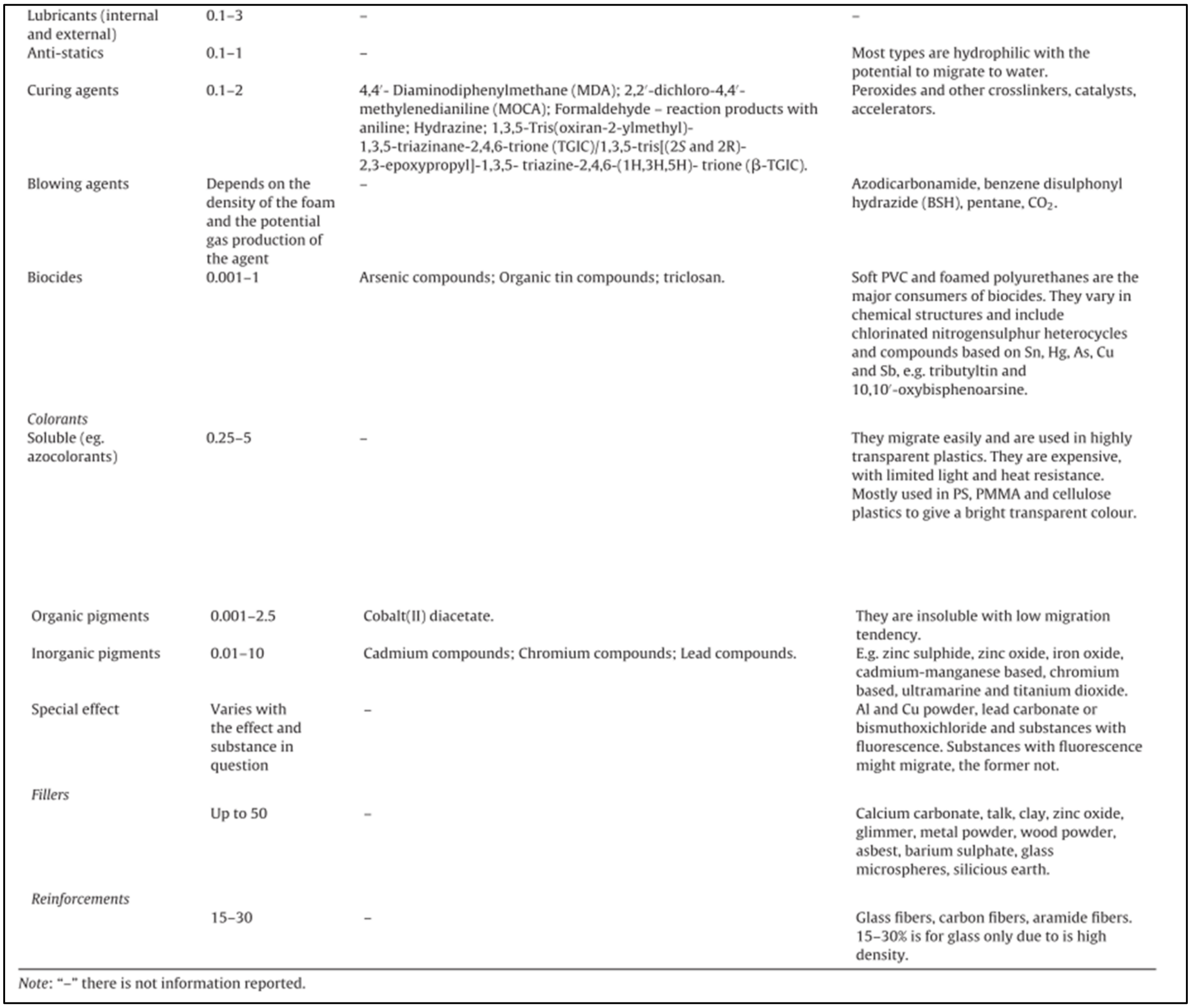

Lubricants (internal and external)	0.1–3	–	–
Anti-statics	0.1–1	–	Most types are hydrophilic with the potential to migrate to water.
Curing agents	0.1–2	4,4′- Diaminodiphenylmethane (MDA); 2,2′-dichloro-4,4′-methylenedianiline (MOCA); Formaldehyde – reaction products with aniline; Hydrazine; 1,3,5-Tris(oxiran-2-ylmethyl)-1,3,5-triazinane-2,4,6-trione (TGIC)/1,3,5-tris[(2*S* and 2R)-2,3-epoxypropyl]-1,3,5- triazine-2,4,6-(1H,3H,5H)- trione (β-TGIC).	Peroxides and other crosslinkers, catalysts, accelerators.
Blowing agents	Depends on the density of the foam and the potential gas production of the agent	–	Azodicarbonamide, benzene disulphonyl hydrazide (BSH), pentane, CO_2.
Biocides	0.001–1	Arsenic compounds; Organic tin compounds; triclosan.	Soft PVC and foamed polyurethanes are the major consumers of biocides. They vary in chemical structures and include chlorinated nitrogensulphur heterocycles and compounds based on Sn, Hg, As, Cu and Sb, e.g. tributyltin and 10,10′-oxybisphenoarsine.
Colorants			
Soluble (eg. azocolorants)	0.25–5	–	They migrate easily and are used in highly transparent plastics. They are expensive, with limited light and heat resistance. Mostly used in PS, PMMA and cellulose plastics to give a bright transparent colour.
Organic pigments	0.001–2.5	Cobalt(II) diacetate.	They are insoluble with low migration tendency.
Inorganic pigments	0.01–10	Cadmium compounds; Chromium compounds; Lead compounds.	E.g. zinc sulphide, zinc oxide, iron oxide, cadmium-manganese based, chromium based, ultramarine and titanium dioxide.
Special effect	Varies with the effect and substance in question	–	Al and Cu powder, lead carbonate or bismuthoxichloride and substances with fluorescence. Substances with fluorescence might migrate, the former not.
Fillers			
	Up to 50	–	Calcium carbonate, talk, clay, zinc oxide, glimmer, metal powder, wood powder, asbest, barium sulphate, glass microspheres, silicious earth.
Reinforcements			
	15–30	–	Glass fibers, carbon fibers, aramide fibers. 15–30% is for glass only due to is high density.

Note: "–" there is not information reported.

Figure 28– Typical plastic additives, and their uses, continued (Hahladakis et al. 2018).

Appendix B: Additional CFD Images and Data

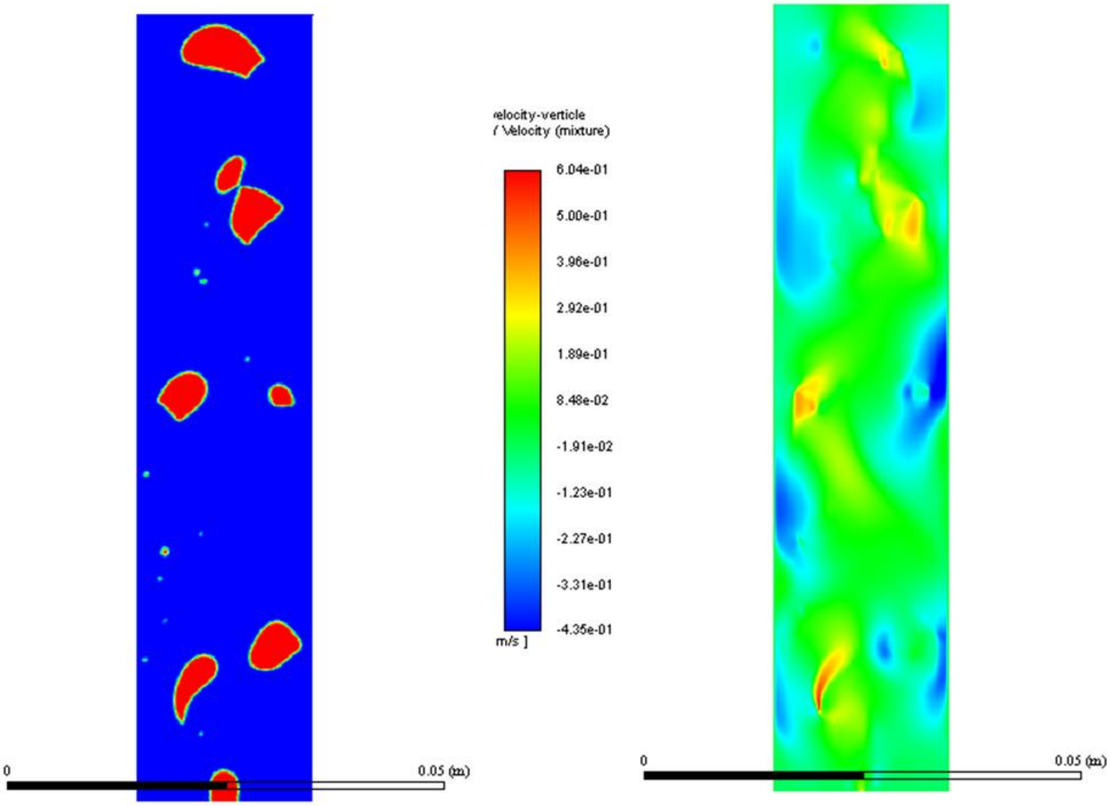

0.75 sec

0.75 sec

Figure 29 - VOF and Velocity Contours at 0.75 seconds.

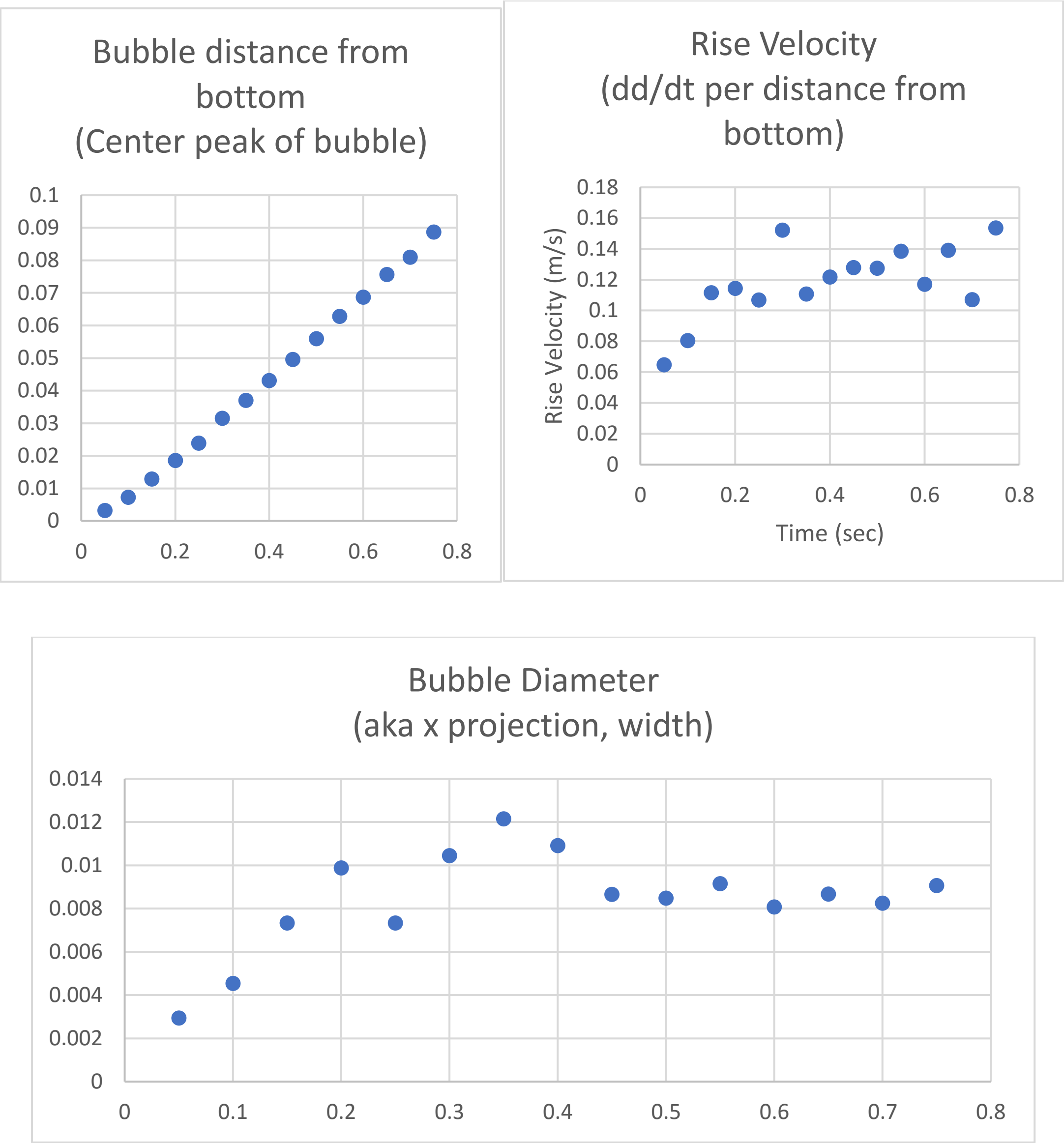

Figure 30 – Characteristics of the first bubble to rise in the ANSYS Simulation.

Appendix C: Deconvolution Method

The key metrics for reaction progression in the Ethane Dehydrogenation Reaction (EDH) are conversion of Ethane, and selectivity of Ethene. The data recovered from the in-line mass spec is ion current per particular masses A_i (Amps), which is calibrated to return the concentration of species according to a response factor, R. Due to the multiple species in the system, there are data for signal, concentration, and response factor matrixes. A simple matrix inversion is not possible to solve the system due to the non-square shape of response and selectivity matrix, and so the response factor is found the least squares regression. The mass spec signals will drift, and so the response factor should be validated before each day of experiment against known mixes of ethane and ethene.

$$[C_i]*[R_i]=[A_i] \qquad \text{Equation C.1}$$

Once the response factor is known, then the concentrations can be found using the same equation with known response factor and signals. The molar fraction of each species can be determined from the total concentrations of the system.

$$Y_i = \frac{C_{i\,out}}{\sum C_{i\,out}} \qquad \text{Equation C.2}$$

Once the response factor is known, one can then determine the concentration of each species in the reaction products. This concentration can be used to determine the conversion via a known flow rates in and out.

$$\text{Conversion} = N_{\text{ethane out}} - N_{\text{ethane in}} = Y_{\text{ethane in}} * N_{\text{total in}} - Y_{\text{ethane out}} * N_{\text{total out}} \qquad \text{Equation C.3}$$

$N_{\text{total in}}$ is known from the mass flow controllers, and Y_{ethane} in is found via Equation 1 and 2 when the ethane is flown through a bypass line directly into the mass flow controller. $N_{\text{total out}}$ is determined through the use of an internal standard of Argon. As argon is an inert gas it is assumed to not be consumed or generated during the course of reaction.

$$N_{\text{Argon in}} = N_{\text{Argon out}} = Y_{\text{Argon out}} * N_{\text{total out}}$$ **Equation C.4**

The selectivity of products is determined by

$$S_i = \frac{N_{i\,out}}{\sum N_{i\,out}}$$ **Equation C.5**

For each cycle of Mass Spec data, the conversion is found via a python script that performs a least squares regression of Equation 1, calculation of molar fraction for each species via Equation 2, calculation of molar flow via Equation 4, calculation of conversion via Equation 3, and calculation of selectivity of each species in equation 5.

Appendix D: SEM Images

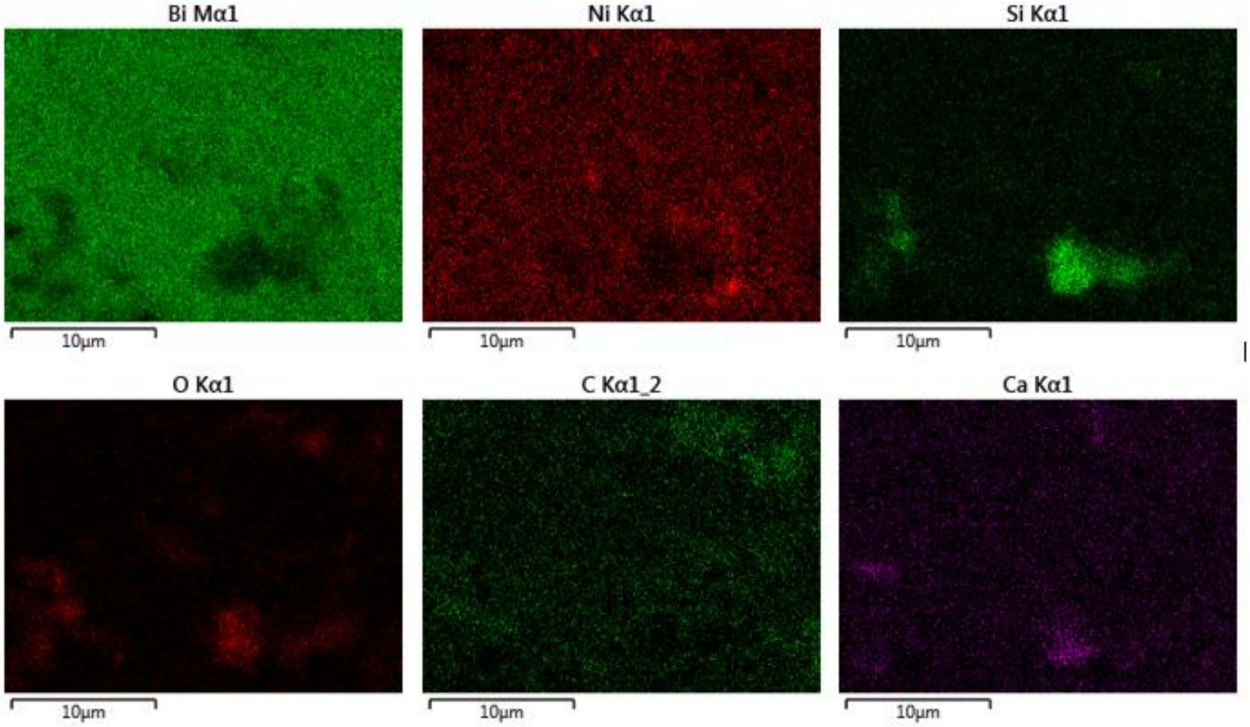

Figure 31 – Bitmaps of detected metals via EDS analysis on recovered Bismuth / 10% weight Nickel LMC from the stagnation point reactor after an EDH experiment.

Appendix E: Mixed Plastic Waste Sorting Methodology

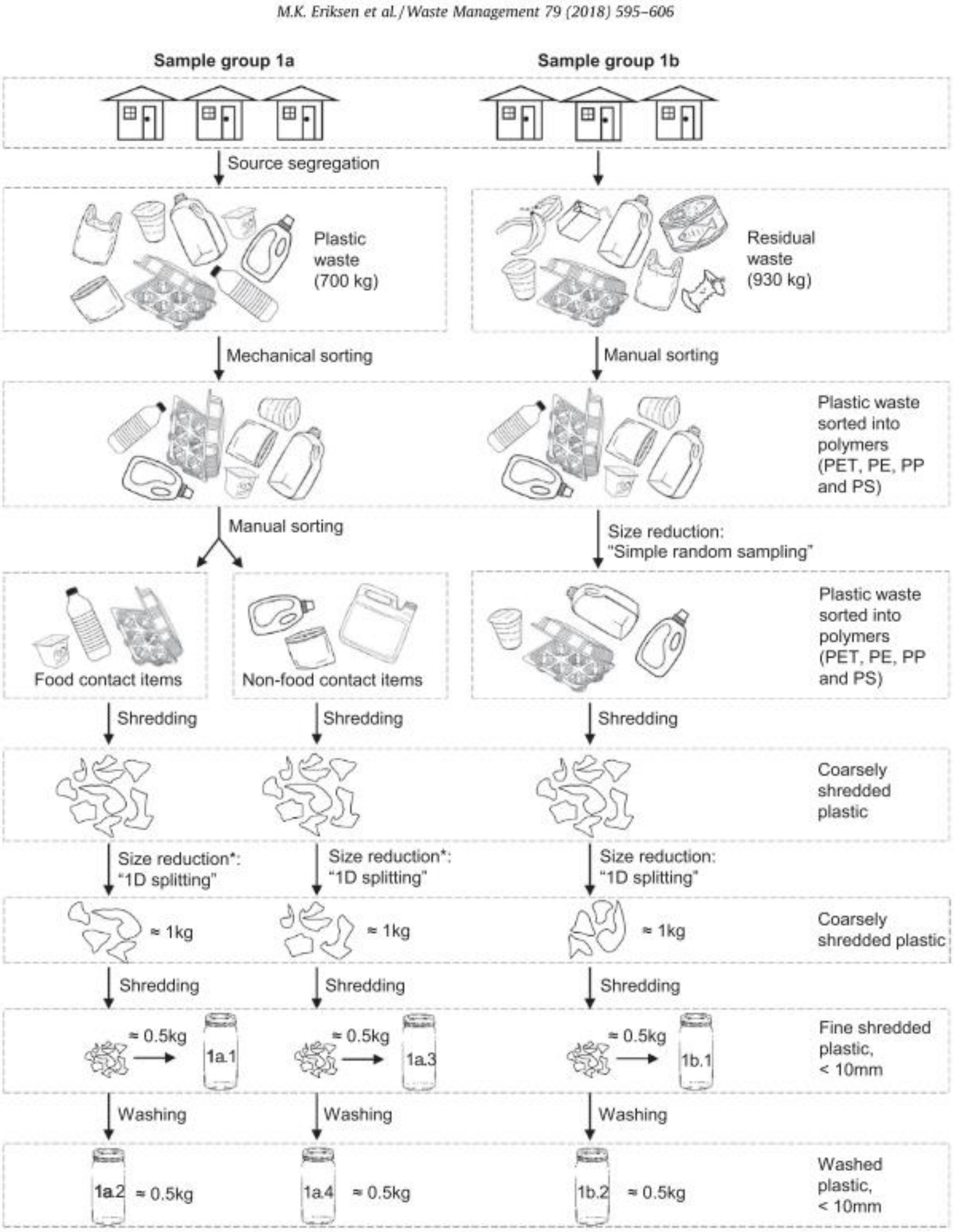

Figure 32 – Illustration of collection, selection, and preparation of post-consumer plastic waste (Erikson et al. 2018).

Bibliography:

1. Achilias, D. S., & Antonakou, E. V. (2015). Chemical and Thermochemical Recycling of Polymers from Waste Electrical and Electronic Equipment. *Recycling Materials Based on Environmentally Friendly Techniques, July*. https://doi.org/10.5772/59960
2. Achilias, D. S., Giannoulis, A., & Papageorgiou, G. Z. (2009). Recycling of polymers from plastic packaging materials using the dissolution–reprecipitation technique. *Polymer Bulletin*, *63*(3), 449–465. https://doi.org/10.1007/s00289-009-0104-5
3. Achilias, D. S., Roupakias, C., Megalokonomos, P., Lappas, A. A., & Antonakou, E. V. (2007). Chemical recycling of plastic wastes made from polyethylene (LDPE and HDPE) and polypropylene (PP). *Journal of Hazardous Materials*, *149*(3), 536–542. https://doi.org/10.1016/J.JHAZMAT.2007.06.076
4. Aguado, J., Serrano, D. P., & San Miguel, G. (2007). Analysis of products generated from the thermal and catalytic degradation of pure and waste polyolefins using Py-GC/MS. *Journal of Polymers and the Environment*, *15*(2), 107–118. https://doi.org/10.1007/s10924-007-0051-x
5. *Altshuller, Genrich (1984). Creativity as an Exact Science. New York, NY: Gordon & Breach. ISBN 978-0-677-21230-2.*
6. ANSYS FLUENT Theory Guide. Release 12.0 © ANSYS, Inc. 2009-01-23. https://www.afs.enea.it/project/neptunius/docs/fluent/html/th/node298.htm
7. Arabiourrutia, M., Elordi, G., Lopez, G., Borsella, E., Bilbao, J., & Olazar, M. (2012). Characterization of the waxes obtained by the pyrolysis of polyolefin plastics in a conical spouted bed reactor. *Journal of Analytical and Applied Pyrolysis*, *94*, 230–237. https://doi.org/10.1016/j.jaap.2011.12.012
8. Arenova, A., Kodama, S., & Sekiguchi, H. (2019). Biomass pyrolysis in Sn-Bi molten metal for synthesis gas production. *Journal of Analytical and Applied Pyrolysis*, *137*(November 2018), 61–69. https://doi.org/10.1016/j.jaap.2018.11.010
9. Artetxe, M., Lopez, G., Amutio, M., Elordi, G., Bilbao, J., & Olazar, M. (2012). Light olefins from HDPE cracking in a two-step thermal and catalytic process. *Chemical Engineering Journal*, *207–208*, 27–34. https://doi.org/10.1016/j.cej.2012.06.105
10. Assael, M. J., Antoniadis, K. D., Wakeham, W. A., Huber, M. L., Fukuyama, H., Imperial, L. P., & Division, M. (2017). *Reference Correlations for the Thermal Conductivity of Liquid Bismuth, Cobalt, Germanium and Silicon*. *46*(3), 1–22. https://doi.org/10.1063/1.4991518.Reference
11. Balooch, M., Siekhaus, W. J., & Olander, D. R. (1984). Reactions of chlorine with liquid metals. 2. Lead. *Journal of Physical Chemistry*, *88*(16), 3529–3531. https://doi.org/10.1021/j150660a030
12. Bauer, T., Maisel, S., Blaumeiser, D., Vecchietti, J., Taccardi, N., Wasserscheid, P., Bonivardi, A., Görling, A., & Libuda, J. (2019). Operando DRIFTS and DFT Study of Propane Dehydrogenation over Solid- and Liquid-Supported GaxPty Catalysts. *ACS Catalysis*, *9*(4), 2842–2853. https://doi.org/10.1021/acscatal.8b04578

13. Bergstrom, F. W., & Carson, J. F. (1941). Alkali and Alkaline Earth Metals as Catalysts in the Hydrogenation of Organic Compounds. *Journal of the American Chemical Society*, *63*(11), 2934–2936. https://doi.org/10.1021/ja01856a019
14. Besagni, G., Inzoli, F., & Ziegenhein, T. (2018). Two-phase bubble columns: A comprehensive review. ChemEngineering, 2(2), 1–80. https://doi.org/10.3390/chemengineering2020013
15. Catalan, L. J. J., & Rezaei, E. (2020). Coupled hydrodynamic and kinetic model of liquid metal bubble reactor for hydrogen production by noncatalytic thermal decomposition of methane. *International Journal of Hydrogen Energy*, *45*(4), 2486–2503. https://doi.org/10.1016/j.ijhydene.2019.11.143
16. Daeneke, T., Khoshmanesh, K., Mahmood, N., De Castro, I. A., Esrafilzadeh, D., Barrow, S. J., Dickey, M. D., & Kalantar-Zadeh, K. (2018). Liquid metals: Fundamentals and applications in chemistry. In *Chemical Society Reviews* (Vol. 47, Issue 11, pp. 4073–4111). Royal Society of Chemistry. https://doi.org/10.1039/c7cs00043j
17. Das, P., & Tiwari, P. (2017). Thermal degradation kinetics of plastics and model selection. *Thermochimica Acta*, *654*(May), 191–202. https://doi.org/10.1016/j.tca.2017.06.001
18. Das, P., & Tiwari, P. (2018). Valorization of packaging plastic waste by slow pyrolysis. *Resources, Conservation and Recycling*, *128*(June 2017), 69–77. https://doi.org/10.1016/j.resconrec.2017.09.025
19. Della Zassa, M.; Favero, M.; Canu, P. Two-steps selective thermal depolymerization of polyethylene. 1: Feasibility and effect of devolatilization heating policy. J. Anal. Appl. Pyrolysis 2010, 87, 248− 255.
20. Desai, D., & Baker Rivest, J. L. (2019). *SYSTEM AND METHOD FOR PYROLYSIS USING A LIQUID METAL CATALYST* (Patent No. 2019/0055173 A1). United States Patent Office.
21. Dimitris S. Achilias, Lefteris Andriotis, Ioannis A. Koutsidis, Dimitra A. Louka, Nikolaos P. Nianias, Panoraia Siafaka, Ioannis Tsagkalias and Georgia Tsintzou (2012). Recent Advances in the Chemical Recycling of Polymers (PP, PS, LDPE, HDPE, PVC, PC, Nylon, PMMA), Material Recycling - Trends and Perspectives, Dr. Dimitris Achilias (Ed.), ISBN: 978-953-51-0327-1
22. Eriksen, M. K., Pivnenko, K., Olsson, M. E., & Astru, T. F. (2018). Contamination in plastic recycling: Influence of metals on the quality of reprocessed plastic. *Waste Management*, *79*, 595–606.
23. Fathi Aqra, Ahmed Ayyad. Surface tension of pure liquid bismuth and its temperature dependence: Theoretical calculations, Materials Letters, Volume 65, Issue 4,2011, Pages 760-762, ISSN 0167-577X, https://doi.org/10.1016/j.matlet.2010.11.038.
24. Geyer, R., Jambeck, J. R., & Law, K. L. (2017). Production, use, and fate of all plastics ever made. *Science Advances*, *3*(7), e1700782. https://doi.org/10.1126/sciadv.1700782
25. Ginter, G., Gasser, J. G., & Kleim, R. (1986). The electrical resistivity of liquid bismuth, gallium and bismuth-gallium alloys. Philosophical Magazine B: Physics of Condensed Matter; Statistical Mechanics, Electronic, Optical and Magnetic Properties, 54(6), 543–552. https://doi.org/10.1080/13642818608236869
26. Gulevich, A. V., Martynov, P. N., Gulevsky, V. A., & Ulyanov, V. V. (2008). Technologies for hydrogen production based on direct contact of gaseous hydrocarbons and evaporated water with molten Pb or Pb-Bi. *Energy Conversion and Management*, *49*(7), 1946–1950. https://doi.org/10.1016/j.enconman.2007.12.028

27. Hahladakis, J. N., Velis, C. A., Weber, R., Iacovidou, E., & Purnell, P. (2018). An overview of chemical additives present in plastics: Migration, release, fate and environmental impact during their use, disposal and recycling. *Journal of Hazardous Materials*, *344*, 179–199. https://doi.org/10.1016/j.jhazmat.2017.10.014

28. Hamad, K., Kaseem, M., & Deri, F. (2013). Recycling of waste from polymer materials: An overview of the recent works. *Polymer Degradation and Stability*, *98*(12), 2801–2812. https://doi.org/10.1016/J.POLYMDEGRADSTAB.2013.09.025

29. Harrison K., 3DChem.com - Polyethylene (Molecule of the Month for April 2007). https://www.3dchem.com/Polyethylene.asp#

30. Hillman, D. E. (1971). Characterization and Analysis of Waxes by Gel Permeation Chromatography. *Analytical Chemistry*, *43*(8), 1007–1013. https://doi.org/10.1021/ac60303a023

31. *Hoffman A., Smith J.,Soukup S.,* Boston University, S. of M. (1999). *Molten Metal Technology, Case study*. 1–27.

32. Honda, K., Takahashi, K., & Ogino, Y. (1980). BUTADIENE YIELDS IN THE REACTIONS OF BUTENES OVER BINARY LIQUID ALLOY CATALYSTS CONTAINING K OR Na. *Chemistry Letters*, *9*(5), 553–556. https://doi.org/10.1246/cl.1980.553

33. Horodytska, O., Cabanes, A., & Fullana, A. (2020). Non-intentionally added substances (NIAS) in recycled plastics. *Chemosphere*, *251*, 126373. https://doi.org/10.1016/j.chemosphere.2020.126373

34. International Atomic Energy Agency. (2007). Liquid Metal Cooled Reactors: Experience in Design and Operation. *Atomic Energy*, *December*, 272.

35. Kashiwadate, K., Saito, Y., Miyamoto, A., & Ogino, Y. (1971). The Dehydrogenation of Butyl Alcohols by the Molten-metal Catalysts. *Bulletin of the Chemical Society of Japan*, *44*(11), 3004–3009.

36. Keplinger, O., Shevchenko, N., & Eckert, S. (2019). Experimental investigation of bubble breakup in bubble chains rising in a liquid metal. *International Journal of Multiphase Flow*, *116*, 39–50. https://doi.org/10.1016/j.ijmultiphaseflow.2019.03.027

37. Kettner, M., Maisel, S., Stumm, C., Schwarz, M., Schuschke, C., Görling, A., & Libuda, J. (2019). Pd-Ga model SCALMS: Characterization and stability of Pd single atom sites. *Journal of Catalysis*, *369*, 33–46. https://doi.org/10.1016/j.jcat.2018.10.027

38. Komiyama, M., Nojima, S., & Ogino, Y. (1982). Studies on catalysis by molten metals. 14. Catalytic cracking of asphalts at low temperature. *Fuel*, *61*(6), 542–548.

39. Lithner, D. (2011). Environmental and health hazards of chemicals in plastic polymers and products. In *Department of Plant and Environmental Sciences: Vol. Ph.D. thes*.

40. Liu, J., Sheng, L., & He, Z.-Z. (2019). *Liquid Metal Soft Machines Principles and Applications*. https://www.springer.com/gp/book/9789811327087

41. Lopez, G., Artetxe, M., Amutio, M., Bilbao, J., & Olazar, M. (2017). Thermochemical routes for the valorization of waste polyolefinic plastics to produce fuels and chemicals. A review. *Renewable and Sustainable Energy Reviews*, *73*(January), 346–368. https://doi.org/10.1016/j.rser.2017.01.142

42. Luff, P., & White, M. (1968). Thermal degradation of polyethylene and polytetrafluoroethylene during vacuum evaporation. *Vacuum*, *18*(8), 437–440. https://doi.org/10.1016/0042-207X(68)90336-9

43. Marcilla, A., Beltrán, M. I., Hernández, F., & Navarro, R. (2004). HZSM5 and HUSY deactivation during the catalytic pyrolysis of polyethylene. *Applied Catalysis A: General*, *278*(1), 37–43. https://doi.org/10.1016/j.apcata.2004.09.023

44. Matsuura, M., Matsunaga, S. I., Ozawa, S., & Ogino, Y. (1981). Volcano-shaped relation between heats of oxide formation of metals and coal-liquefaction activities of liquid-metal catalysts. *Journal of the Chemical Society, Chemical Communications*, *14*, 721–722. https://doi.org/10.1039/C39810000721

45. Miyamoto, A., & Ogino, Y. (1972). Studies on Catalysis by Molten Metal. V. Kinetics of the Dehydrogenation of sec-Butyl Alcohol over the Liquid Indium Catalyst. *Journal of Catalysis*, *27*, 311–321.

46. Miyamoto, A., & Ogino, Y. (1976). Studies on catalysis by molten metals. X. Hydrogen transfer reactions between alcohols and ketones on liquid indium catalyst. *Journal of Catalysis*, *43*(1–3), 143–153. https://doi.org/10.1016/0021-9517(76)90301-8

47. Munera Parra, A. A., & Agar, D. W. (2017). Molten metal capillary reactor for the high-temperature pyrolysis of methane. *International Journal of Hydrogen Energy*, *42*(19), 13641–13648. https://doi.org/10.1016/j.ijhydene.2016.12.044

48. Nagel C., Bach R.; Molten Metal Technology, Inc. (1996). United States patent 5,543,558. Method for producing unsaturated organics from organic-containing feeds.

49. Nakakubo, K., Yoshioka, H., Morita, K., Ishimatsu, R., Kiani, A., Hallen, H., Dickey, M. D., & Oki, Y. (2021). Dynamic control of reflective/diffusive optical surfaces on EGaIn liquid metal. *Optical Materials Express*, *11*(7), 2099. https://doi.org/10.1364/ome.425432

50. Onwudili, J. A., Insura, N., & Williams, P. T. (2009). Composition of products from the pyrolysis of polyethylene and polystyrene in a closed batch reactor: Effects of temperature and residence time. *Journal of Analytical and Applied Pyrolysis*, *86*(2), 293–303. https://doi.org/10.1016/j.jaap.2009.07.008

51. Orbetron - 50 Series Feeder [https://www.orbetron.com/product/orbetron/50-series-feeder]

52. Painter, Paul C., and Michael M. Coleman. 1997. *Fundamentals of polymer science: an introductory text*. Lancaster, Pa: Technomic Pub. Co.

53. Palmer, C., Tarazkar, M., Kristoffersen, H. H., Gelinas, J., Gordon, M. J., McFarland, E. W., & Metiu, H. (2019). Methane Pyrolysis with a Molten Cu-Bi Alloy Catalyst. *ACS Catalysis*, *9*(9), 8337–8345. https://doi.org/10.1021/acscatal.9b01833

54. Palmer, C., Upham, D. C., Smart, S., Gordon, M. J., Metiu, H., & McFarland, E. W. (2020). Dry reforming of methane catalysed by molten metal alloys. *Nature Catalysis*, *3*(1), 83–89. https://doi.org/10.1038/s41929-019-0416-2

55. Park, S. H., Park, C., Lee, J. Y., & Lee, B. (2017). A Simple Parameterization for the Rising Velocity of Bubbles in a Liquid Pool. *Nuclear Engineering and Technology*, *49*(4), 692–699. https://doi.org/10.1016/j.net.2016.12.006

56. Payne, J., McKeown, P., & Jones, M. D. (2019). A circular economy approach to plastic waste. *Polymer Degradation and Stability*, *165*, 170–181. https://doi.org/10.1016/J.POLYMDEGRADSTAB.2019.05.014

57. Peterson, J. D., Vyazovkin, S., & Wight, C. A. (2001). Kinetics of the thermal and thermo-oxidative degradation of polystyrene, polyethylene and poly(propylene). *Macromolecular Chemistry and Physics*, *202*(6), 775–784.

58. *Physical Properties of Bismuth.* http://bismuth.atomistry.com/physical_properties_bismuth.html

59. Plevan, M., Geißler, T., Abánades, A., Mehravaran, K., Rathnam, R. K., Rubbia, C., Salmieri, D., Stoppel, L., Stückrad, S., & Wetzel, T. (2015). Thermal cracking of methane in a liquid metal bubble column reactor: Experiments and kinetic analysis. *International Journal of Hydrogen Energy*, *40*(25), 8020–8033. https://doi.org/10.1016/j.ijhydene.2015.04.062

60. Prata, J. C., Patr, A. L., Mouneyrac, C., Walker, T. R., Duarte, A. C., & Rocha-santos, T. (2019). Solutions and Integrated Strategies for the Control and Mitigation of Plastic and Microplastic Pollution. *International Journal of Environmental Research and Public Health*, *16*(2411), 1–19.

61. Ragaert, K., Delva, L., & Van Geem, K. (2017). Mechanical and chemical recycling of solid plastic waste. *Waste Management*, *69*(August), 24–58. https://doi.org/10.1016/j.wasman.2017.07.044

62. Ragaert, K., Hubo, S., Delva, L., Veelaert, L., & Du Bois, E. (2018). Upcycling of contaminated post-industrial polypropylene waste: A design from recycling case study. *Polymer Engineering and Science*, *58*(4), 528–534. https://doi.org/10.1002/pen.24764

63. Raman, N., Maisel, S., Grabau, M., Taccardi, N., Debuschewitz, J., Wolf, M., Wittkämper, H., Bauer, T., Wu, M., Haumann, M., Papp, C., Görling, A., Spiecker, E., Libuda, J., Steinrück, H. P., & Wasserscheid, P. (2019). Highly Effective Propane Dehydrogenation Using Ga-Rh Supported Catalytically Active Liquid Metal Solutions. *ACS Catalysis*, *9*(10), 9499–9507. https://doi.org/10.1021/acscatal.9b02459

64. Regan, M., Pershan, P., Magnussen, O., & Ocko, B. (1997). X-ray reflectivity studies of liquid metal and alloy surfaces. *Physical Review B - Condensed Matter and Materials Physics*, *55*(23), 15874–15884. https://doi.org/10.1103/PhysRevB.55.15874

65. Saito, H., & Sekine, Y. (2020). Catalytic conversion of ethane to valuable products through non-oxidative dehydrogenation and dehydroaromatization. *RSC Advances*, *10*(36), 21427–21453. https://doi.org/10.1039/d0ra03365k

66. Sasse, F., & Emig, G. (1998). Chemical recycling of polymer materials. *Chemical Engineering and Technology*, *21*(10), 777–789. https://doi.org/10.1002/(SICI)1521-4125(199810)21:10<777::AID-CEAT777>3.0.CO;2-L

67. Schultz, I., & Agar, D. W. (2015). Decarbonisation of fossil energy via methane pyrolysis using two reactor concepts: Fluid wall flow reactor and molten metal capillary reactor. *International Journal of Hydrogen Energy*, *40*(35), 11422–11427. https://doi.org/10.1016/j.ijhydene.2015.03.126

68. Schwab, G. (1976). Catalysis on Liquid Metals. *Berichte Der Bunsengesellschaft Fur Physikalische Chemie*, *80*(8), 746–749.

69. Serban, M., Lewis, M. A., Marshall, C. L., & Doctor, R. D. (2003). Hydrogen production by direct contact pyrolysis of natural gas. *Energy and Fuels*, *17*(3), 705–713. https://doi.org/10.1021/ef020271q

70. Shu, Y., Yu, D., Hu, W., Wang, Y., Shen, G., Kono, Y., Xu, B., He, J., Liu, Z., & Tian, Y. (2017). Deep melting reveals liquid structural memory and anomalous ferromagnetism in bismuth. Proceedings of the National Academy of Sciences of the United States of America, 114(13), 3375–3380. https://doi.org/10.1073/pnas.1615874114

71. Simon, Peter. (2004). Isoconversional methods - Fundamentals, meaning and application. Journal of Thermal Analysis and Calorimetry. 76. 10.1023/B:JTAN.0000027811.80036.6c.

72. Steinberg, M. (1996). The Carnol process for CO2 mitigation. *Energy Conversion and Management*, *37*(6–8), 843–848.

73. Stelmachowski, M. (2010). Thermal conversion of waste polyolefins to the mixture of hydrocarbons in the reactor with molten metal bed. *Energy Conversion and Management*, *51*(10), 2016–2024. https://doi.org/10.1016/j.enconman.2010.02.035

74. Strumpf, E. (2017). Experimental study on rise velocities of single bubbles in liquid metal under the influence of strong horizontal magnetic fields in a flat vessel. *International Journal of Multiphase Flow*, *97*, 168–185. https://doi.org/10.1016/j.ijmultiphaseflow.2017.08.001

75. Sun, H., Guo, W., Liu, J., Feng, Z., Li, R., Zhou, X., & Huang, J. (2018). Supported rhodium liquid metal catalysts for the hydroformylation of olefins. *Applied Organometallic Chemistry*, *32*(12), 1–9. https://doi.org/10.1002/aoc.4555

76. Taccardi, N., Grabau, M., Debuschewitz, J., Distaso, M., Brandl, M., Hock, R., Maier, F., Papp, C., Erhard, J., Neiss, C., Peukert, W., Görling, A., Steinrück, H. P., & Wasserscheid, P. (2017). Gallium-rich Pd-Ga phases as supported liquid metal catalysts. *Nature Chemistry*, *9*(9), 862–867. https://doi.org/10.1038/NCHEM.2822

77. Takahashi, K., & Ogino, Y. (1978). Promoting Effect of Selenium on the Catalysis of Liquid Tellurium in the Dehydrogenation of Polynuclear Hydrocarbons. *Chemistry Letters*, *7*(5), 549–552. https://doi.org/10.1246/cl.1978.549

78. Thiounn, T., & Smith, R. C. (2020). Advances and approaches for chemical recycling of plastic waste. *Journal of Polymer Science*, *March*, 1347–1364. https://doi.org/10.1002/pol.20190261

79. Tyrer, D. (1931). *PRODUCTION OF HYDROGEN* (Patent No. 5,147,678). United States Patent Office.

80. Upham, D. C., Agarwal, V., Khechfe, A., Snodgrass, Z. R., Gordon, M. J., Metiu, H., & Mcfarland, E. W. (2017). *Catalytic molten metals for the direct conversion of methane to hydrogen and separable carbon*.

81. Victory M. and Tudball M.. March 12, 2021. Sustainable Plastics. Current recycled polymer price competitiveness fuelling switch away from virgin material. https://www.sustainableplastics.com/news/current-recycled-polymer-price-competitiveness-fuelling-switch-away-virgin-material

82. Wei, T. T., Wu, K. J., Lee, S. L., & Lin, Y. H. (2010). Chemical recycling of post-consumer polymer waste over fluidizing cracking catalysts for producing chemicals and hydrocarbon fuels. *Resources, Conservation and Recycling*, *54*(11), 952–961. https://doi.org/10.1016/j.resconrec.2010.02.002

83. Wittkämper, H., Maisel, S., Wu, M., Frisch, J., Wilks, R. G., Grabau, M., Spiecker, E., Bär, M., Görling, A., Steinrück, H. P., & Papp, C. (2020). Oxidation induced restructuring of Rh-Ga SCALMS model catalyst systems. In *Journal of Chemical Physics* (Vol. 153, Issue 10). https://doi.org/10.1063/5.0021647

84. Yang, L., Yu, X. Y., Zhu, Z., Iedema, M. J., & Cowin, J. P. (2011). Probing liquid surfaces under vacuum using SEM and ToF-SIMS. *Lab on a Chip*, *11*(15), 2481–2484. https://doi.org/10.1039/c0lc00676a

85. Young, H.D. and Freedman, R. A., University Physics, 11th Ed., Pearson, 2004.

86. Zahedi, P., Saleh, R., Moreno-Atanasio, R., & Yousefi, K. (2014). Influence of fluid properties on bubble formation, detachment, rising and collapse; Investigation using volume of fluid method. *Korean Journal of Chemical Engineering*, *31*(8), 1349–1361. https://doi.org/10.1007/s11814-014-0063-x

87. Zhang, J. (2009). A review of steel corrosion by liquid lead and lead-bismuth. *Corrosion Science*, *51*(6), 1207–1227. https://doi.org/10.1016/j.corsci.2009.03.013

88. Zhou, Y., Yao, J., Ding, Y., Yu, J., Hua, X., Evans, J. E., Yu, X., Lao, D. B., Heldebrant, D. J., Nune, S. K., Cao, B., Bowden, M. E., Yu, X. Y., Wang, X. L., & Zhu, Z. (2016). Improving the Molecular Ion Signal Intensity for In Situ Liquid SIMS Analysis. *Journal of the American Society for Mass Spectrometry*, *27*(12), 2006–2013. https://doi.org/10.1007/s13361-016-1478-x

89. Zuraiqi, K., Zavabeti, A., Allioux, F. M., Tang, J., Nguyen, C. K., Tafazolymotie, P., Mayyas, M., Ramarao, A. V., Spencer, M., Shah, K., McConville, C. F., Kalantar-Zadeh, K., Chiang, K., & Daeneke, T. (2020). Liquid Metals in Catalysis for Energy Applications. *Joule*, *4*(11), 2290–2321. https://doi.org/10.1016/j.joule.2020.10.012